EVALUATION OF THE CARDIOPROTECTIVE EFFECTS OF *Olea*

CONTAINING LIPOSOMES

by

SAMANTHA INGA CAIRNCROSS

A mini-thesis submitted in partial fulfillment of the requirements for the degree of

Magister Scientiae in the Department of Medical Bioscience (Nanoscience),

The University of the Western Cape.

SUPERVISOR: PROF. D. DIETRICH

CO-SUPERVISOR: Dr. R. JOHNSON

2017

DECLARATION

I declare that *"Evaluation of the cardioprotective effects of Olea containing liposomes"* is my own work, that it has not been submitted before for any degree or examination in any other university, and that all the sources I have used or quoted have been indicated and acknowledged as complete references.

Signed: _____

Samantha Inga Cairncross

June 2017

UNIVERSITY *of the*
WESTERN CAPE

ACKNOWLEDGEMENTS

Firstly, I would like to thank God for all the blessings in my life. God was always there to protect love and guide me through all of my trials.

I would like to record my gratitude to Professor Daneel Dietrich for kindly accepting me as her Master's student. I am very appreciative of her support and supervision during this project. She has provided valuable consultations, discussions, advice, and suggestions throughout the year. I also enjoyed the freedom to express my ideas. I am very thankful that Prof provided a very friendly atmosphere that made me feel relaxed and comfortable.
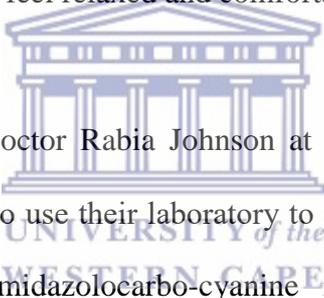
I am very thankful to Doctor Rabia Johnson at the Medical Research Council (MRC) for allowing me to use their laboratory to do the 5, 5′, 6, 6′-tetrachloro-1, 1′, 3, 3′-tetraethylbenzimidazolocarbo-cyanine iodide (JC-1) and adenosine triphosphate (ATP) assays. I am grateful for the advice, insight, and suggestions that was kindly offered.

I would like to give a huge thank you to Doctor Phiwayinkosi Dludla at the MRC for assisting me with my JC-1 and ATP assays in the laboratory. His time sacrifice and patience was really invaluable to me. Furthermore, I would like to thank Samukelisiwe Shabalala at the MRC for her sacrifices in assisting me the first few sessions in the laboratory.

I would like to express gratitude to Valencia Jamalie for placing my orders very diligently. I would like to thank Taahirah Boltman for sacrificing her time to demonstrate how liposomes were made.

I am very grateful to my group of friends at the campus for all the fun times that we had. I really appreciate all the support they gave me through the difficult times. I really enjoyed the jokes and mindful discussion that we had.

Lastly, I would like to thank my family for their sacrifices that enabled me to have the opportunity to complete my degree. I would like to thank my father and mother for always picking me up very late at night when I finished my work and for having to stand up very early in the morning to drop me off again. I am thankful that I have the privilege of having parents that make all these sacrifices asking for no reward. I would like to thank my younger brothers for always being there for me and supporting me. I would also like to thank my close aunts, uncles, and cousins. For the past two years, I have been working very hard on my thesis and have spent a lot of time away from home. I am very grateful for your support and understanding that everyone has offered me.

DEDICATION

I would like to dedicate this thesis to my family - Vicky, Steve, Justin, and Logan. Without the solid foundation of love that you provide for me, I would not be able to build my future.

ABSTRACT

The evaluation of the cardioprotective effects of *Olea* containing liposomes

Cairncross, S. I.

MSc thesis, Department of Medical Bioscience, University of the Western Cape

Background: High levels of free oxygen radicals, induced by many biological or environmental factors, result in damage and dysfunction of the mitochondria which causes cardiovascular and other diseases. Cardiotherapies employing antioxidants has been suggested to be a useful approach to scavenge excess reactive oxygen species (ROS). Many phytomedicines have antioxidant properties. The outcome of many clinical trials in which phytomedicines were used is however often disappointing.
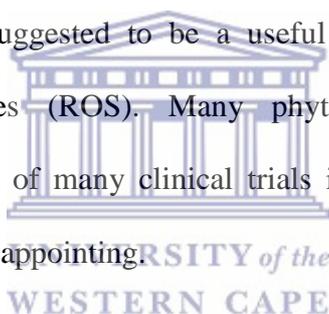
Aqueous leaf extracts of *Olea africana* (OA) has been used in South Africa as traditional medicine. Oleuropein (OL), the main active constituent in the leaf extract, has been proven to have antioxidant properties. The nature of the compounds extracted, like many other bioactive compounds found in plants, are water-soluble molecules. Their poor lipid solubility limits its ability to cross the cell membrane because of the lipid-rich bilayer. Nano-drug delivery systems, such as liposomes, are able to improve the biodistribution of drugs. The vesicles are attractive because of their drug carrying versatility, biocompatibility and ability to carry drugs into cells.

The *main objectives* of the study were to:

- Prepare an aqueous extract of OA and *O exasperata* (OE)

- Develop a nano-drug delivery system for aqueous extracts of OA, OE or OL

- Evaluate potential *in vitro* cardioprotective effects of OA, OE or OL as a free drug and as a liposomal encapsulated drug

Methods: Aqueous extracts of OA and OE were prepared. The OL content of the OA and OE was quantified using high-performance liquid chromatography (HPLC) and the presence of the OL peak was confirmed using mass spectrometry (MS). The HPLC method for the identification and quantification of OL was evaluated based on accuracy, precision, limit of detection (LOD), limit of quantification (LOQ), linearity and range.
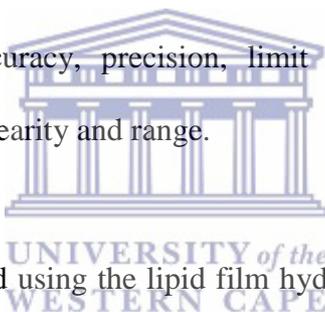
Liposomes were prepared using the lipid film hydration technique and liposomes were characterized based on size, polydispersity index (PDI) and zeta potential using photon correlation spectroscopy. Confocal microscopy was used to assess whether liposomes tagged with rhodamine -123 (rh - liposomes) were able to enter H9c2 cardiomyoblasts. The compounds, OA and OL which was selected to be encapsulated, were added during the aqueous phase of liposome formation and the encapsulation efficiency was determined, using OL as a standard for the encapsulation determination.

H9c2 cells were exposed to different concentrations of hydrogen peroxide (H_2O_2) (between 100 µM and 550 µM) for 24 hours to determine a concentration that will reduce cell viability to approximately 50%. Cell viability was assessed using the

MTT assay. Cells were treated with different concentrations of OA (range 1000 µg/ml to 0.1 µg/ml) or OL (range 100 µg/ml to 0.01 µg/ml) for 24 hours to test the toxicity and proliferation ability of OA and OL. Cell viability and proliferation was assessed using the MTT assay. Cells were pretreated with different concentrations of OA (1000 µg/ml, 100 µg/ml, 10 µg/ml, 1 µg/ml and 0.1 µg/ml) or OL (100 µg/ml, 10 µg/ml, 1 µg/ml, 0.1 µg/ml, 0.01 µg/ml and 0.005 µg/ml) for 24 hours before exposure to H_2O_2 for a further 24 hours. At the end of the experiment, the cell viability was assessed using the MTT assay or the JC-1 assay. A selected concentration of OA (1000 µg/ml) and OL (0.01 µg/ml) was encapsulated in liposomes. Cells were treated with different liposome concentrations (1000 µg/ml 10 µg/ml 1 µg/ml and 0.1 µg/ml) for 24 hours to evaluate the toxicity of the liposomes and/or encapsulated drugs. Cell viability was assessed by the MTT assay. H9c2 cells were pretreated with encapsulated OA (1000 µg/ml) or OL (0.01 µg/ml) at different liposome concentrations (1000 µg/ml 10 µg/ml 1 µg/ml and 0.1 µg/ml) for 24 hours before exposure to H_2O_2 for 24 hours. At the end of the experiment cell viability was assessed using the MTT and JC-1 assay. In order to further evaluate the protective effects of the compounds doxorubicin was used as stressor and cell viability was assessed by the ATP assay, thus H9c2 cells were pretreated with different concentrations of OA (1000 µg/ml, 100 µg/ml, 10 µg/ml and 1 µg/ml) or OL (10 µg/ml, 1 µg/ml, 0.1 µg/ml, 0.01 µg/ml) for 24 hours before exposure to 5 µM doxorubicin for 24 hours. A selected concentration of OA (1000 µg/ml) and OL (0.01 µg/ml) was encapsulated in liposomes. Cells were treated with different liposome concentrations (1000 µg/ml 10 µg/ml 1 µg/ml and 0.1 µg/ml) for 24 hours before exposure to doxorubicin. At the end of these experiments, cell viability was assessed by the ATP assay.

*Result*s: The aqueous extracts prepared from OA – and OE leaves gave yields of 33% and 12% respectively. The OL compound was found to be present in 0.1% in an OA extract. There was no OL present in the OE extract and the extract was not used in subsequent studies. The HPLC method for the identification and quantification of OL was then validated and showed good accuracy – and precision, selectivity for OL and linearity (r^2=0.9991) over a wide range. The limit of detection was 1 ppm and the limit of quantitation was 4 ppm. The liposomes had an average diameter of 109.6 nm and a charge of -20.3 mV. Liposomes were monodispersed and remained stable over the 6 months period. Furthermore, liposomes had an encapsulation efficiency of 24%. Confocal microscopy results reveal that liposomes were inside the cells after 24 hours. The OA and OL concentrations tested were not toxic to H9c2 cells and did not cause cell proliferation. Hydrogen peroxide at a concentration of 550 µM reduced cell viability significantly ($p<0.05$) to 58%. OA and OL pretreatment, either as a free drug or encapsulated in liposomes, could not protect the H9c2 cells against H_2O_2 – induced stress at any of the concentrations tested ($P>0.05$) as assessed by the MTT and JC-1 assays. Furthermore, OA and OL pretreatment, either as a free drug or encapsulated in liposomes, could not protect the H9c2 cells against doxorubicin (dox) induced oxidative stress as assessed by the more sensitive ATP assay ($P>0.05$)

In conclusion, we were able to prepare liposomes with a diameter of 109.6 nm and a charge of -20.3 mV. The liposomes were monodispersed and were stable over the 6 months tested. The liposomes encapsulated OL with an efficiency of 24% (something we would like to improve). Liposomes prepared were able to enter H9c2

cells. In this study, a 24-hour pretreatment of OA or OL as a free – or encapsulated

drug was unable to protect H9c2 cells against H_2O_2 - or doxorubicin-induced stress.

June 2017

UNIVERSITY *of the*
WESTERN CAPE

KEYWORDS

Antioxidant

Cardioprotection

Doxorubicin

H9c2 cells

Hydrogen Peroxide

Liposomes

Nanomedicine

Olea europaea subsp. *africana*

Olea exasperata

Oleuropein

Oxidative stress

Reactive oxygen species

LIST OF FIGURES

LIST OF TABLES

LIST OF ABBREVIATIONS

µm	micrometre
µM	micromolar
µl	microlitres
ADP	Adenosine diphosphate
AIDS	Acquired immunodeficiency virus
ATP	Adenosine triphosphate
CAT	Catalase
CVD	Cardiovascular disease
dox	doxorubicin
ETC	Electron Transport Chain
FDA	Food and drug administration
GaAsP	Gallium arsenide phosphide
GIT	Gastrointestinal tract
GPx	Glutathione Peroxidase
GR	Glutathione reductase
HEPES	4-(2-Hydroxyethyl)piperazine-1-ethanesulfonic acid
HPLC	High-Performance Liquid Chromatography
H_2O_2	Hydrogen Peroxide
HT	Hydroxytyrosol
I/R	Ischemic-Reperfusion
JC-1	1-5, 5′, 6, 6′-tetrachloro-1, 1′, 3, 3′-tetraethylbenzimidazolocarbo-cyanine iodide
KCL	Potassium chloride

l	Litres
LDL	Low-density lipoprotein
ml	millilitres
mM	millimolar
MMP	Mitochondrial membrane potential
MS	Mass spectrometer
MTT	3-(4,5-dimethylthiazol-2-yl)-2,5-diphenyl tetrazolium bromide
Na_2HPO_4	Disodium hydrogen phosphate
$NaH_2PO_4H_2O$	Sodium Dihydrogen Phosphate Monohydrate
nm	nanometre
NRF	National Research Foundation
O_2	Oxygen
O_2^-	Superoxide radical
OH^-	Hydroxyl radical
OA	*Olea europaea* subsp. *africana*
OE	*Olea exasperata*
OL	Oleuropein
PDI	Polydispersity index
ppm	part per million
RES	Reticuloendothelial system
rh-liposomes	Rhodamine - liposomes
ROS	Reactive Oxygen Species
SA	South Africa
SOD	Superoxide dismutase
TPx	Thioredoxin reductase

UV   Ultraviolet

CONTENTS

UNIVERSITY *of the*
WESTERN CAPE

PREFACE

"There is plenty of space at the bottom"

These are the famous words of the Nobel physicist Richard P. Feyman who prophesied that machine tools so small, as to manipulate processes on a nanoscale, is something that "*cannot be avoided*". Aware that these tiny tools could have medical applications, he proposed a miniature surgeon that can be introduced into the body, go the heart and cure heart disease. In 1959 Feyman urged to consider the possibility that we can create machines that can be manipulated on a cellular level (Freitas, 2005).

Nanotechnology is a fast growing field and has become very popular in recent years. (Lazarovits *et al*., 2015). Nanoparticles are considered a discovery of the twentieth century. However, there is evidence of artisans in the nineth century utilizing nanosized materials on the surface of ceramic vessels to obtain a glittering effect (Strambeanu *et al*., 2015). These particles can be defined as having at least one dimension in the nanoscale (1-100nm for naturally occurring nanoparticles and 1 - 1000 nm for colloidal particles) (Wagner *et al*., 2014).

Nanomaterials have unique magnetic, electrical, luminescent, and catalytic properties that can offer many advantages in diagnostics and therapeutics in the biomedical field. However, the advanced properties as a result of enhanced physical and chemical characteristics is also the cause of toxicity of nanoparticles in living organisms (Gatoo *et al*., 2014).

There are plenty of complaints concerning health and ecological implications as living organisms are becoming continuously exposed to potentially toxic Nanoparticles. Despite all of the safety concerns on Nanoparticles, their beneficial applications in medicine are difficult to ignore. The nanoscale dimensions of the particles allow for therapeutic and diagnostic applications that are less discomforting and more accurate (Demming, 2011).

Very recent successes in nanomedicine have increased the awareness of the area and with the increase in attention- came an increase in funding. More funds resulted in the heightened discovery of more complex nanoscale systems and thus more excitement over the potential of Nanoparticles (Mitragotri *et al*., 2017).

CHAPTER 1: INTRODUCTION

Plants have been used in the prevention, treatment, and curing of diseases for centuries. Towards the end of the twentieth century, the use of botanical-derived therapies has been replaced by synthetic products as remedies. The synthetic remedies often had no association with natural products. The increase in synthetic medicine was a big achievement and lead to countless lives being saved (Raskin *et al*., 2002). Natural products are however considered safer and cheaper than synthetic drugs. There has been an increase in the preferred use of natural products (Esmaeili and Sonboli, 2010, Rice-Evans *et al*., 1997). Also, the benefits of modern medicine are mostly experienced in developed countries. Many developing countries still rely on ethnomedicine (Lall and Kishore, 2014).
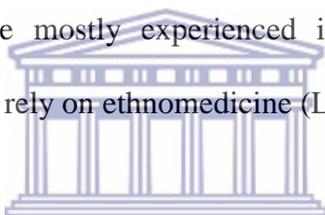
In the past natural products were enhanced through chemical modification. The therapeutic effect of the drug is 'improved' by the isolation of a single bioactive compound. More recently, natural products are used as a mixture of compounds, as found in an extract. A mixture of compounds which complement each other could provide a heightened therapeutic effect (Adams *et al*., 2006, Zhou *et al*., 2016). The olive leaf extract and its pure phenolics have both been shown to have antioxidant effects. Both synergistic and antagonistic effects may enhance the antioxidant potency (Mylonaki *et al*., 2008).

South Africa (SA) has a rich botanical diversity. Many of these indigenous plants have been used since ancient times in ethnomedicine. Very few of these have however been fully investigated scientifically. A large proportion of the SA

population makes use of traditional medicines for their physical and psychological needs (Lall 2014).

The research focussing on the olive plant tend to focus on the olive fruit and olive oil. There is very limited research focussing on the health benefits of the olive leaf extract. The main constituent in the olive plant is oleuropein (OL). It is not plentiful in olive oil and olive fruits. This is due to the constituents being hydrolyzed during processing and maturation. However, OL is abundant in the leaves of the olive plant. This is because the leaves undergo very little changes during maturation (Bock *et al*., 2013).
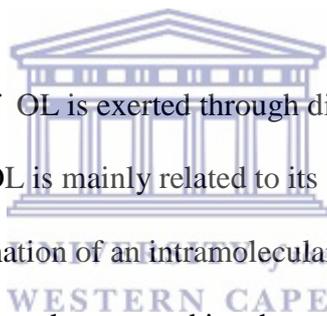
The antioxidant effect of OL is exerted through different mechanisms. The antioxidant potential of OL is mainly related to its ability to improve radical stability through the formation of an intramolecular hydrogen bond between the free hydrogen of the hydroxyl group and its phenoxyl radicals. Oleuropein may counteract oxidative stress demonstrating an antioxidant potential similar to that exerted by ascorbic acid (vitamin C) and α-tocopherol (vitamin E) (Barbaro *et al*., 2014). Oleuropein is present in the *Olea europaea* subsp. *africana* (Long *et al*., 2010).

CVDs are a significant cause of disability, morbidity, and mortality (Cook *et al*., 2014, Dai and Rabinovitch, 2009, Sahoo *et al*., 2007). The disease is very prevalent in western societies. In recent years, it has become evident that mitochondrial dysfunction is implicated in a variety of CVDs (Bulotta *et al*., 2014).

When ROS are present at high concentrations and the endogenous radical scavenging systems become depleted, it results in oxidative stress that can cause damage to the mitochondria of cells. This results in an increase in mitochondrial ROS, which in turn further damages the organelle. Damage to the mitochondria reduces the function of cells and organs, such as the heart (Dai and Rabinovitch, 2009, Wallace, 2006, Zorov et al., 2014).

Superoxide ion (O_2^-), a free-oxygen radical, is rapidly converted to hydrogen peroxide (H_2O_2). The dismutation of O_2^- to H_2O_2 occurs through the catalyzation by superoxide dismutase (SOD). H_2O_2 is a very stable molecule and is readily membrane permeable, thus enabling its diffusion into the cell (Schröder and Eaton, 2008). When O_2^- is converted to H_2O_2, the H_2O_2 diffuses out of the mitochondria and into the cytoplasm (Yamada 2008). H_2O_2 is decomposed by many cytosolic and mitochondrial antioxidant enzymes. Glutathione peroxidase (GPx), catalase (CAT) and thioredoxin reductase (TPx) are all antioxidant systems involved in the decomposition of H_2O_2 (Armstrong, 1997, Esmaeili and Sonboli, 2010, McCord and Fridovich, 1969, Van Bladeren, 2000). However, if H_2O_2 is not eliminated, it forms a hydroxyl radical (OH^-) which is highly reactive. Its strong oxidizing potential allows OH^- to damage almost every kind of macromolecule. Unlike O_2^- and H_2O_2, OH^- cannot be detoxified by enzymatic conversion. Therefore OH^- is extremely dangerous to an organism (Sheu et al., 2006).

Preclinical testing of new drugs is important to eliminate unsuitable compounds before the expenses of clinical research. The use of tissue culture system as an initial preclinical screening of compounds is very common. The cultured cells selected

can represent the disease or associated biochemical anomalies (Van Tonder *et al*., 2015). The H9c2 cells are a clonal cell line that is derived from embryonic rat heart tissue. The cells exhibit similar properties to cardiac muscle, including its electrophysiological properties and its ion channels- and receptor composition. Despite not being fully differentiated, H9c2 cells have frequently been employed as a model for cardiac cells and are considered a good model for cardiomyocyte experiments (Ekhterae *et al*., 1999, Hescheler *et al*., 1991, Ranki *et al*., 2002, Takahashi *et al*., 2006). H_2O_2 has been frequently employed to induce oxidative stress in cardiomyocytes (Chen *et al*., 2000, Duarte and Jones, 2007, Han *et al*., 2004, Heo *et al*., 2007, Jeong *et al*., 2009, Witting *et al*., 2006). Oxidative damage has been reported to cause cell death in many experiments (Chen *et al*., 2000).
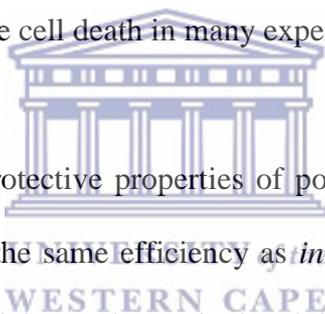
Many times when the protective properties of polyphenols are tested in clinical trials, they fail to show the same efficiency as *in vitro*. Reasons for this include poor bioavailability, toxicity and gastric breakdown and poor cellular uptake (Atale *et al*., 2013, Chen *et al*., 2001, Lindgren *et al*., 2000). Most of the bioactive compounds in plants are polar or water-soluble molecules. Water-soluble phytoconstituents (e.g. flavonoids, tannins, terpenoids etc.) are poorly absorbed. This is due to their large molecule size which cannot be absorbed by passive diffusion. It is also their poor lipid solubility that severely limits their ability to pass over the lipid-rich biological membranes. The emerging trends in nanotechnology can assist in overcoming bioavailability problems associated with natural products use as drugs (Kumari *et al*., 2012, Saraf, 2010b, Shi *et al*., 2010). A suitable method for altering the biodistribution pattern of water-soluble agents is the encapsulation in liposomes (Sachse *et al*., 1993, Schneider *et al*., 1995).

The problem with traditional medicine is that it does not keep pace current scientific and technological advancement. Encapsulating an extract of a local plant is thus important.

Research questions

- Can aqueous extracts of *Olea exasperata* (prepared in our lab), *Olea africana* (prepared in our lab) or OL protect the H9c2 cell line from hydrogen peroxide-induced oxidative stress?

- Will the aqueous extracts of *Olea exasperata* or *Olea africana*, that we prepared, contain OL?

- When encapsulated in liposomes, will the aqueous extracts of *Olea exasperata*, *Olea africana* or OL provide enhanced protection against hydrogen peroxide-induced stress as compared to the unencapsulated drug?
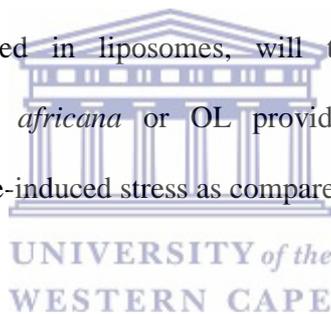
Aim and objectives:

- To develop a nano - liposomal drug delivery system for OA, OE, and OL.
    - Firstly, an aqueous extract will be prepared and evaluated to determine its oleuropein content.
    - Liposome vesicles with an average diameter of 100 nanometres (nm) will be produced and characterized based on size, size distribution and charge.
    - The uptake of liposomes into cardiomyoblasts will be evaluated.
    - The drugs of interest will be encapsulated in the nanoparticles and the encapsulation efficiency will be determined.

- To prepare an aqueous extract of OA or OE and determine the OL content of the extracts.

- To evaluate the potential cardioprotective effect of the free compounds and the encapsulated compounds.

UNIVERSITY *of the*

WESTERN CAPE

CHAPTER 2: LITERATURE REVIEW

2.1 Oxygen and the heart

Around 10% of all oxygen in the body is consumed by the heart at rest. The oxygen consumption of the heart can increase 4-5 fold during exertion. This is because the heart uses more energy than any other organ in the body (Goffart *et al*., 2004). Adenosine triphosphate (ATP) is the major source of energy for the cell and is crucial for cell survival (Guimarães-Ferreira, 2014). The mitochondria generate ATP via the electron transport chain (ETC). Thus the heart has the highest density of mitochondria. Under anaerobic conditions, the heart cannot produce sufficient energy for normal cellular functions to be maintained. This can result in irreversible cell damage or cell death (Giordano, 2005).
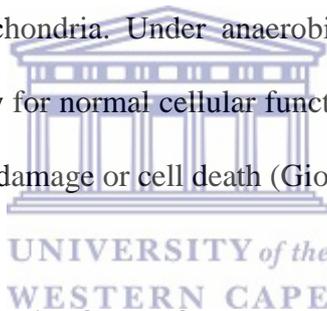
Free-radicals are highly reactive forms of oxygen produced by aerobic cells as a result of oxygen consumption. In the ETC, oxygen serves as the final electron acceptor. The oxygen atom contains two unpaired electrons in the outer shell. Any atom or molecule with unpaired electrons is known as a free-radical. Free-radicals are highly reactive molecules (Kaul *et al*., 1993, Singal *et al*., 1988). Molecular oxygen (O_2) is described as being diradical. Therefore, in the ETC, it requires four electrons to be reduced to water (Singal *et al*., 1988). The input of only one electron in the O_2 molecule would result in the formation of a superoxide radical (O_2^-) (Kaul *et al*., 1993). The donation of only two electrons produces peroxide. Further protonation of peroxide yields, a non-radical oxygen species, hydrogen peroxide

32 | P a g e

(H_2O_2) (Münzel *et al*., 2015). The addition of a third electron results in the formation of a hydroxyl radical (OH^-) (Kaul *et al*., 1993).

Figure 2.1: The formation of ROS species (Cristiana *et al*., 2012)

Reactive oxygen species (ROS) have the ability to react with lipids, proteins and nucleic acids and cause damage to these structures (Münzel *et al*., 2015). Oxygen and its reactive metabolites were a huge threat to a primitive eukaryotic cell in early evolution (Ott *et al*., 2007). Thus, developing mechanisms to protect cells from these highly reactive molecules became critical to surviving in an aerobic environment. When the "negative" side of oxygen was controlled, it became possible to use molecular oxygen for essential biochemical reactions (Finkel and Holbrook, 2000, Ott *et al*., 2007).

ROS are maintained at physiological levels by numerous endogenous antioxidant systems. Superoxide dismutase (SOD), catalase, glutathione peroxidases and glutathione reductase (GR) are all antioxidant enzymes assisting in the control of ROS levels (Bulotta *et al*., 2014). Additional protection is provided by non-

enzymatic defences such as glutathione, vitamin C and vitamin E (Ames *et al*., 1993, Esmaeili and Sonboli, 2010, Halliwell, 1994).

The regulation of ROS levels is extremely important, as low levels of ROS slightly alter the redox state of the cell. This plays a major role in the cellular stress response. Cellular signaling, via ROS, occurs in both eukaryotic and prokaryotic organisms. Given that the response occurs in more primitive cells, shows that it is an evolutionarily conserved mechanism and this demonstrates the importance of redox regulation (Finkel and Holbrook, 2000).

A cellular stress response can be induced by a disturbance within the extra- and intracellular environment. When conditions become unfavourable, the cells need to react to restore homeostasis. The survival of the cells depends on the ability to adapt or resist stress. Cell signaling pathways drive a response for cells to repair, replace or remove the damaged cells which help to preserve the organism (Finkel and Holbrook, 2000). There are also other adaptions to advance resistance to the stressor. During the cellular stress response, there is an upregulation of cytoprotective proteins to counteract the stressor (Jiang *et al*., 2011). If the attempt fails to prevent harm to cellular components, it could result in permanent damage. When the cell is permanently impaired, it undergoes apoptosis, a programmed cell death (Bonavita *et al*., 2003, Jiang *et al*., 2011).

ROS acts as a double-edged sword. At non-toxic levels, ROS plays an important role in normal cellular signal mechanisms, such as those in cellular processes, including inflammatory responses, cellular adhesion, differentiation and proliferation, etc. (Zhang *et al*., 2016). ROS, however, accelerates cellular dysfunction when present in excess (Allen *et al*., 2005, Choi *et al*., 2015, Sauer *et al*., 2001). Oxidative stress is marked by an accumulation of ROS within the cell. The presence of excess radicals is associated with depleted defence mechanisms. This redox state results in damage to proteins, lipids, deoxyribonucleic acids (DNA), cell membrane and cellular organelles (Finkel and Holbrook, 2000, Giasson *et al*., 2000). Given that ROS causes damage to tissue, these have become important molecules implicated in disease (Halliwell, 1987, Kaul *et al*., 1993).
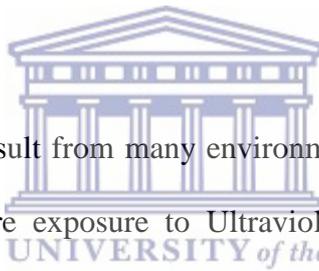
In the body, ROS can result from many environmental or biological factors. The environmental factors are exposure to Ultraviolet (UV) light, x-ray radiation, smoking, pollution, ozone, certain drugs (for example, doxorubicin), chemicals or pesticides. Biologically, the mitochondria are the main source of ROS (Pryor, 1986, Zou *et al*., 2010). Oxidative stress, in particular, causes damage to the mitochondria of cells. This results in an increase in mitochondrial ROS which in turn damages the organelle. Damage to the mitochondria results in functional declines in the cells and organs, such as the heart (Dai and Rabinovitch, 2009, Wallace, 2006, Zorov *et al*., 2014). The heart is very susceptible to a radical attack. A brief exposure to oxygen radicals has been shown to cause a decrease in high energy phosphates, loss of contractile function and structural abnormalities in isolated perfused hearts (Singal *et al*., 1998).

As the main source of energy in the cell, mitochondrial dysfunction is characterized by an inoperative ETC chain and consequently an impeded oxidative phosphorylation pathway, thus decreases energy production. The supply of energy by the mitochondria depends on the chemiosmotic gradient across the inner membrane. This gradient, or proton motive force, is generated by three respiratory enzyme complexes. These complexes use the free energy released from the electron transport chain to translocate protons from the mitochondrial matrix to the intermembrane space (Škárka and Oštádal, 2002).

The proton motive force consists of two components, these are the mitochondrial membrane potential (MMP) and pH gradient. The MMP results from the net movement of positive charge across the inner membrane. Energy stored in the gradient is a result of the MMP. The MMP is used as an indicator for the energization state of the mitochondria. In normal cellular function, the MMP is maintained as it is important for ATP production (Škárka and Oštádal, 2002). Insufficient energy adversely affects cardiomyocyte functions (Green and Reed, 1998, Wallace, 2006, Yamada *et al.*, 2007). Thus, impaired mitochondrial function is present in many cardiac diseases, such as the aging heart, I/R injury, hypertrophy of the myocardium and heart failure (Schwart *et al.*, 2014).

Aging is marked by a physiological decline in the physiological functioning of the body. Thus, in aged individuals, there is an increased risk of morbidity and mortality. The cause of the body's decline is not well known. However, sustained damage caused by endogenous ROS has been implicated in the progression of aging (Miyoshi *et al.*, 2006).

Aging is a risk factor for the development of cardiovascular disease (Dai and Rabinovitch, 2009). Intrinsic cardiac aging is defined as a progressive, age-dependent degeneration and decline in cardiac function (Dai and Rabinovitch, 2009). Mitochondria in the aged show morphological changes, produce more oxidant species and synthesize less ATP. Damaged cells thus accumulates/ during aging (Miyoshi *et al*., 2006), making the heart more susceptible to stress (Dai and Rabinovitch, 2009).

2.2 *Olea* as medicine

As mentioned previously, oxidative stress arises from an imbalance between the production of reactive oxygen species (ROS) and their removal by cellular antioxidant systems (Sieprath *et al*., 2016). It is, therefore, logical to suggest that introducing an antioxidant could assist in relieving the redox-imbalance (Dai *et al*., 2014).

Plant products contain many bioactive compounds that can scavenge radicals (Block *et al*., 1992). This gives plant medicines the potential to be used as therapeutics to treat disorders caused by ROS (Esmaeili and Sonboli, 2010, Halliwell, 1999).

Plants have been used in the prevention, treatment, and curing of diseases for centuries (Raskin *et al*., 2002). Towards the end of the twentieth century, the use of botanical-derived therapies has been replaced by synthetic products as remedies. The synthetic remedies often have no association with natural products. The increase in synthetic medicine was a big achievement and lead to countless lives being saved. The mass produced chemical medicines have however not proven to be the universal panacea that researchers had hoped for (Raskin *et al*., 2002). Research has now thus gone back to exploring plant sources for health care (Esmaeili and Sonboli, 2010, Rice-Evans *et al*., 1997).

A traditional Mediterranean diet consists of a plentiful intake of olive oil, fruit, nuts, vegetables, and cereals (Estruch *et al*., 2013, Willett *et al*., 1995). There is a moderate consumption of fish and poultry. Also, the diet has a low intake of dairy products, red meat, processed meat, and sweets. Wine is often consumed with meals (Estruch *et al*., 2013, Willett *et al*., 1995). The health benefits associated with the Mediterranean diet include, decreasing the risk factors for hyperlipidaemia, hypertension, diabetes, inflammation, stroke, obesity and coronary heart disease (Carluccio *et al*., 2003, Kratzb and Cullenc, 2002, Manna *et al*., 1997, Rose *et al*., 1986, Trichopoulou and Critselis, 2004, Tuck and Hayball, 2002, Visioli *et al*., 1995, Visioli and Galli, 1994, Waterman and Lockwood, 2007, Willett *et al*., 1995). Most of the beneficial properties of the diet have been attributed to olive oil, a main constituent of the diet, and olive fruit as this is a popular dietary component (Fitó *et al*., 2007, Rose *et al*., 1986, Tuck and Hayball, 2002).

The olive tree has been used for the production of olive oil, canned fruit, and wood for centuries. The leaves were used for herbal tea because they contain beneficial polyphenols (Breton *et al*., 2012). There has been a lot of interest in olive polyphenols in recent years. The olive tree (Olea europaea L.) contains biophenols such as oleuropein (OL) and its break-down products including, verbascoside, ligostride, tyrosol and hydroxytyrosol (HT) (Japón-Luján and Luque de Castro, 2007). Quantitatively, these compounds vary within the different parts of the plant (Ryan and Robards, 1998).

The flowering of the olive tree is indicative of olive fruit development beginning. The olives mature over a period of 6-8 months. There are three phases involved in maturation. The first phase is the growth phase, which is marked by the accumulation of OL. This is followed by the green, then black maturation phases. When the olive fruit matures, enzymatic reactions result in chemical changes in the fruit (Amiot *et al*., 1989). During the manufacturing of olive oil, the olive plant is subjected to many hydrolytic processes to extract the oil. The alterations during processing and maturation result in these components having high levels of hydroxytyrosol (HT) (Cimato *et al*., 1989, Tuck and Hayball, 2002, Ryan *et al*., 1999). The olive leaves, which makes up a large part of the olive tree mass (Ahmad-Qasem *et al*., 2013b), undergo very little chemical changes during maturation. Therefore, OL is well conserved and present in high concentrations in the leaves (Bulotta *et al*., 2014a, Rada *et al*., 2007).

2.2.1 Oleuropein

The leaves of the olive tree are often just considered a byproduct of olive fruit pruning. The leaves are thus used in animal feeds or disposed of by burning (Ahmad-Qasem *et al*., 2013a, de Castro and Capote, Mylonaki *et al*., 2008, Rada *et al*., 2007). The olive tree leaves, however, contain high concentrations of OL which is said to exhibit many biological activities (Dekanski *et al*., 2011, El Sedef and Karakaya, 2009). Extracts from the olive tree leaves have been shown to have to exhibit superior antioxidant activity as compared to vitamin E or the common food antioxidant additive butylated hydroxytoluene (BHT) (Mylonaki *et al*., 2008).

OL is the main polyphenol glycoside in the olive plant. All bioactive components in the olive are said to originate from OL (Hashmi *et al*., 2015).OL has thus become renowned as a substance with high pharmacological potency due to the many bioactivities of the compound (Mylonaki *et al*., 2008).
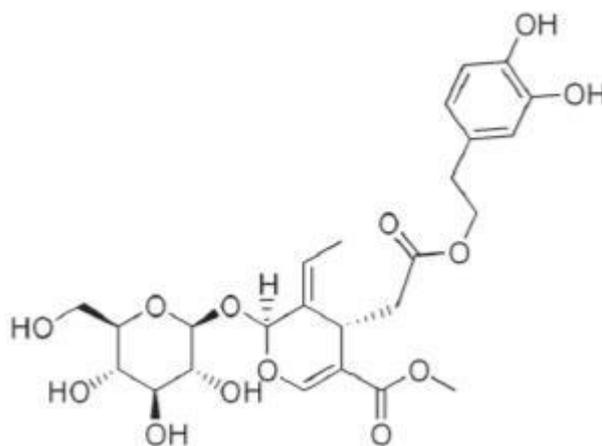
Figure 2.2: Chemical structure of OL (Choi *et al*., 2015)

OL has many beneficial biochemical properties. It was shown that OL is a good radical scavenger (Tuck and Hayball, 2002). Other benefits include anti-inflammatory properties, anti-thrombotic activities, prevention of platelet aggregation etc. (Carluccio *et al*., 2003, Petroni *et al*., 1995, Mourtzinos *et al*., 2007). OL has also been shown to have protective effects against the oxidation of low-density lipoprotein (LDL). This means that it could protect against the development of atherosclerosis (Coni *et al*., 2000, Visioli and Galli, 1994, Wiseman *et al*., 1996). In an isolated perfused heart model, OL was able to protect against I/R injury (Manna *et al*., 2004).

2.2.2 *Olea europaea* subspecies *africana*
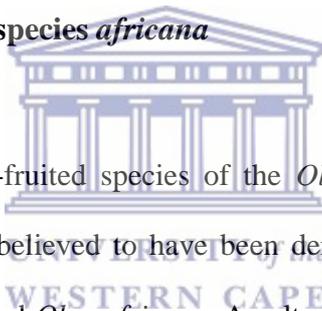
Olea africana is a small-fruited species of the *Oleaceae* family. The commercial olive, *Olea europaea*, is believed to have been derived from it. The African Wild olive, was previously named *Olea africana*. An alternative name for *Olea africana* is, *Olea europaea* subsp. *cuspidata*. The African wild olive has been popularly used in South Africa by Sotho, Xhosa, and Zulu tribes. The plant is found widespread throughout Southern Africa, East Africa and into Erithrea (Somova *et al*., 2003). In traditional medicine, the plants are used as a diuretic, hypotensive agent, an emollient, febrifuge and tonic (Hutchings *et al*., 1996). The plant has also been used for headaches, urinary tract- and bladder infections (Hutchings *et al*., 1996).

When comparing the bark of OA to the bark of *Olea europaea* subsp *europaea*, Tsukamoto *et al* (1984) found no differences in the concentration of ligans, coumarinds or secoirioids (Tsukamoto *et al*., 1984a, Tsukamoto *et al*., 1984b).

The biological effects of any compound are related to the concentration and time of drug exposure at the target tissue site. Therefore, it is critical to understand the bioavailability of compounds in the body. Bioavailability can be influenced by factors such as administration route, genetic phenotype, age, gender, food interactions with the drug etc. (Koch-Weser, 1974).

An olive leaf extract (OLE) is traditionally ingested orally. After ingestion, it is important that the stability, bioactivity, and bioavailability of polyphenols are preserved for it to be effective (Kumari *et al*., 2012).

Polyphenols ingested orally have huge challenges. The gastric residence time, low permeability of the compounds, solubility in the gut are all trials that bioactive compounds need to overcome. The other trials are the instability of the compounds in the gastrointestinal (GIT) include the pH, enzymes and the presence of other nutrients (Kumari *et al*., 2012).
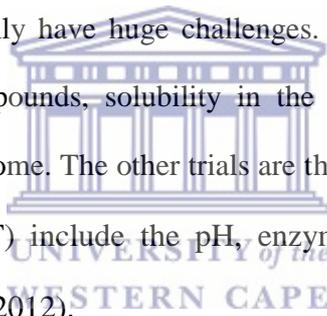
There are many studies on the bioavailability and metabolism of OL. The results of these studies are however conflicting. Del Boccio *et al* (2003) reported that OL is rapidly absorbed following oral administration and reaches a maximum plasma concentration after 2 hours (Del Boccio *et al*., 2003). Edgecombe *et al*., (2000), using an *in situ* intestinal perfusion model, found that OL was poorly absorbed in the intestine (Edgecombe *et al*., 2000). Garcia-Villalba *et al*. (2014) reported that OL has a high stability in gastric - and duodenal fluid. However, the uptake was poor in the perfused intestine model. This would indicate that OL is poorly absorbed which was also shown in the studies above. Also, other studies show that OL is hydrolyzed to HT and elenolic acid in the upper gastrointestinal tract (García-Villalba *et al*., 2014), meaning that it might not have a high stability in the gastric - and duodenal fluid. The oral route remains the route of preference for the drug. Many of the limitations experienced with using conventional 'free drugs' can be overcome with the use of drug delivery systems (DDS) (Allen and Cullis, 2004). Drug delivery systems have become very important to medicine and healthcare in recent years.

Drug delivery is an important component of drug development. Drug delivery systems are designed to enhance the stability, absorption and therapeutic concentration of the drug within the targeted tissue. Drug loading onto nanoparticles allows for improved tissue distribution for therapy. It can also improve drug efficiency (Parveen *et al*., 2012). The employment of nanoparticles in drug delivery systems has become very popular (De Jong and Borm, 2008).

2.3 Nanotechnology

Nanotechnology involves the science and engineering in the design, synthesis, characterization, and applications of nanoparticles. Nanoparticles can be defined as materials having at least one dimension in the nanometer (nm) (1×10^{-9}) range or colloidal particles that fall between 1-1000 nm (Sahoo *et al*., 2007, Silva, 2004, Wagner *et al*., 2014). A nanometer is equivalent to the width of 6 carbon atoms or ten water molecules (Sahoo *et al*., 2007, Silva, 2004). Biological units such as deoxyribonucleic acid (DNA), proteins or cell membranes fall within this dimension. Nanodevices or particles are 100 and up to 3000 times smaller than human cells (Logothetidis, 2006). Reducing the size of macromaterials to micro- and nano-sized materials increases the surface area of the particles. The increase in surface area results in an increase in reactivity (Tsai *et al*., 2012). Cells are thus able to capture nanoparticles more efficiently than larger structures, making nanoparticles useful tools for the transport and release of drugs (Pal'tsev *et al*., 2009).

Pathophysiological conditions result in many functional and anatomical changes in the body, causing distinct differences between the healthy and the diseased state of the body. These dissimilarities can be exploited for site-specific targeting of Nanoparticles (Sahoo *et al*., 2007).

Nanoparticles can penetrate deep into tissues by penetrating fine capillaries. Nanoparticles are also able to cross the fenestrations found by epithelial cells in the liver. Nanoparticles are also efficiently taken up by cells. Together this makes it possible for therapeutics to be more effectively delivered (Prokop and Davidson, 2008).

In the CaCo2 (a model of the intestinal epithelial barrier) cell line, 100 nm particle uptake was 2.5 times more than the uptake of 1 µm particle uptake and 6 times more than that of 10 µm particles. Furthermore, when tested on an intestinal loop, the uptake of 100 nm particles were 15 and 250 fold greater compared to the 1- and 10 µm particles respectively (Singh and Lillard, 2009).
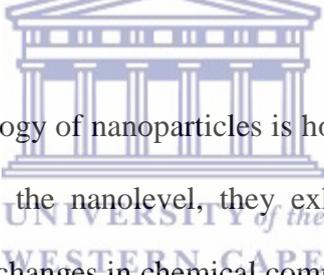
Knowledge of the toxicology of nanoparticles is however still lacking. When bulk materials are reduced to the nanolevel, they exhibit very different properties. These properties include changes in chemical composition and size. The former is the main contributor to toxic properties and the latter is the dominant indicator of toxic effects of Nanoparticles (Logothetidis, 2006).

Biodegradable (natural or synthetic polymers and lipids) and metallic Nanoparticles are the most popular nanocarriers. Biodegradable nanoparticles are preferred as nanocarriers because they tend to be non-toxic and non-immunogenic (Pal'tsev et al., 2009).

2.4 Liposomes

Liposomes are considered as one of the most successful drug carriers known to date (Bozzuto and Molinari, 2015). Liposomes used as a drug delivery system are extensively studied and used in clinical trials and were the first system approved for clinical purposes (Bozzuto and Molinari, 2015). The use of liposomes as DDS for medical applications dates back to 1965 when lipid vesicles were the first controlled release polymer systems of macromolecules (Farokhzad and Langer, 2006). In 1995 the Food and drug administration (FDA) approved Doxil, doxorubicin (dox) encapsulated liposomes for the treatment of acquired immunodeficiency syndrome (AIDS) associated Kaposi's sarcoma. Since then, numerous other liposomal formulations have been approved (Table 2.1) (Farokhzad and Langer, 2006).
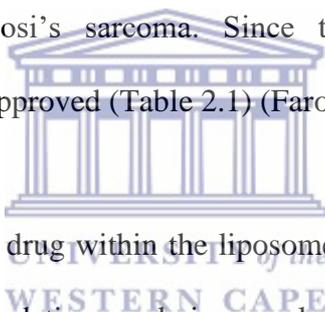
The encapsulation of the drug within the liposome affords protection of the drug against enzymatic degradation and immunological or chemical activation. Liposomes, therefore, protect the drug from being metabolized and simultaneously reduce the exposure of the drug to healthy tissue during circulation in the blood, thereby limiting undesired effects which the free drug may have (Bozzuto and Molinari, 2015). Furthermore, liposomes are non-toxic, biodegradable and non-immunogenic (Akbarzadeh *et al*., 2013), thereby increasing its biocompatibility and making them suitable for any route of administration without any adverse effects. Liposomes are therefore very popular nanoparticles used as drug carriers (Asili *et al*., 2011, Cabral *et al*., 2004).

Table 2.1: Different liposomal approved drugs (Zhang *et al*., 2013)

Liposomal product name	Technology	Treatment
Doxil	Pegylated liposomal doxorubicin	A variety of cancers
Daunoxome	Liposomal Daunorubicin	Advanced HIV- associated Kaposi's sarcoma
Ambisome	Liposomal amphotericin B	Fungal infections
Depocyt	Liposomal cytarabine	Lymphomatous meningitis
Visudyne	Liposomal verteporfin	Age-related macular degeneration
Depodur	Liposomal morphine sulfate	Postoperative pain

2.4.1 Liposome structure

When there is interaction with water, polar lipids would self-assemble and form self-organized colloidal particles. Hydrophilic compounds orientate towards the water. Hydrophobic compounds would orientate away from the water. The positioning of polar lipids would form a bilayer. Consequently, water-soluble compounds are trapped in the center and lipid-soluble compounds are incorporated

in the lipid compartment (Barenholz, 2003, Nii and Ishii, 2005, Ohnishi et al., 2013, Saraf, 2010a). Figure 2.3 shows the packing of phospholipids in lipid bilayer structures, illustrating a liposome structure on the left. The hydrophobic tails (yellow) and the hydrophilic heads surrounding the aqueous core and faces outward.
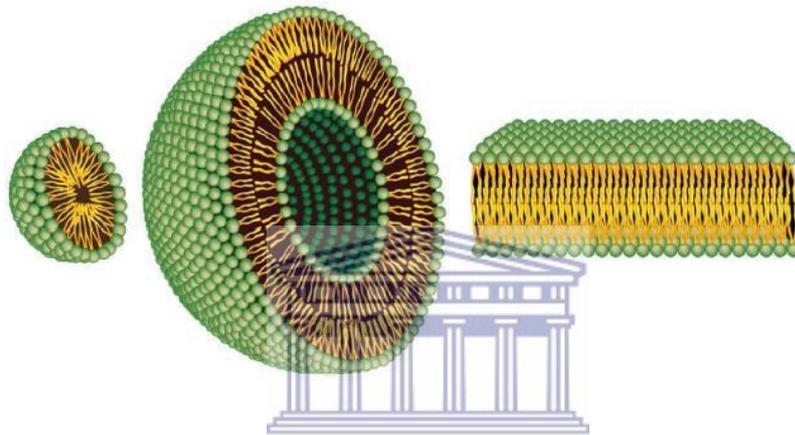
Figure 2.3: Lipid bilayer structures (Bozzuto and Molinari, 2015).

The liposome can vary from small (0.020 μm) to large (>0.5 μm) in size and can vary in the number of bilayers. The vesicle size can be used to determine the circulation half-life of liposomes, and both size and number of bilayers affect the amount of drug encapsulated in liposomes.
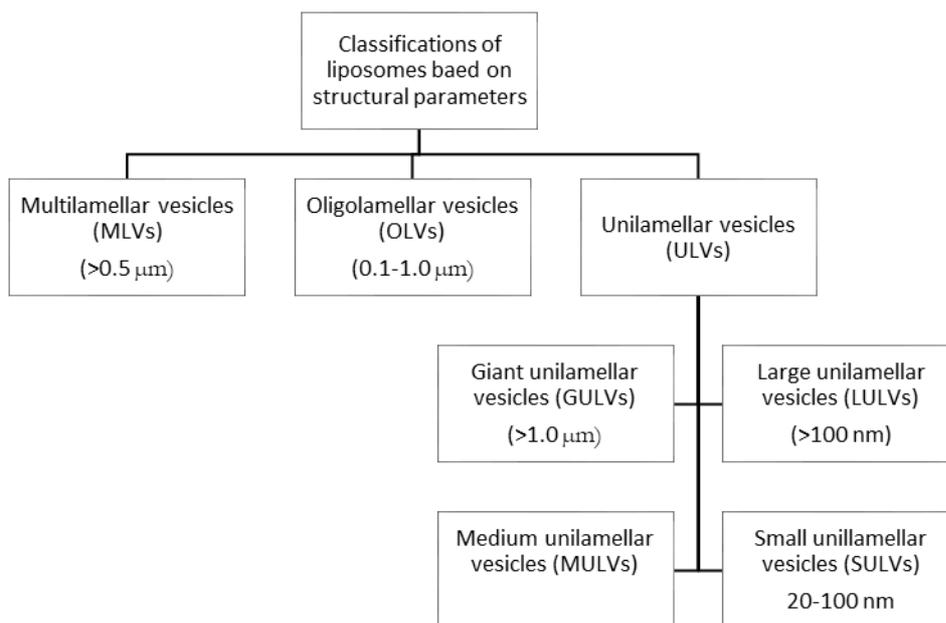
Figure 2.4: The classification of liposomes based on structural parameters (Rani, 2013).
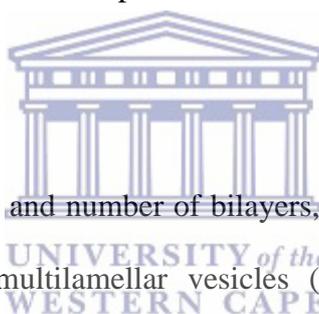
On the basis of their size and number of bilayers, the liposomes can be classified into 3 categories, i.e. multilamellar vesicles (MLVs), oligolamellar vesicles (OLVs) and unilamellar vesicles (ULVs). The ULVs can be further classified into giant unilamellar vesicles (GULVs), large unilamellar vesicles (LULVs) and small unilamellar vesicles (SULVs). The MLVs and OLVs have an onion structure, consisting of many lipid bilayers. In unilamellar liposomes, the vesicles have a single phospholipid bilayer sphere that encloses an aqueous core (Akbarzadeh *et al*., 2013, Sachse *et al*., 1993, Schneider *et al*., 1995). To ensure liposomes have the desired size, lamellarity and homogeneity properties postformation processing of the vesicles are required. Multilamellar liposome vesicles consist of many lipid bilayers and their size may increase into the millimetre range.

The spaces between the bilayers are determined by Van Der Waals forces which causes attraction. Furthermore, there are repulsion forces such as the electrostatic and hydration forces between adjacent lamellae. For the delivery of drugs, SULVs are desired in most cases. (Pagano and Weinstein, 1978).

The small radius of curvature in the small unilamellar vesicles (SUVs) imposes strains on the packing of the lipids. Thus, SULVs demonstrate different physic-chemical characteristics compared to MLV and larger ULVs (Pagano and Weinstein, 1978).

Particle size can be engineered to precise dimension and high monodispersity. Size plays an important role in the particle half-life, extravasation through leaky vasculature and macrophage uptake *in vivo*. Nanoparticles with a diameter of less than 5 nm, undergo renal clearance upon intravenous administration. The non-continuous endothelia with vascular fenestrations that measure 50 - 100 nm are present in the liver, leading to the nonspecific accumulation of larger particles. Retention of particles of >200 nm accounts for splenic filtration, due to 200 - 50 nm inter-endothelial cell slits in the spleen. Particles that have size ranges of 2 - 5 μm accumulate within capillaries of the lungs. There are resident macrophages in the liver, spleen, and lungs that contribute to substantial particle uptake. Taken together, nanoparticles with an average diameter of approximately 100 nm generally have been proven to be longer lasting in the circulation and can selectively prolong circulation lifetimes and subsequently enhance accumulation at specific sites of interest (Blanco *et al*., 2015).

ULVs and MLVs have different release kinetics. ULVS of sizes about 130 nm in hydrodynamic size has a faster release rate than the MLVs. The release rate is due to the number of bilayers the drug needs to cross. Size is a very important property in the function of liposomes. Experimenting with liposomal size, it was found that liposomes with smaller sizes (<100 nm), interacted less with plasma proteins. Smaller particles subsequently evaded the reticuloendothelial system, while larger particles could not escape RES uptake. Smaller particles did, however, have a poor drug uptake (Bozzuto and Molinari, 2015).

Liposomes can be positively, negatively or neutrally charged (Akbarzadeh *et al*., 2013, Sachse *et al*., 1993, Schneider *et al*., 1995). Surface charge is another feature that can be tailored to prolong circulation times. Nanoparticles that have a neutral or negative surface have been shown to reduce the adsorption of serum proteins, thus resulting in longer half-lives in circulation. Furthermore, it has been shown that neutral nanoparticles (1.3 mV) and negatively charged particles (-10.6 mV) resulted in the lower accumulation in the liver and spleen. The liver and spleen are filter organs and remove nanoparticles from the circulation. The surface charge of liposomes will also affect cellular uptake, as the plasma membrane is negatively charged (Arvizo *et al*., 2010). Positively charged nanoparticles, thus have a high rate of nonspecific uptake in the majority of cells. Negatively charged nanoparticles are therefore best for intravenous administration as they last longer in the circulation (Blanco *et al*., 2015).

Stability of nanoparticles is critical to ensure the safety and efficacy of drug products. When injected intravenously, unstable nanosuspensions can form aggregates. These aggregations form larger particles which can block of capillaries or cause emboli. Thus, drug particle size and size distribution need to be monitored during storage (Wu *et al*., 2011).

Particles in suspension can either settle down or cream up. This depends on the particle density compared to that of the solution. The sedimentation rate is described by Stoke's law, a mathematical equation which "describes" the relationship between of size, medium viscosity and the density difference between the particles and the medium. The decrease of particle size is the most common method of avoiding sedimentation (Wu *et al*., 2011). Nanoparticles have a large surface area. This results in the nanoparticles having a high surface energy. Accordingly, this makes nanoparticles thermodynamically unfavourable, causing it to then agglomerate to minimize the surface energy. The sedimentation rate of the particles increases as they grow larger in size. A common way to stabilize colloidal suspensions is electrostatic repulsion (Wu *et al*., 2011).

The zeta electric potential is the electric potential at the shear plane, which is the boundary of the surrounding liquid layer attached to the moving particles in the medium. The zeta potential is the key parameter used to predict the suspension stability. The higher the zeta potential, the more stable a suspension is. The size and size distribution of nanoparticles are important parameters to evaluate the physical stability of nanoparticles. Techniques such as photon correlation spectroscopy or dynamic light scattering are commonly used for particle size and size distribution (Wu *et al*., 2011).

The size distribution is the polydispersity index (PDI) of the suspension. The PDI values of 0.1 to 0.25 would indicate a narrow size distribution. A PDI of greater than 0.5 indicates a broad distribution. In general, a zeta potential of above 60 mV yields excellent stability. Whereas, a zeta potential of 30mV, 20mV have short-term stability. A charge of less than 5 mV has fast particle aggregation (Wu *et al*., 2011).

2.4.2 Liposome formation

Natural or synthetic lipids can be used for the formation of liposomes. There can also be the addition of cholesterol. The lipid most often used is phosphatidylcholine (lecithin). Many phospholipids can, however, be used (Table 3) to confer the desired charge (Pagano and Weinstein, 1978). All liposomes must be prepared above the lipid phase transition temperature (Pagano and Weinstein, 1978), the temperature at which the lipids move from a gel-like state to a more fluid state. At a temperature below the phase-transition temperature, the lipids are in a rigid state. When liposomes are prepared at a temperature above the lipid-phase transition temperature, the bilayer is less rigid and it allows for fluidity, which makes liposome formation easier (Figure 2.5).
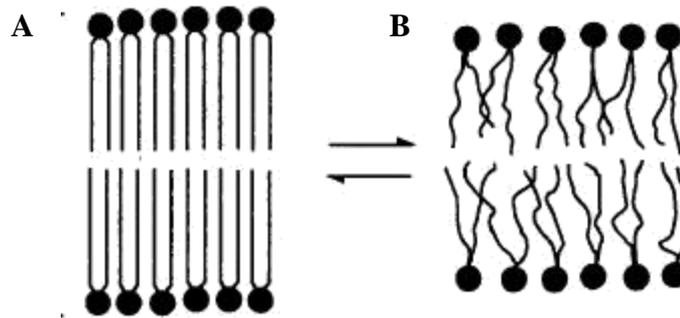
Figure 2.5: The effect of phase transition temperature on lipid structure. The gel state of phospholipids below the phase transition temperature (A) and the liquid crystalline state of phospholipids at a temperature above the phase transition temperature (B), modified image from Eze (1991).

Cholesterol is a major component of the mammalian cell plasma membrane. It plays a role in cell functioning through the regulation of membrane fluidity. (Pagano and Weinstein, 1978). The addition of cholesterol into the lipid bilayer decreases the permeability of the vesicle. Cholesterol is a hydrophobic molecule and would be incorporated into the core of the membranes as a stabilizer, which increases both the *in vitro* and *in vivo* stability. This is because the cholesterol allows for the close packing of the phospholipids. Cholesterol can also be used as an anchor for other molecules such as polyethylene glycol (PEG) and deoxyribonucleic acid (DNA) (Bozzuto and Molinari, 2015).

Table 2.2: Different lipids used in liposome formation, their charge and phase transition temperature (Pagano and Weinstein, 1978).

LIPID	ABBREVIATION	CHARGE	T_c (°C)
Egg phosphatidylcholine	Egg PC	0	-15 to -7
Dioleoyl phosphatidylcholine	DOPC	0	-22
Dilauryl phospahtidylcholine	DLPC	0	0
Dimyristoyl phosphatidylcholine	DMPC	0	23
Dipalmitoyl phosphatidylcholine	DPPC	0	41
Dilauryl phosphatidylcholine	DSPC	0	58
Diisostearoyl phosphatidylcholine	DIPC	0	
Bovine brain sphingomyelin	Brain SM	0	32
Egg phosphatidylethanolamine	Egg PE	0	0
Dimyristoyl phosphatidylethanolamine	DMPE	0	48
Dimyristoyl phosphatidylglycerol	DMPG	-	23
Dimyristoyl phosphatidic acid (PH 6)	DMPA	-	52

Bovine brain phosphatidylserine	Brain PS	-	5
Dicetyl phosphate	DCP	-	
Stearylamine	SA	+	

2.4.3 Proposed mechanism of liposome interaction with cells

Many *in vitro* and *in vivo* studies have demonstrated that the main mechanism of liposome uptake is simple absorption or endocytosis (Banerjee *et al*., 2004). Simple absorption involves the interaction of cell surface components by electrostatic forces or non-specific weak hydrophobic interactions. Binding to surface receptors may also occur (Figure 2.6A, Figure 2.6B and Figure 2.8). The fusion of the vesicle with the cell membrane, with the simultaneous release of the drug, is very rare. Interestingly, when multilamellar vesicles interact with the plasma membrane of cells, the outermost layer may fuse with the membrane releasing its content into the cytoplasm, whereas ULVs would release their content after fusion (Pagano and Weinstein, 1978) as shown in Figure 2.7.
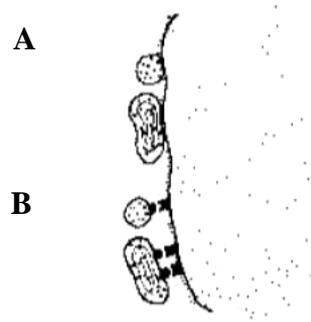
Figure 2.6: The simple absorption of liposomes to the cell membrane, either by non-specific adsorption (A) or interaction with receptors (B), modified from Pagano and Weinstein (1978).

Figure 2.7: The fusion of ULVs (A) and MLVs (B) modified from Pagano and Weinstein (1978).
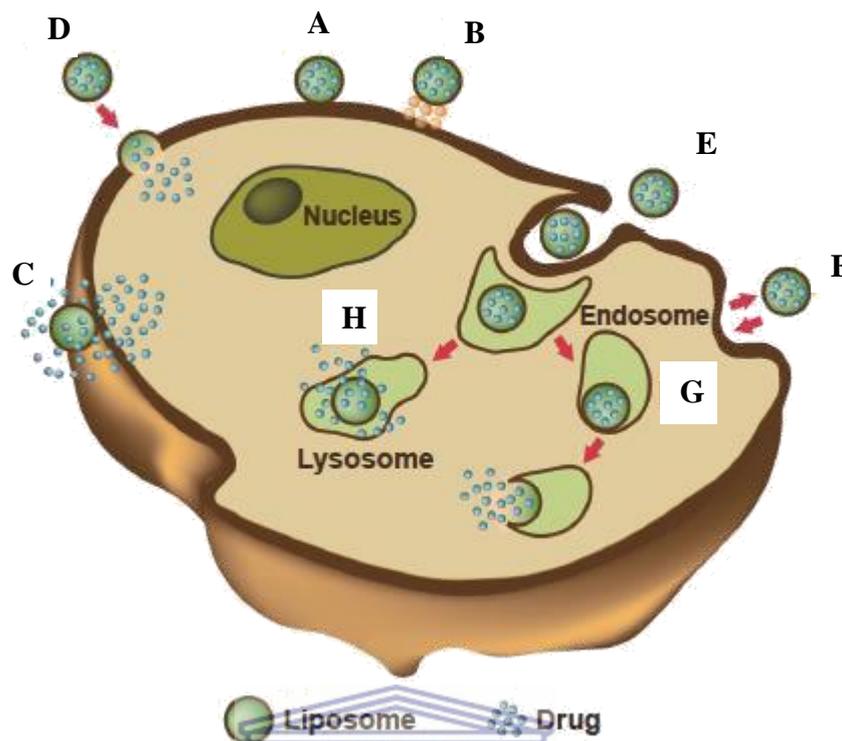
Figure 2.8: The different ways of nanoparticle uptake by the cell (Bozzuto and Molinari, 2015).

Liposomes containing drug can interact by binding to the plasma membrane surface through electrostatic interactions (A) or by means of receptors (B). The delivery of the drug into the cytoplasm of the cell can occur through different modes. When interacting with the cell, the structure of the liposome can be affected and the cargo released (C) or the nanocarriers can fuse with the plasma membrane and discharge drugs into the cell (D). The exchange of carrier-lipid components with the cellular membrane can also occur. Another possible mechanism of liposome transportation is the exchange of liposome and bilayer components. Cholesterol and membrane-bound molecules are all components that can be exchanged (E). Liposomes can be internalized by endocytosis (F) and after that has different fates depending on their physicochemical characteristics. In one scenario, liposomes can release their drugs after fusion or destabilization of the endocytic vesicle (G) or endosomes can fuse with lysosomes (H) and the drug gets released (Bozzuto and Molinari, 2015).

The various pathways of liposome uptake are not necessarily mutually exclusive and

a combination of uptake is possible.

2.5 NANOTECHNOLOGY FOR PLANT EXTRACTS

Worldwide today, there is a demand for natural products, organic living and healthy lifestyles (Pinsuwan *et al*., 2010). Extracts of *Roselle calyses* possess antioxidant activity used in cosmetic products. The *Roselle* extract, however, has low skin permeation and causes dermal irritation. These problems were overcome when the extract was encapsulated in liposomes (Pinsuwan *et al*., 2010). Encapsulating an *Aloe vera* leaf gel in liposomes was also able to enhance the activity of the plant formulation (Takahashi *et al*., 2009). Tsai *et al* (2012) encapsulated a hydrophilic ginseng root extract and found that the antioxidant activity of the ginseng extract was improved (Tsai *et al*., 2012).

SA has a wide plant biodiversity and many of these plants are used for medicinal treatments. Furthermore, indigenous communities still use and have knowledge of plants used to treat various ailments (Richter, 2003). The renewed interest in traditional or natural pharmacopoeias has led to an increase in markets for herbal products, thus leading to economic possibilities and research and business interest. In SA more than 20000 tons of traditional plants are harvested, processed and sold annually (Taylor *et al*., 2001).

The OA plant is found in Africa and SA. The olives of the plant are not edible, but the leaves roots and stem barks possess medicinal properties, as they contain bioactive constituents. Most of the biologically active constituents of extracts, such as flavonoids, tannins, and trepenoids, are highly water-soluble, but demonstrate low absorption, as they are unable to cross lipid membranes. This results in loss of bioavailability and efficiency of the plant extracts (Bonifácio *et al*., 2014).

The strategy of applying nanotechnology to plant extracts has been cited widely in the literature. This is because nanostructured systems could potentiate the action of plant bioactive compounds (Bonifácio *et al*., 2014). Furthermore, it could promote a sustained release of active constituents, reduce the required dose and decrease the required dose (Bonifácio *et al*., 2014). The modernization of traditional plant extracts can thus offer better efficiency of the medicine. Also, encapsulating a South-African plant extract could help our country to keep pace with the current trend of scientific and technological advancement by the employment of nanotechnology. This advancement could help us promote traditional medicine and contribute to the economy of the country.

CHAPTER 3: MATERIALS AND METHODS

3.1 Materials

All consumable plasticware was purchased from Whitehead Scientific (Pty) Ltd.

Table 3.1: List of biological materials used in this study and the source from which it was obtained.

BIOLOGICAL MATERIAL	SOURCE
H9c2 cells	Medical Research Council of South Africa
Olea africana (OA)	See section 3.2.1
Olea exasperata (OE)	See section 3.2.2

Table 3.2: List of chemical reagents used in the study and the manufacturer of the reagents.

Reagents	Manufacturer
Acetonitrile	Sigma-Aldrich, USA
Chloroform	Sigma-Aldrich, USA
Cholesterol (sheep wool)	Sigma-Aldrich, Japan
Dimethyl sulfoxide (DMSO)	Sigma-Aldrich, France
Dulbecco's Modified Eagles Medium (DMEM)	Gibco® by Life technologies™
Ethanol	Kimix, South Africa
Extracellular matrix	Sigma-Aldrich
Foetal bovine serum (FBS)	Gibco® by Life technologies™
HiPerSolv CHROMANORM (HPLC-grade water)	Kimix, France
JC-1 reagent	Sigma-Aldrich, USA
Methanol	Sigma-Aldrich, France
MTT- reagent	Sigma-Aldrich, USA
Oleuropein	Sigma-Aldrich, China
Penicillin-streptomycin (PenStrep)	Lonza, BioWhittaker®, USA
Phosphate buffered saline (PBS)	Lonza, BioWhittaker®, Belgium
Phosphatidylcholine powder (egg yolk)	Sigma-Aldrich, USA
Rhodamine 123	Sigma-Aldrich, Germany
Trypsin	Lonza, BioWhittaker®, Belgium
ViaLight™ plus ATP kit	Lonza, Basel, Switzerland

3.2 Methods
3.2.1 Collection of plant material and preparation of the extracts
3.2.1.1 Collection of *Olea africana* and *Olea exasperata*

The leaves of *Olea europaea* subsp. *africana* (OA) was collected in 2012 on the grounds of the University of the Western Cape. OA leaves were authenticated by Mr. Franz Weitz from the Department of Biodiversity and Conservation Biology, UWC. The leaves were dried at room temperature, ground finely (Figure 3.1) and stored in a glass container, away from light, until use.

Figure 3.1: Finely ground leaves of OA.

The leaves of the *Olea exasperata* (OE) plant was collected in May 2014 in the Cape Nature Reserve at the University of the Western Cape. The plant was identified and authenticated by Mr. Franz Weitz from the Department of Biodiversity and Conservation Biology at the University.

The leaves were rinsed to remove any dust or other impurities and left to air-dry at room temperature in a dark room. After drying, the OE leaves (Figure 3.2) were ground finely (Figure 3.3) and stored away from light until use.

Figure 3.2: Young and mature OE leaves dried for extraction and mature. The leaves maintained a deep green colour.

Figure 3.3: Leaves of OE finely ground before extraction.

3.2.1.2 Preparation of aqueous plant extracts

6.25 grams of grounded leaves of OA or OE were dissolved in 125 millilitres (ml) of water and left overnight. The solutions were then filtered through a Whatman no. 4 filter, followed by another filtration using a Whatman no.1 filter. The extracts were freeze-dried to obtain a fine powder. The round bottom flask in which each extract was prepared was weighed before and after it contained the freeze-dried product, to determine the yield. The powdered product of OA and OE were found to be hygroscopic. The freeze-dried products were thus dissolved in HPLC-grade water, aliquoted at a known concentration, and stored at -20 °C away from light.

3.2.2 Quantification of OL using Ultra-High Performance Liquid Chromatography-Mass Spectrometry (UHPLC-MS) method

Principle

High-Performance Liquid chromatography (HPLC) is a technique used to separate and quantify dissolved molecules in a solution. Molecules can be separated based on differences in their composition and structure. The procedure involves a stationary phase and a mobile phase. The mobile phase flows over the stationary phase and carries the components or molecules of the sample mixture injected with it. The molecules in the sample will have different affinities and interactions with the stationary support. Components that interact strongly will move slower and those with weaker interactions move faster. This leads to molecules being separated (Kupiec, 2004). The composition and type of the mobile phase will affect the separation of components. In normal-phase HPLC the solvent is non-polar. The reverse-phase HPLC is used when the solvent is a polar organic solvent, normally with a mixture of water (Kupiec, 2004).
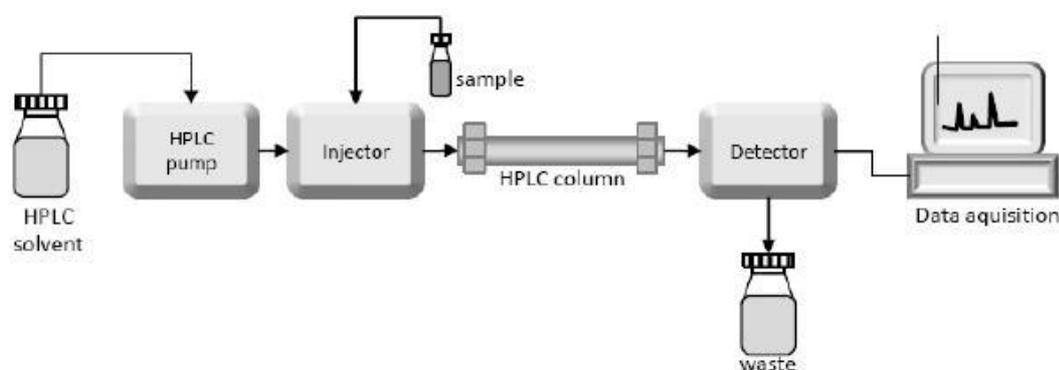

Figure 3.4: A schematic diagram of a HPLC equipment (Czaplicki, 2013).

The HPLC instrument consists of a mobile phase reservoir, which can be as simple as a glass bottle connected to a tube that contains the solvent. A pump is used to push the mobile phase through the packed stationary phase. An injection port allows for the sample to be injected into the system. The column represents the stationary phase where the molecules get separated. The HPLC detector, located at the end of the column, detects the analytes as they elute from the chromatographic column. The detector is the component that turns a physical or chemical attribute of an analyte into a measurable signal that corresponds to the identity or concentration of the analyte (Swartz, 2010). In our system, we used a mass spectrometer as a detector. The mass spectrometer signals were integrated by computer software. The software used is the Chromera version 3.4.4.5945 (Copyright 2006-2014 PerkinElmer, Inc.) and the SQ 300 MS Driver version 1.1.0.0193 (Copyright 2000-2011 PerkinElmer, Inc.). The chromatogram is then displayed on a computer screen and stored on the computer (Kupiec, 2004).
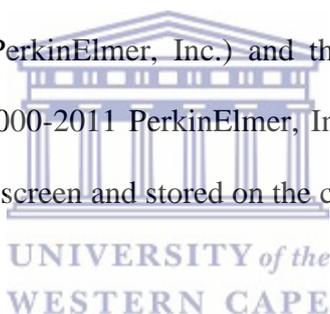
3.2.2.1 HPLC and MS methods

The specifications of the system used and UHPLC conditions were as follows:

An HPLC system (Perkin Elmer Flexar FX-15 UHPLC, USA) with an LC 275 Series Ultra High Res Binary Pump (FX15Pump-2), a Flexar Autosampler (FXASCO-1), Flexar Column Oven (FXOven-3) and Photo Diode Array Detector (PDADet-4) was used. The reverse-phase column used was a Kinetex® 2.6 μm EVO C_{18} 100Å, with a size of 100×2.1 mm. The HPLC system was equipped with a Liquid Chromatography-Mass Spectrometer. The injection volume was set to 1.4

microliters (µl). The mobile phase of acetonitrile and water containing 0.1% acetic acid was used in a ratio of 80:20 volume/volume (v/v). Isocratic elution was at a flow rate of 0.4 ml/minute and detection was performed at 240 nanometres (nm). Reverse-phase high-performance liquid chromatography (HPLC) coupled to mass spectrometry (MS) enables the accurate detection of phenols in plant extracts (Peragón *et al*., 2015). For the detection of OL, Mass spectra were scanned over the range m/z 500-600. The software used was the Chromera version 3.4.4.5945 (Copyright 2006-2014 PerkinElmer, Inc.) and the SQ 300 MS Driver version 1.1.0.0193 (Copyright 2000-2011 PerkinElmer, Inc.).

3.2.2.2 Validation of the HPLC method
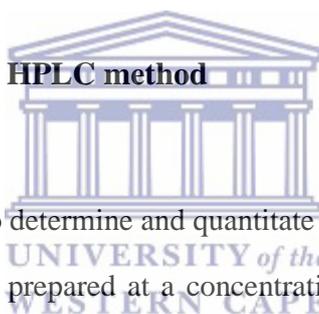
The HPLC method used to determine and quantitate OL was validated in this study. A stock solution of OL was prepared at a concentration of 1000 ppm in HPLC-grade water. Thirteen solutions of OL (1 ppm, 2 ppm, 3 ppm, 4 ppm, 5 ppm, 15 ppm, 25 ppm, 50 ppm, 100 ppm, 150 ppm, 200 ppm, 250 ppm and 300 ppm) were prepared from the stock solution, with HPLC-grade water as a diluent. All thirteen solutions were used to determine the linearity and range of the method. Concentrations of 2 ppm, 50 ppm, and 300ppm were used for the accuracy of the study. Three concentrations, 5 ppm, 50 ppm and 300 ppm, were used to study the precision of the method. The limit of detection (LOD) and limit of quantitation (LOQ) was also determined. The LOD was selected as the concentration that gives a signal-to-noise (S/N) ratio between 3 and 10. The LOQ was the concentration that had an S/N ratio of 10 and 20 (Al-Rimawi, 2014). The accuracy was determined by the ratio of the measured value over the expected value for concentration 2 ppm, 50 ppm, and 300 ppm.

3.2.3 Production and storage of liposomes

Principle

Liposomes were prepared using the lipid film hydration technique. The lipid film hydration, or Bangham method is the most popular method used to produce liposomes. Lipids are dissolved in an organic solvent which is evaporated, leaving a thin lipid film. The film is then hydrated by the addition of an aqueous medium, resulting in the formation of liposomes. Hydrophobic drugs can be added during the organic solvent phase. Hydrophilic drugs can be added during the aqueous phase (Bozzuto and Molinari, 2015). The size and size distribution/polydispersity index (PDI) of nanoparticles are important parameters to evaluate the physical stability of nanoparticles (Wu *et al*., 2011). For this study, vesicles of approximately 100 nm were desired, as this is often assumed to be the ideal size of a drug delivery system (Lammers, 2013).
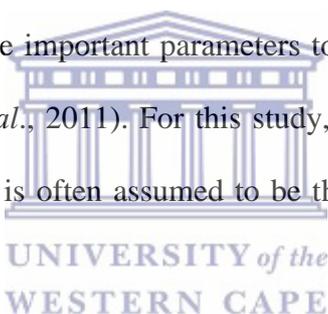
The zeta potential is the key parameter used to predict the suspension stability. The higher the zeta potential the more stable the suspension is. Liposomes include components, such as cholesterol, that can confer a charge. Any lack of surface charge will cause liposomes to aggregate. Positively or negatively charged liposomes are more stable as they have electrostatic repulsion, with the result that liposomes do not aggregate or flocculate (Bozzuto and Molinari, 2015).

3.2.3.1 Formation of liposomes

Liposomes were prepared in a round bottom flask at a concentration of 10 mg/ml. Phosphatidylcholine and cholesterol (7:3 w/w) were dissolved in chloroform. The solvent was removed by rotary evaporation above the lipid phase transition temperature (25 °C). This resulted in the deposition of a thin film on the walls of the round bottom flask. The dry lipid film was hydrated with plain HPLC-grade water or HPLC-grade water containing OA or OL (drugs were added during the aqueous phase). Liposomes formed were then incubated in a shaking water bath at a temperature above the lipid-phase transition temperature (25 °C). The extract of OE was not encapsulated in liposomes for reasons explained in the results.
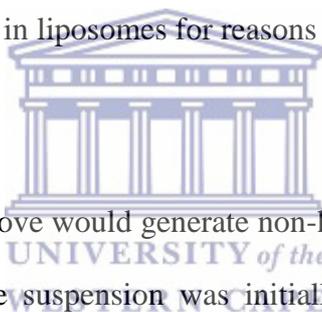
The method described above would generate non-homogenous large multilamellar liposomes. The liposome suspension was initially extruded through a 200 nm polycarbonate filter membrane to reduce the liposome vesicle diameter. The liposome suspension was then passed through a 100 nm polycarbonate filter membrane, to form 100 nm vesicles. Extrusion took place at a temperature above the lipid-phase transition temperature (25 °C) using a mini-extruder (Avanti Polar Lipids Inc.), shown in Figure 3.5. A total of 25 passages were used for one extrusion protocol.

The size, PDI and zeta potential were determined using the Malvern Zetasizer NanoZs (Malvern instruments, Ltd., UK). For size and PDI determination, 1 ml of the liposomal suspension was added to a disposable capillary cell and 800 µl of the

liposomal suspension was added to a capillary cell containing gold electrodes for zeta potential determination.

Liposomes were centrifuged at 14000 rpm for 30 min at 4 °C. The liposome pellet was washed with HPLC-grade water and centrifuged again. This was repeated three times to purify liposomes before use.
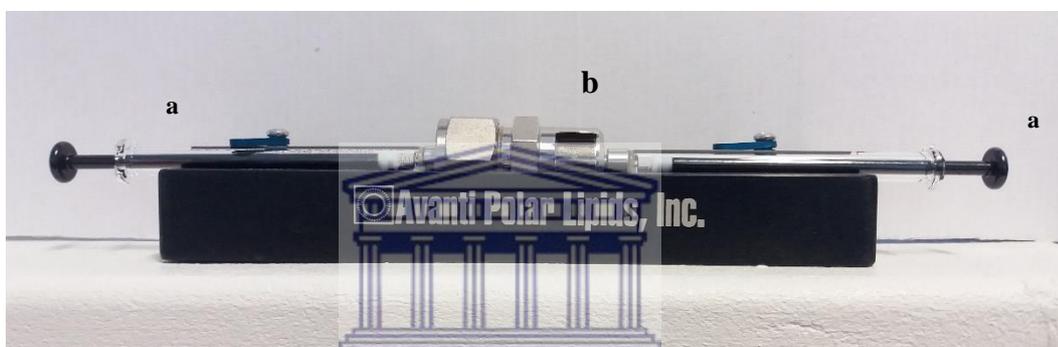
Figure 3.5: Extruder showing (a) Hamilton syringes and (b) compartment that contains a filter.

3.2.4 Encapsulation Efficiency of liposomes

Liposomes were encapsulated with 1mg/ml of OL. The liposomes were then extruded and purified using methods described above. Liposomes were disrupted using an organic solvent consisting of ethanol-methanol (75:25 v/v) in a 1:3 ratio. Thereafter, the suspension was added to 1 ml Phree^{TM} Phospholipid removal tubes and the resulting supernatant was injected into the HPLC-MS system for analysis.

The encapsulation efficiency was calculated using the formula below:

$$\%EE = \frac{amount\ of\ drug\ after\ encapsulation}{amount\ of\ drug\ initially\ used\ for\ encapsulation} \times 100$$

The data used to calculate the encapsulation efficiency is shown in the appendix (Table A1).

3.2.5 Incorporation of rhodamine 123 into liposomes

Rhodamine 123 (a hydrophobic fluorophore) was added during the lipid-phase of liposome formation at a concentration of 5 µg/ml dissolved in methanol. Thereafter, the organic solvent was removed, resulting in lipid deposition on the round bottom flask. The lipid film was hydrated with distilled water for vesicle formation. Liposomes were extruded and purified as previously described in section 3.2.5.3. The liposomes containing rhodamine (rh-liposomes) was used in the cell culture experiments and confocal microscopy experiments described later.

3.2.6 Cell culture experiments

### 3.2.6.1 Maintenance of H9c2 cells

H9c2 cells were cultured in complete Dulbecco's Modified Eagle's Medium (DMEM), supplemented with 10% Foetal Bovine Serum (FBS) and antibiotics (1% Penicillin-Streptomycin). The cells were maintained at 37 °C and at a 5% CO_2 humidified atmosphere. The media in the flask was changed every 2 days. The H9c2 cells were split when they reached 70 - 80% confluency.

3.2.6.2 Counting of H9c2 cells

When H9c2 cells reached 80% confluency, they were trypsinized and used in experiments. Detached cells were washed after trypsinization with medium (to neutralize the trypsin) and centrifuged at 1500 rpm for 3 min. After centrifugation, the supernatant containing trypsin was removed and the pellet containing cells were re-suspended in a known volume of complete DMEM. Equal parts of the cell culture and trypan blue (0.40%) were mixed and 10 µl was added to a counting chamber. Cell counts were done using a $TC20^{TM}$ automated cell counter (BIO-RAD).

3.2.7 Treatment of H9c2 cells
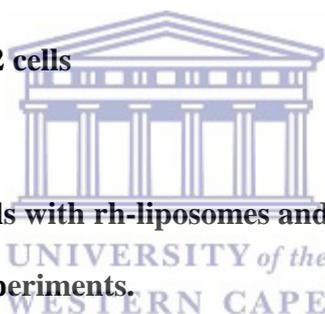
3.2.7.1 Treatment of cells with rh-liposomes and subsequent fixation for confocal microscopy experiments.

Microscope glass coverslips (22 × 22 mm) were sterilized using 70% ethanol and is left to air-dry in a laminar flow hood. Extracellular matrix (ECM) at a concentration of 100 µg/ml was made up in cold HEPES buffered PBS (6 mM KCl, 1 mM Na2HPO4, 0.2 mM, NaH2PO4.H20, 1.4 mM MgSO4.7H20, 128 mM NaCl, 1.2 mM Ca^{2+}, 10 mM HEPES, pH 7.4). The coverslips were placed in 6-well tissue culture plates (Corning Inc.) and each coverslip was coated with 25 µl of ECM. After a 3 hour incubation at 37 °C, the coverslip was rinsed with HEPES buffered PBS and stored at 4°C until use.

Cells were seeded, as described previously, in 6-well plates containing the coverslips that were coated with extracellular matrix. The H9c2 cells were treated with 100 μg/ml of rh-liposomes for 1 hour or 24 hours. After the incubation period, the medium was removed and the monolayers were washed twice with PBS. The cells were treated with 3.7 - 4% formaldehyde diluted in PBS. Thereafter, the cells were incubated for 15 minutes at room temperature. Following the incubation period, the fixed cells were washed 3 times, with a 5-minute shake in between washes. The cells were stored under PBS until the following day when confocal microscopy images were taken.
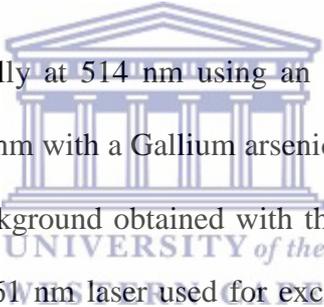
Cells were excited initially at 514 nm using an Argon laser and emission was detected from 531 – 703 nm with a Gallium arsenide phosphide (GaAsP) detector, but there was a high background obtained with these settings. The settings were changed and instead a 561 nm laser used for excitation was used with emission detected between 410-695 nm. A GaAsP detector was used to detect emission. Images were captured using the LSM780 with ELYRA PS1 platform, with software ZEN 2012 (Zeiss, Germany). The EC Plan-Neofluar 10x/0.30 objective was used for wide view images. Higher resolution images were taken with the Plan-Apochromat 63x/1.4 Oil DIC objective.

3.2.7.2 Treatment of H9c2 cells with OL and OA as free drugs and encapsulated in liposomes

Cells were seeded in 96-well plates at a density of $1x10^6$ cells/ml. When cells reached 80% confluence they were treated with serum-free medium for 24 hours to allow the synchronization of the cell cycle among the cells. Cells were then subjected to one of the protocols below. At the end of each experiment cell viability was assessed either by the MTT assay, JC-1 assay or the ATP assay.

Protocol 1:

H9c2 cells were exposed to different concentrations of H_2O_2 (100 μM, 300 μM, 350 μM, 400 μM, 450 μM, 500 μM and 550 μM) for 24 hours to determine a concentration that will reduce cells viability to approximately 50%. At the end of the experiments, cell viability was assessed using the MTT assay.

Protocol 2

Cells were treated with different concentrations of OA (1000 µg/ml, 100 µg/ml, 10 µg/ml, 1 µg/ml and 0.1 µg/ml) or OL (100 µg/ml, 10 µg/ml, 1 µg/ml, 0.1 µg/ml and 0.01 µg/ml) for 24 hours to test its toxicity. At the end of the experiments, cell viability and proliferation was assessed using the MTT assay.
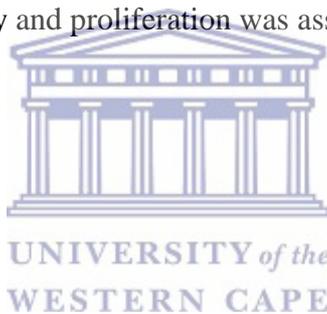
Protocol 3:
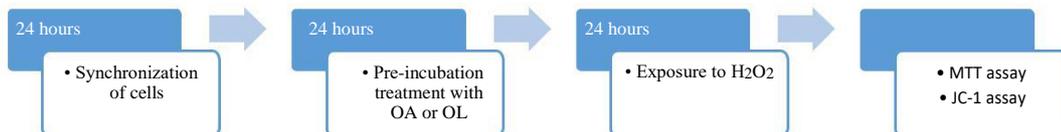
Cells were pretreated with different concentrations of OA (1000 µg/ml, 100 µg/ml, 10 µg/ml, 1 µg/ml and 0.1 µg/ml) or OL (100 µg/ml, 10 µg/ml, 1 µg/ml, 0.1 µg/ml, 0.01 µg/ml and 0.005 µg/ml) for 24 hours before exposure to H_2O_2 for a further 24 hours. At the end of the experiment, the cell viability was assessed using the MTT assay or the JC-1 assay.

Protocol 4:
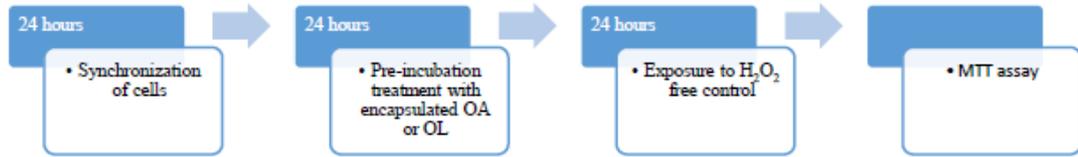
A selected concentration of OA (1000 µg/ml) and OL (0.01 µg/ml) was encapsulated in liposomes. Cells were treated with different liposome concentrations (1000 µg/ml 10 µg/ml 1 µg/ml and 0.1 µg/ml) for 24 hours to evaluate the toxicity of the liposomes and/or encapsulated drugs. At the end of the experiments, cell viability was assessed by the MTT assay
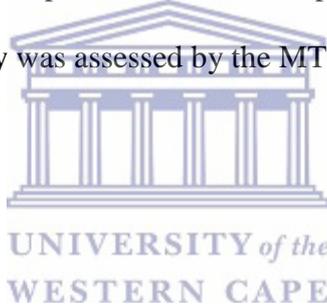
Protocol 5:
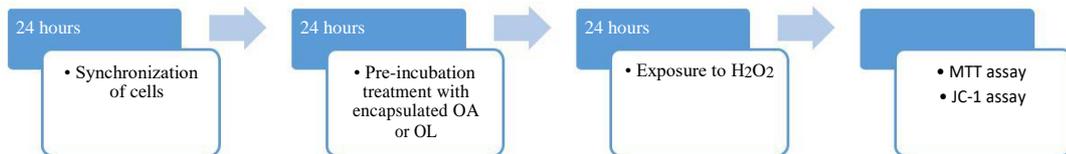
H9c2 cells were pretreated with encapsulated OA (1000 µg/ml) or OL (0.01 µg/ml) at different liposome concentrations (1000 µg/ml 10 µg/ml 1 µg/ml and 0.1 µg/ml) for 24 hours before exposure to H_2O_2 for 24 hours. At the end of the experiment cell viability was assessed using the MTT and JC-1 assay.

Protocol 6:

Cells were pretreated with different concentrations of OA (1000 µg/ml, 100 µg/ml, 10 µg/ml and 1 µg/ml) or OL (10 µg/ml, 1 µg/ml, 0.1 µg/ml, 0.01 µg/ml) for 24 hours before exposure to 5 µM doxorubicin for 24 hours. At the end of the experiments, cell viability was assessed by the ATP assay

Protocol 7
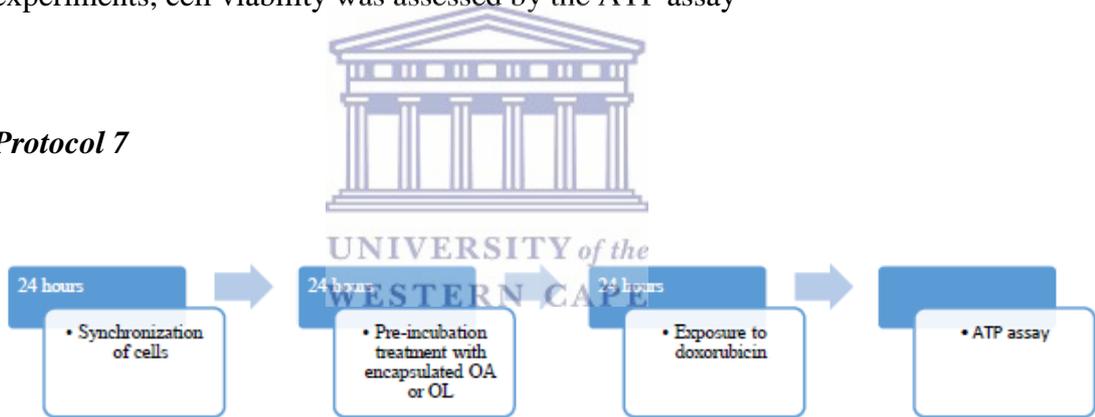
A selected concentration of OA (1000 µg/ml) and OL (0.01 µg/ml) was encapsulated in liposomes. Cells were treated with different liposome concentrations (1000 µg/ml 10 µg/ml 1 µg/ml and 0.1 µg/ml) for 24 hours before exposure to Doxorubicin. At the end of the experiments, cell viability was assessed by the ATP assay

3.2.8 Cell viability assays

3.2.8.1 The MTT assay

Principle

The 3-(4, 5-dimethylthiazol-2-yl)-2, 5-diphenyl tetrazolium bromide (MTT) test has been widely used for cell proliferation, cell viability or drug toxicity. The viability of cells is assessed using the principle of 3,4-dimethyltetrazolium salt (MTT) reduction to insoluble purple formazan product as an indication of viable cells (Maioli *et al*., 2009).

3.2.8.1.1 The MTT assay procedure

10 µl of the MTT reagent was added to a final concentration of 0.05 mg/ml per well. After a 4 hour incubation, the supernatant was carefully removed and the insoluble formazan crystal was dissolved in 100 µl dimethyl sulfoxide (DMSO) on a shaker for 15 minutes at room temperature. The absorbance was then read at 560 nm using a Glomax Multi Detection System plate reader (Promega Corporation, Madison, USA). The Optical Density (OD) readings were used to determine the percentage of viable cells according to the formula:

$$\% \text{ Cell Viability} = \frac{OD \text{ (treatment group)}}{OD \text{ (control)}} \times 100$$

3.2.8.2 Measurement of the mitochondrial membrane potential (MMP)

Principle

In normal cell function, the MMP is maintained as it is important for ATP production. The proton gradient is necessary for the conversion of ADP to ATP (Jia *et al*., 2014). The MMP may thus be used as an indicator for the energization state of the mitochondria. The MMP is highly negative (approximately -180 mV). The use of cationic lipophilic fluorescent indicators, such as the JC-1 dye, to measure the MMP is very common. The JC-1 dye accumulates in the mitochondrial matrix. JC-1 emits light at red or green wavelengths depending on its concentration. When in high concentrations in the in the mitochondrial matrix, the dye forms J - aggregates and emits red light. Low concentrations of the dye, results in the monomer forming and green light is emitted (Perry *et al*., 2011).
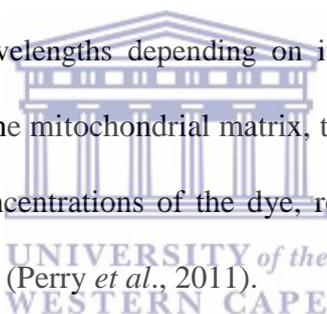
3.2.8.2.1 JC-1 Assay Procedure

The change in the MMP was assessed using 5, 5', 6, 6'- tetrachloro- 1, 1', 3, 3'- tetraethylimidacarbocyanine iodide (JC-1) fluorescent dye. At the end of the experiment, the cell culture medium was removed and cells were incubated in the dark with 100 µl of JC-1 (1 µg/ml) per well for 30min. Cells were washed twice with PBS, and read whilst being suspended in PBS. The fluorescent intensity of the JC-1 multimer was analyzed using a BioTekR FLX 800 plate reader [Excitation at 485 nm, emission at 530±25 nm (green) and 590±35 9 (red)].

3.2.8.3 The ATP assay

Principle

The maintenance of homeostasis in the cell depends on the maintenance of cellular ATP levels (Guimarães-Ferreira, 2014). Minutes after the loss of membrane integrity, the cells lose the ability to synthesize ATP. Any remaining ATP gets destroyed by endogenous ATPases. Thus, ATP is only present in metabolically active cells (Perry *et al*., 2011).

3.2.8.3.1 The ATP assay procedure

The detection of ATP was done using the ViaLight^{TM} plus ATP kit, following the manufacturer's instructions. Briefly, 50 µl of cell culture medium was removed from each well and cells were lysed by the addition of 50µl of the Vialight cell lysis reagent for 10 min. After incubation, 100 µl of the Vialight Plus assay reagent was added to each well. The luminescence was quantified using a BioTekR FLx800 plate reader and Gen 5$^{®}$ software (BioTek Instruments Inc., Winooski, VT, USA).

3.2.9 Statistical analysis

The results are expressed as the mean $\pm$ standard error of the mean (SEM) of three independent experiments. The Kruskal Wallis test and Dunnet's post-hoc test were

used to determine the differences among the means using GraphPad Prism 5. A value of $p < 0.05$ was considered to be statistically significant.

CHAPTER 4: RESULTS

4.1 The HPLC-MS analysis of Oleuropein (OL)

The HPLC chromatogram and mass spectra for OL are shown in Figure 4.1 and Figure 4.2 respectively.
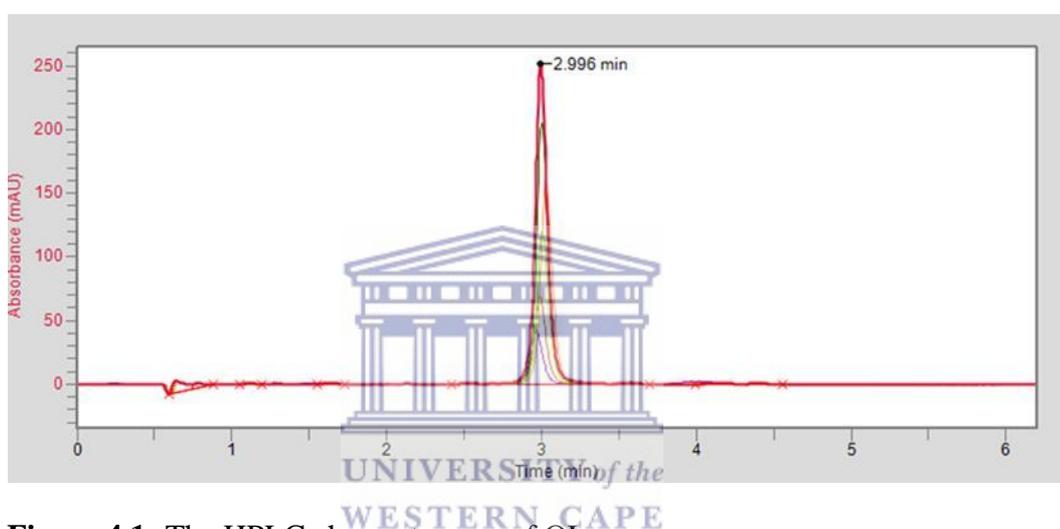
Figure 4.1: The HPLC chromatogram of OL.

Using the isocratic elution method, the HPLC chromatogram shows that the OL standard shows a peak at 2,996 minutes (Figure 4.1). Mass spectra data are represented by a peak with a specific mass-to-charge ratio (m/z) and shows OL has a peak at 538.06 m/z (Figure 4.2).
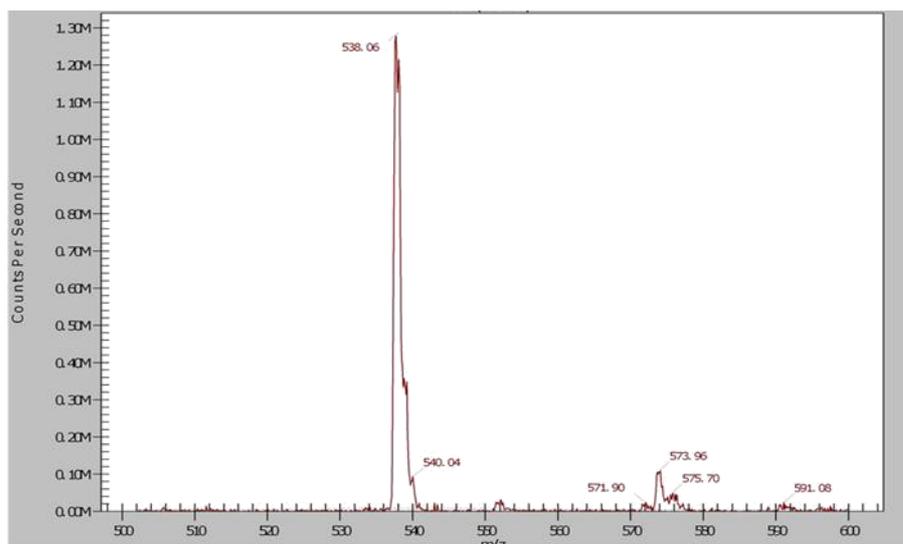
Figure 4.2: Mass spectra of OL

4.2 The HPLC method validation for the identification OL
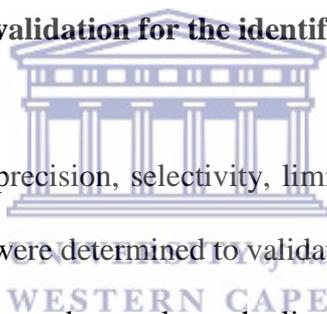
The linearity, accuracy, precision, selectivity, limit of detection (LOD) and limit of quantification (LOQ) were determined to validate the method. Figure 4.3 shows the calibration curve generated to evaluate the linearity of the HPLC method used in this study. Table 4.1 shows the RSD obtained describing the accuracy of the method. The peak purity of the OL peak is shown in Figure 4.4 to describe the selectivity of the method.
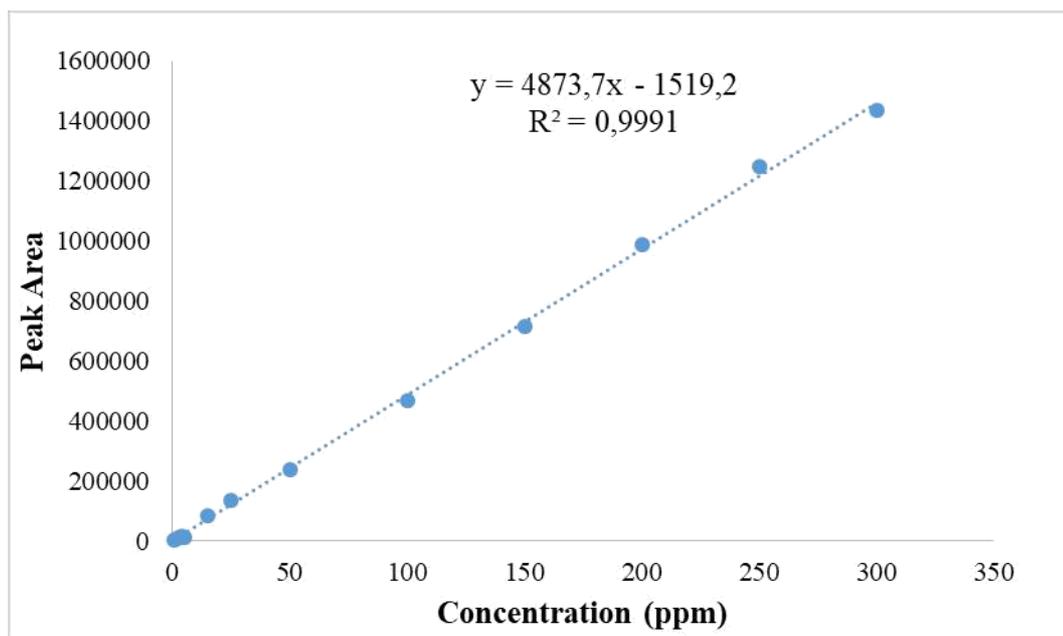
Figure 4.3: A calibration curve for OL (area of the peak versus the concentration of OL in ppm).

A correlation coefficient of 0.9991 was obtained in the graph illustrated in Figure 4.3 which demonstrates the method was linear over the range of 1 ppm to 300 ppm. The LOD was calculated to be 1 ppm and the LOQ was calculated to be 4 ppm. The precision of the method as calculated using the concentrations of 5 ppm, 50 ppm or 300 ppm, showed a relative standard deviation (RSD) of 0.451464%, 0.90289%, 1.059847% respectively.

Table 4.1: The Relative Standard deviation for the determination of the accuracy of the OL concentration. Concentrations of 2 ppm, 50 ppm, and 300 ppm were used.

Concentration:	Peak area/Predicted peak area × 100	mean	Standard deviation (SD)	Relative Standard Deviation (%)
2 ppm	102.379963 101,3141349 103,9680059	102,60	1,34	1,30
50 ppm	99,21358901 97,09266084 98,61804959	98,31	1,09	1,11
300 ppm	97,56312369 98,28625631 99,12577549	98,33	0,78	0,80
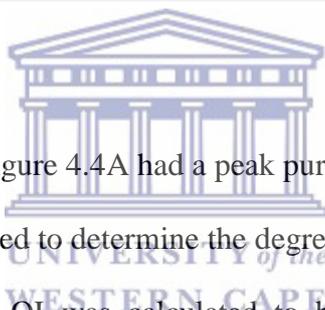
The OL peak shown in Figure 4.4A had a peak purity of 1.41 as shown in Figure 4.4B. Figure 4.5A was used to determine the degree of separation of OL from neighbouring peaks and OL was calculated to be separated from the closest neighbouring peak with a resolution of 0.3.
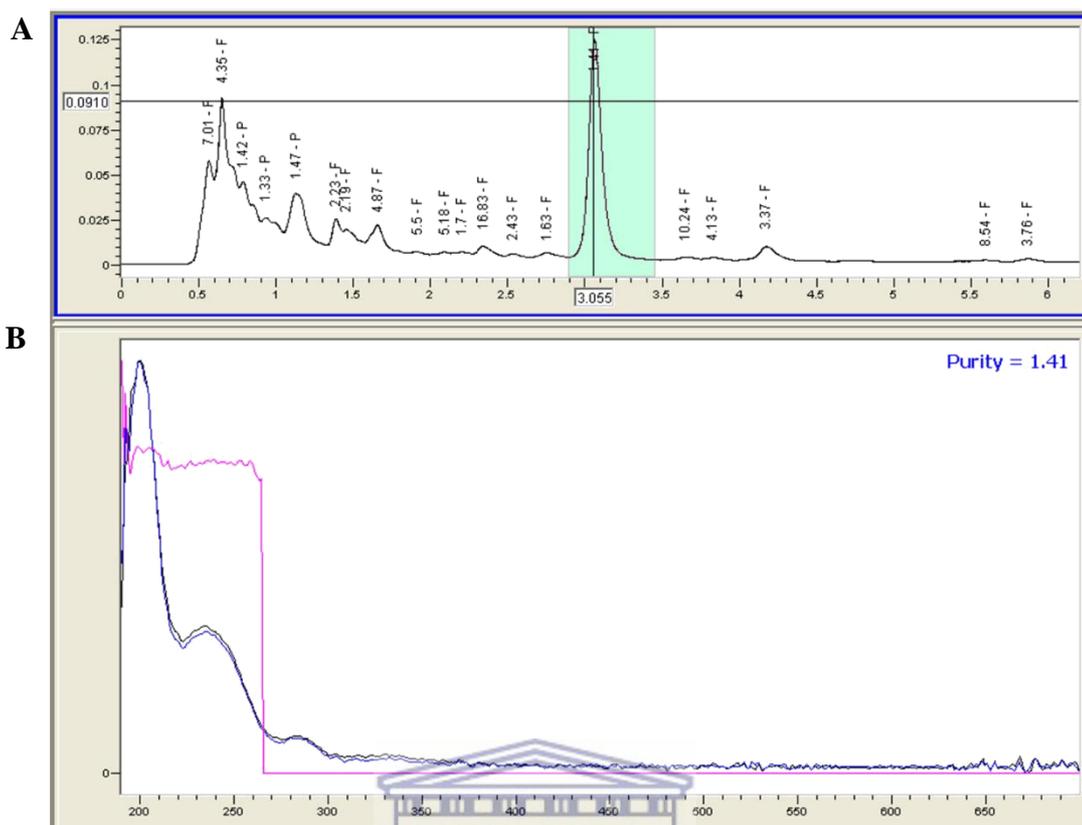
Figure 4.4: The peak of OL on the chromatogram (A) and the purity of the peak (B)

4.3 The HPLC-MS analysis of OA and OE for the identification and quantification of OL

In Figure 4.5A and Figure 4.7A, the peak appearing at close to 2.996 minutes (the time OL peaks in Figure 4.1) was analyzed by ultraviolet (UV) spectra to identify OL present in *Olea africana* (OA) or OE. Furthermore, the presence of OL in the OA or OE extracts was confirmed using mass spectroscopy as shown in Figure 4.6 and Figure 4.8 respectively.
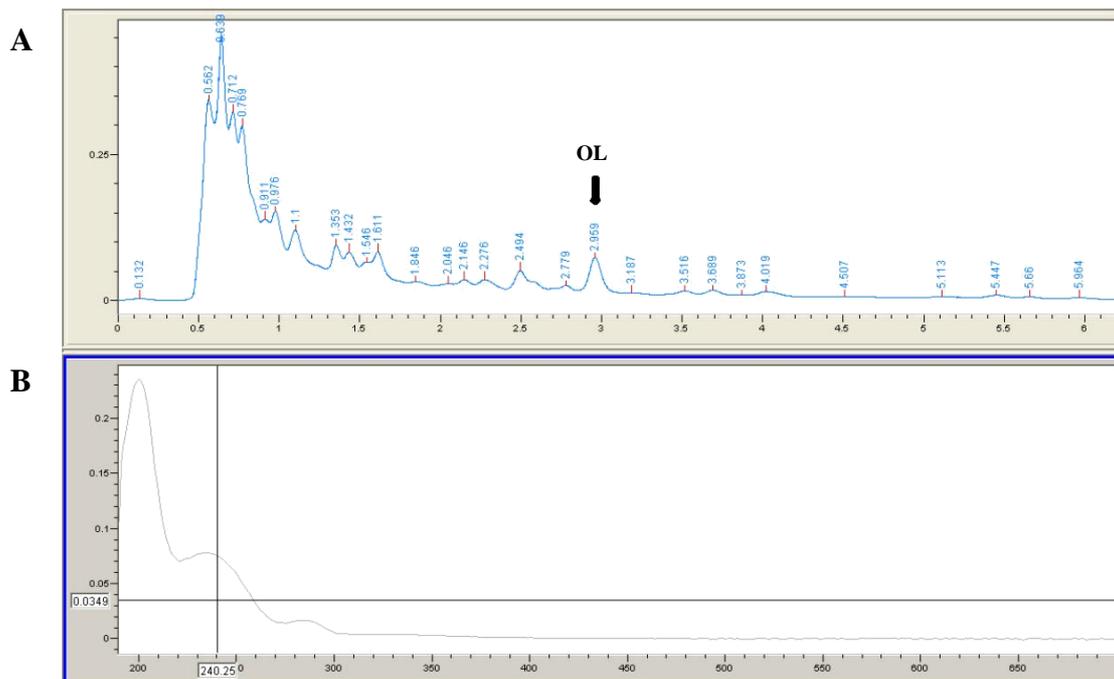
Figure 4.5: The HPLC chromatogram of OA (A) at 240 nm and the UV peak of OL (B).

The yield obtained for OA was 33% and the yield obtained for OE was 12%. The HPLC chromatogram of OA shows a peaked at 2.959 min (Figure 4.5A), which is the approximate time the OL standard peaked (Figure 4.1). The absorption maxima (λ_{max}) for OL is around 240nm and 280nm. The UV-vis analysis of the 2.959 min peak confirms that OL peaks at 240nm and 280nm (Figure 4.5 B).
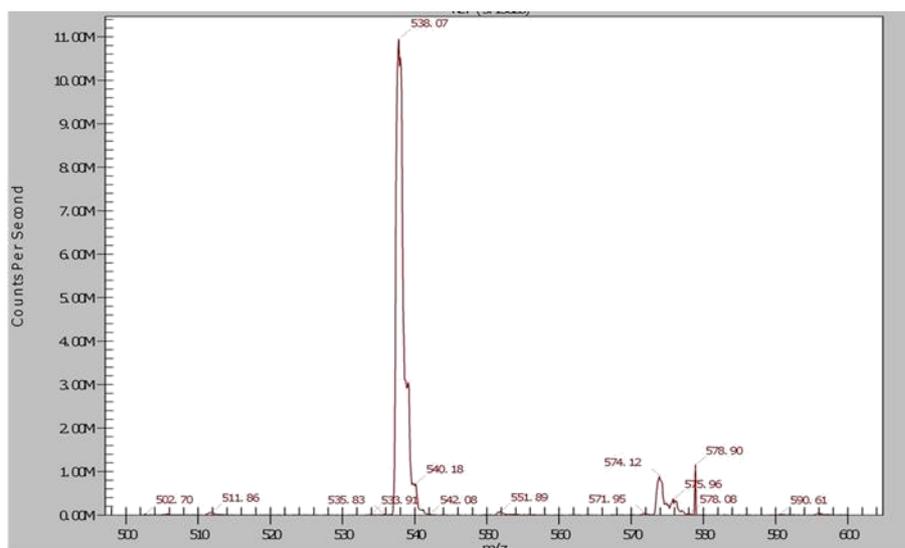
Figure 4.6: The mass spectra of OA to confirm the identification OL.

The mass spectra (Figure 4.6) show a peak at 538.07m/z, confirming the presence of OL in OA. OL was calculated to be present in OA at a concentration of 11.65604424 mg/g.
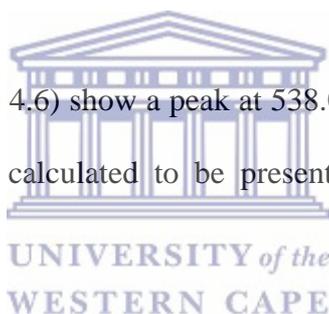
The peak appearing in the HPLC chromatogram of OE at 2.921 minutes was seemingly OL (Figure 4.7A). However, the UV analysis of the peak at 2.921 shows that there were no peaks at 240nm and 280 nm for the 2.921 minute peak (Figure 4.7B). Furthermore, the suspected OL peak was analyzed using mass spectroscopy and there was no indication that OL was present, implicated by an absence of a peak of about 538m/z (Figure 4.8). OL is the main compound of interest in this study. The OE extract was thus not used in subsequent experiments.
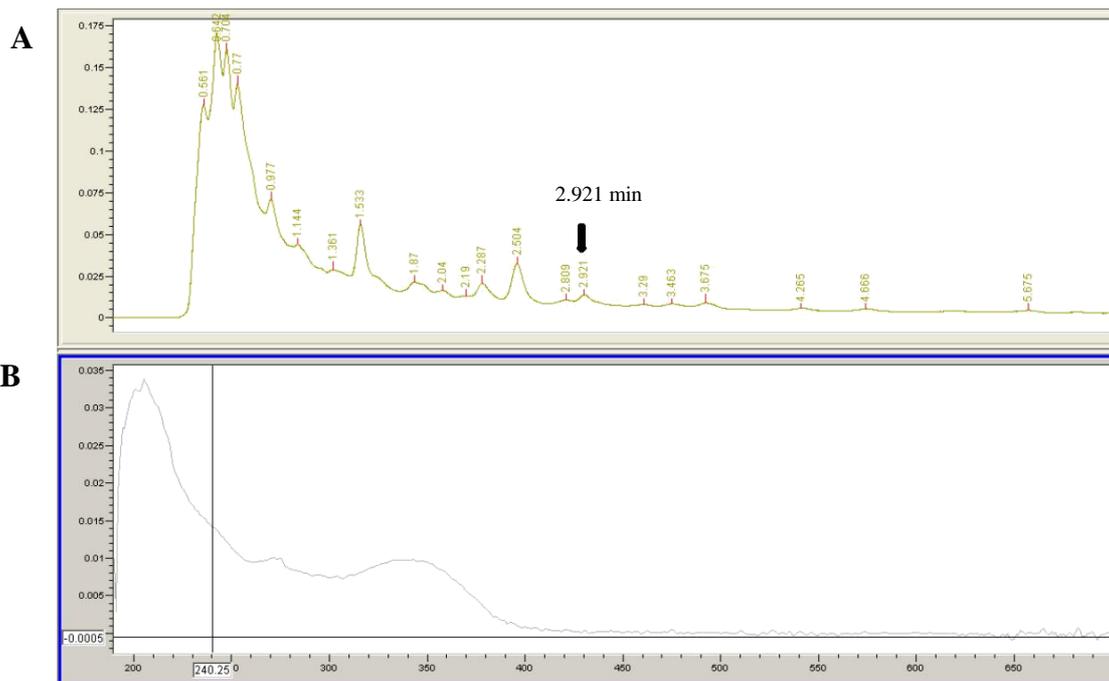
Figure 4.7: The HPLC chromatogram of *Olea exasperata* (OE) (A) and the UV analysis of the peak (B).
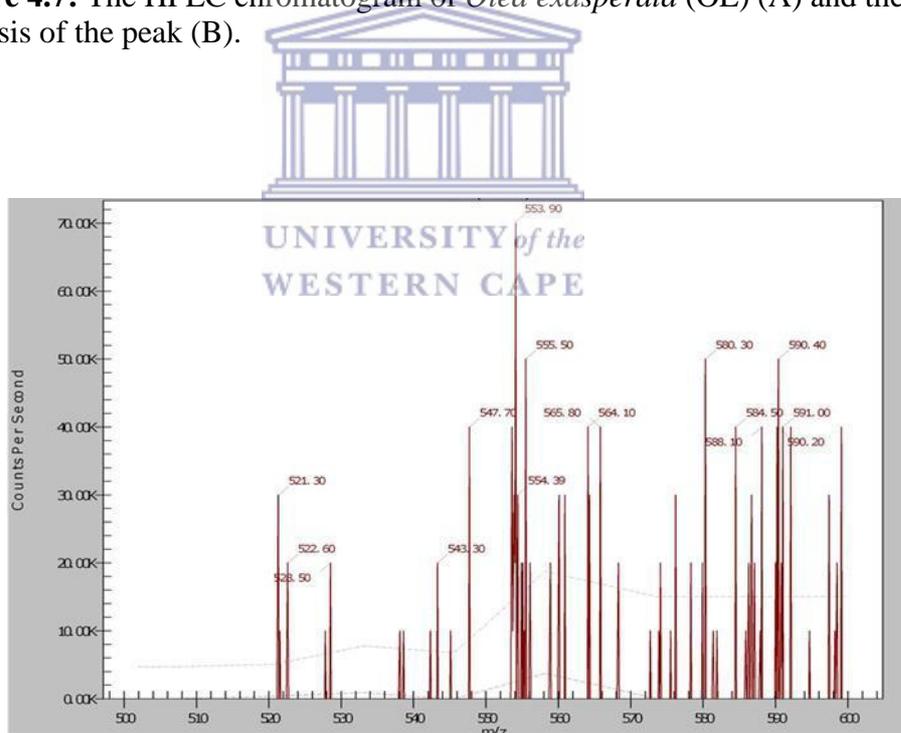
Figure 4.8: The mass spectra of OE.

The next step would be to design and characterize a liposome nanocarrier that is suitable for the encapsulation of OA and OL, as these compounds will be used in experiments to follow.

4.4 The characterization of liposomes

Liposomes were produced as described in section 3.1. The liposomes were characterized based on size (diameter), polydispersity index (PDI) and zeta potential (surface charge). The average size and charge of liposomes are shown in figure 4.9 and 4.10 respectively. The liposomes were stored for 6 months and the average diameter and charge was evaluated and the results are shown in figure 4.11 and 4.12 respectively. The appearance of the batch of liposome prepared was also evaluated for any visible signs for a loss of stability (Figure 4.13).
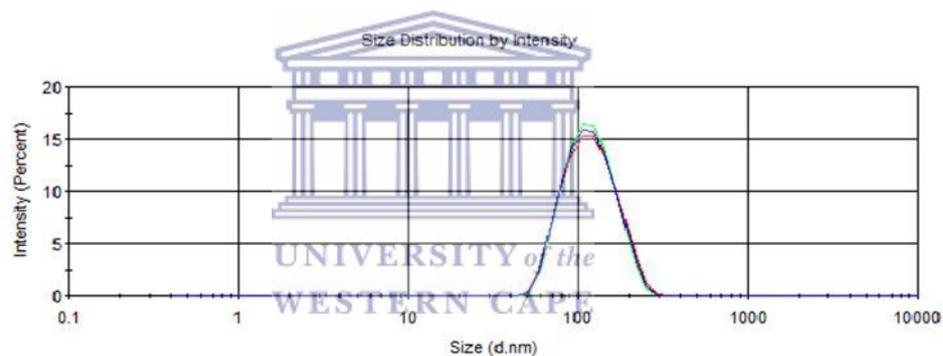
Figure 4.9: The size distribution of the colloidal liposomes particles after extrusion through a 100nm polycarbonate membrane.
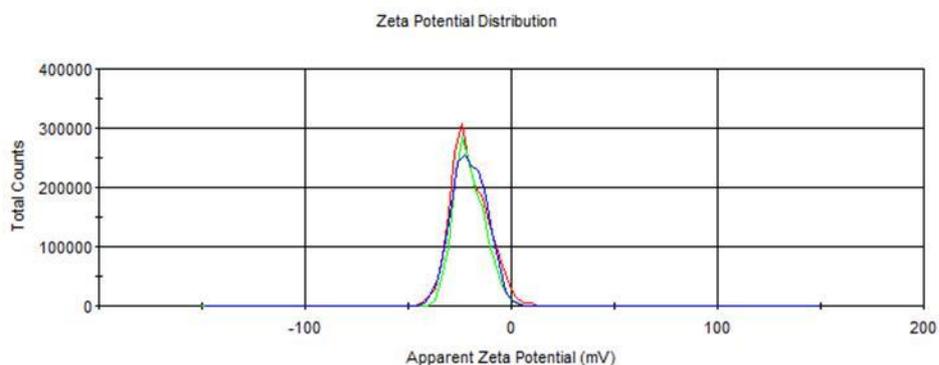
Figure 4.10: The zeta potential of plain liposomes

The average size of the colloidal particles was 109.6 nm (Figure 4.9), with a PDI of 0,098, meaning particles size distribution was monodispersed. The surface charge of plain liposomes determined by photon correlation spectroscopy/dynamic light scattering (DLS) was -20.3mV (Figure 4.10).
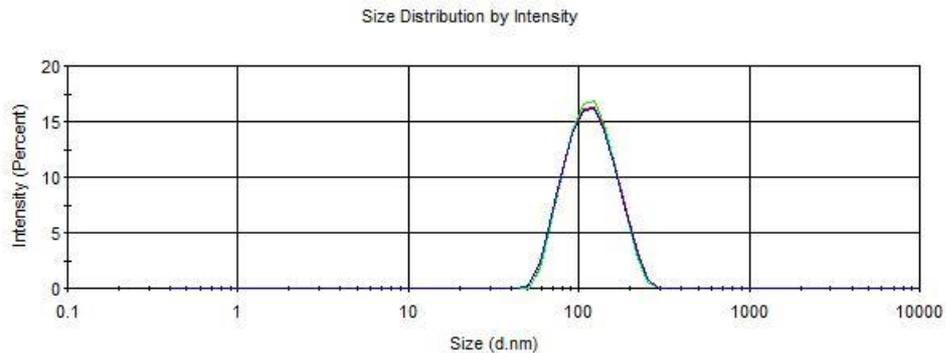
Figure 4.11: The average size of the liposomes after 6 months.
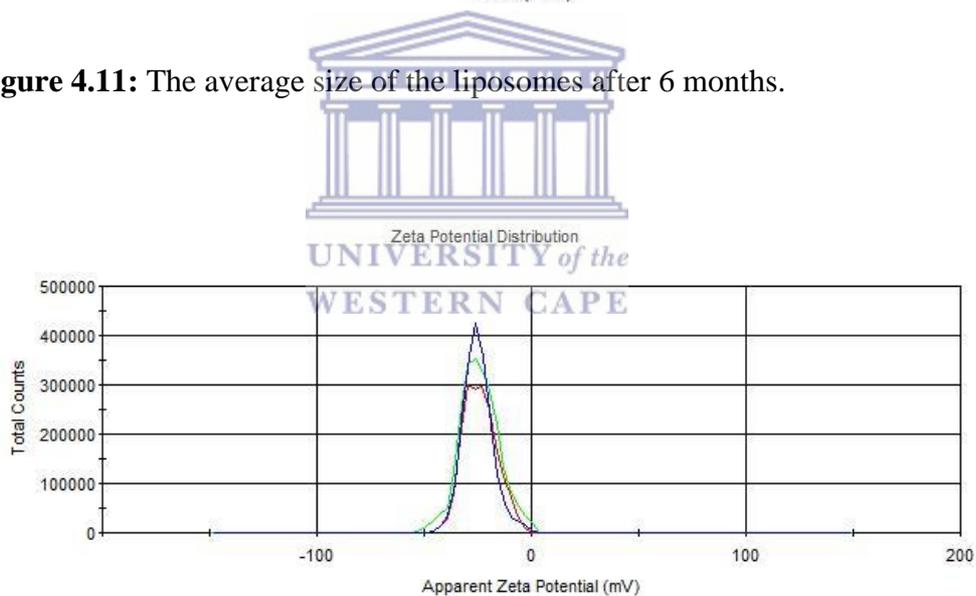
Figure 4.12: The average zeta potential of the liposomes after 6 months.

To test the stability of the liposomes, liposomes were stored for 6-months at 4 °C and the size and PDI were measured using DLS after the 6-month storage. Liposomes had a mean diameter of 111.2 nm (Figure 4.11) and a PDI of 0.098. There was a slight variability in the size of the liposomes, but this most likely was just the batch-to-batch variability that comes with DLS measurements. This was further supported

by the PDI that demonstrated that the liposomes were still monodispersed in size distribution. The average zeta potential of the liposomes was -24 mV showing no decrease of charge on the liposome surface (Figure 4.12). There was no visible creaming or aggregation in the liposomes batch after 6 months (Figure 4.13). The liposomes maintained a white-milky homogenous appearance. The liposomes showed no visible creaming, flocculation or aggregation.

Figure 4.13: The stored liposomes maintained a homogenous mixture with no visible aggregation.

After preparation and characterization of the liposomes, we had to ensure that the liposomes were able to penetrate the H9c2 cells. In preliminary experiments "empty" rhodamine incorporated liposomes (rh-liposomes) were prepared and H9c2 cells were incubated for 1 hour and 24 hours. We chose the 24 hour time point to coincide with our preincubation period. Figure 4.14 shows the confocal images of cells incubated with rh-liposomes for 1 hour (Figure 4.14A) or 24 hours (Figure 4.14B).

A
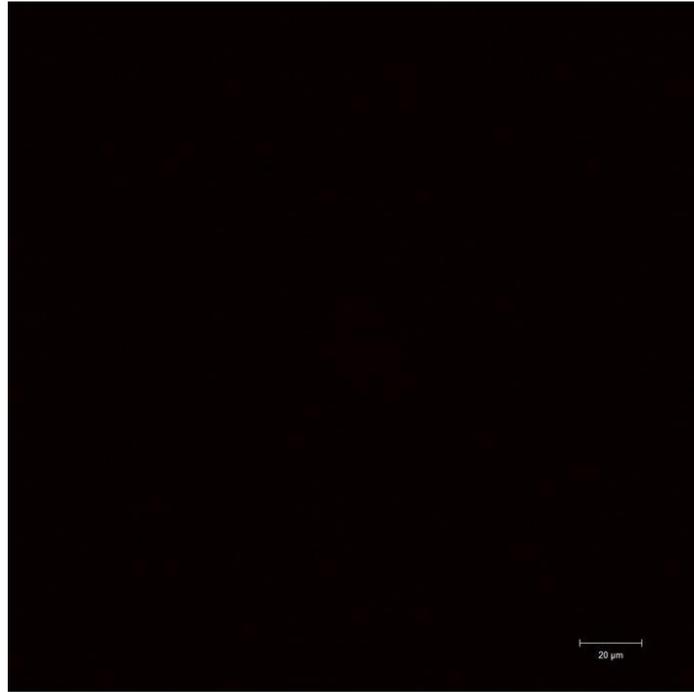
B
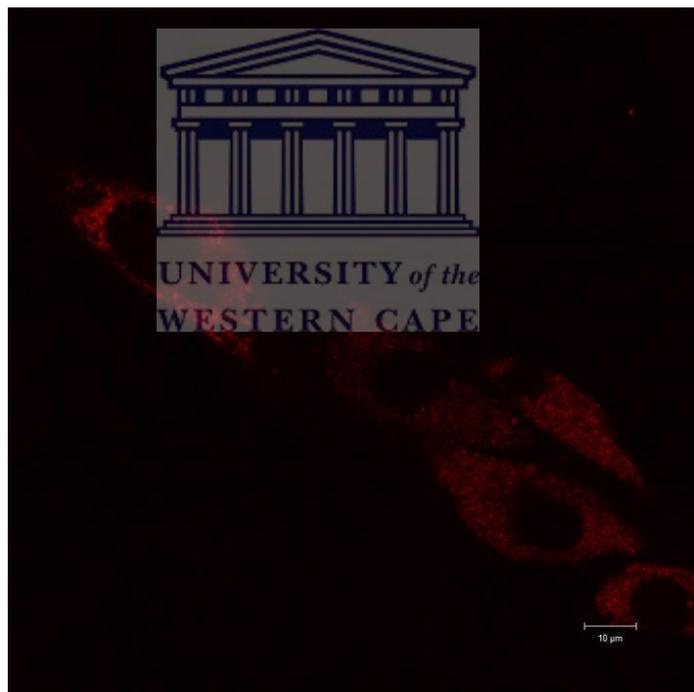
Figure 4.14: Confocal images of rh-lip after 1 hour (A) and 24 hours (B).

Figure 4.14A shows that no rh-liposomes were detected by confocal microscopy in H9c2 cells after 1 hour. Liposomes were, however, present in cells at the 24 hour time point (Figure 4.14B). The nanocarrier designed would thus be suitable for

deliver drugs inside the H9c2 cells. The next step would be to encapsulate OA and OL.

HPLC-MS was used to determine whether OL in the extract and individually was present in the liposomes and how efficiently the liposomes were able to encapsulate the drugs. OL is completely miscible in water. OL was dissolved in distilled water and was added during the aqueous phase of liposome formation. The encapsulation efficiency was calculated to be 24%. The presence of OL was confirmed by the presence of a peak at 3.082 minutes on the HPLC chromatogram and a peak at 538.02 on the MS (Figure A3 and Figure A4 in the appendix).
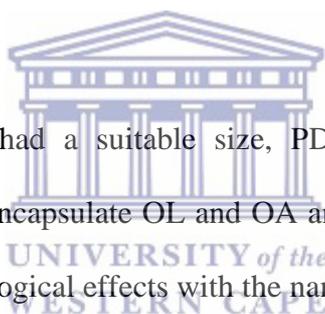
The liposomes formed had a suitable size, PDI, and charge. Furthermore, the liposomes were able to encapsulate OL and OA and enter H9c2 cells. The next step was to determine the biological effects with the nanodelivery of OA and OL.

4.5 The evaluation of the cardioprotective effects of OA and OL applied as a free drug or encapsulated in liposomes.

Oxidative stress was induced in H9c2 cells using hydrogen peroxide. The viability of the cells after 24 hours are shown in Figure 4.15 below.
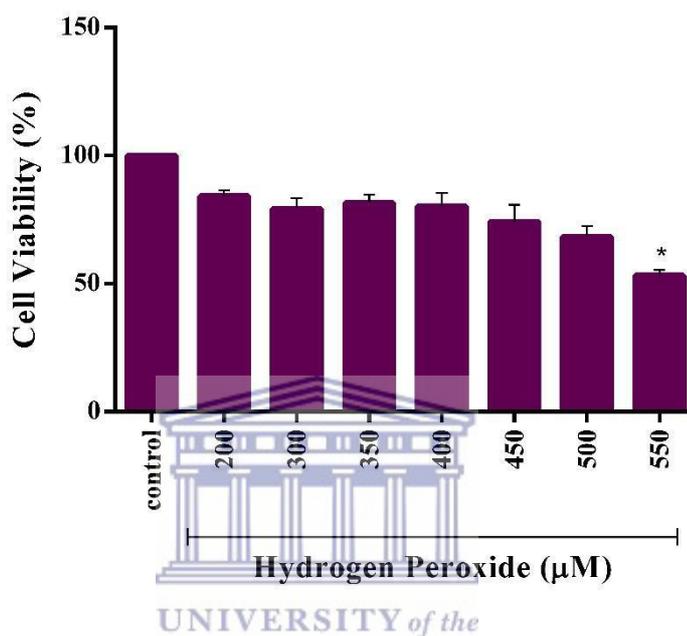
Figure 4.15: The effect of a 24-hour exposure to different concentrations of H_2O_2.
*$p<0.05$ was considered statistically significant as compared to the control.

In this study, cells were treated with different concentration of H_2O_2 (100, μM 300 μM, 350 μM, 400 μM, 450 μM, 500 μM and 550 μM) for 24 hours to determine a concentration that would damage about 50% of cells. At a concentration of 550μM H_2O_2 reduced the cell viability to 53.22±2.04%. Figure 4.15 shows that 550 μM H_2O_2 was the only concentration that reduced cell viability significantly ($p<0.05$). This concentration was used in subsequent experiments. To ensure that the concentrations of OA and OL that were going to be used in subsequent experiments had no toxic or proliferative effects on the H9c2 cells,

cells were exposed to only OA or OL for 24 hours. The results are shown in Figure

4.16A and Figure 4.16B.
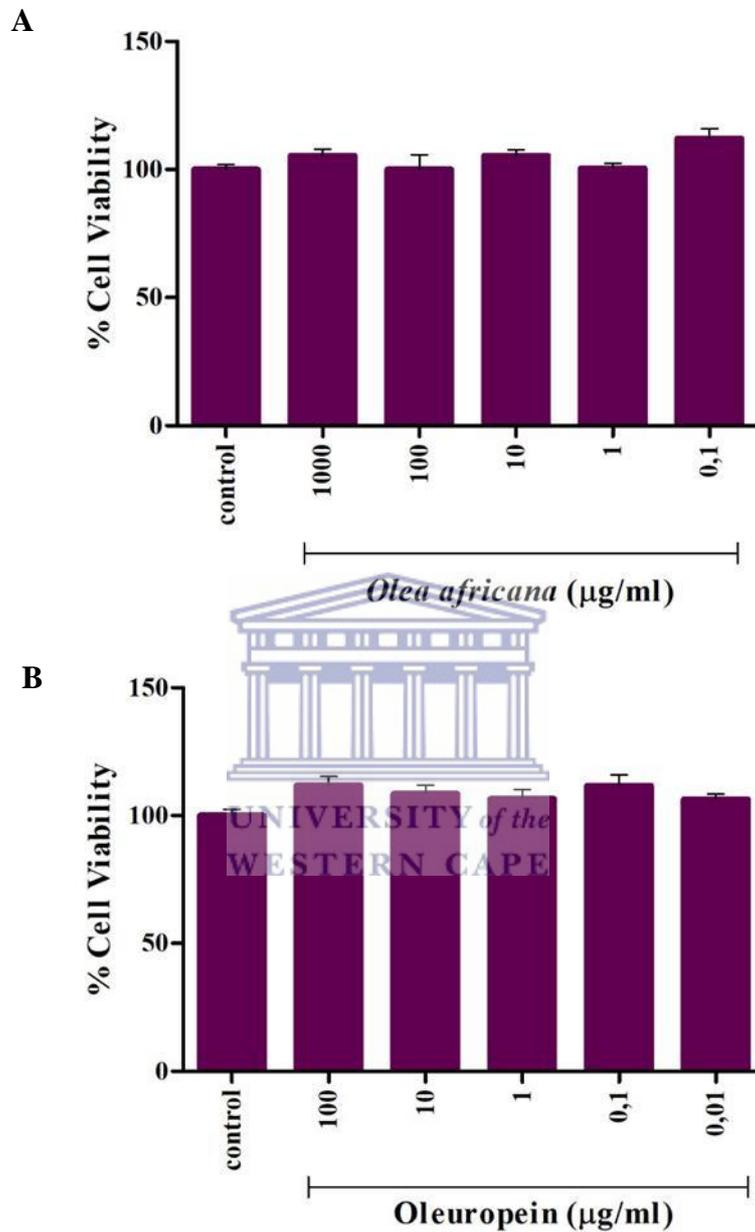
Figure 4.16: The effect of different concentrations of OA (A) or OL (B) on cell
viability, as assessed by the MTT assay.
*$p < 0.05$ was considered statistically significant as compared to the control.

All the concentrations of OA (1000 µg/ml, 100 µg/ml, 10 µg/ml and 0.1 µg/ml) or

OL (100 µg/ml, 10 µg/ml, 1 µg/ml, 0.1 µg/ml and 0.01 µg/ml) tested in this study

did not increase nor decrease cell viability (Figure 4.16A and Figure 4.16B) ($p>0.05$).

Cells were pretreated with OA or OL for 24 hours and then exposed to H_2O_2 to determine whether the treatment could protect H9c2 cells from H_2O_2 induced cell death. The results are shown in Figure 4.17A and Figure 4.17B. H_2O_2 exposure significantly reduced the cell viability of H9c2 cells to $57.73 \pm 3.93\%$, as compared to the untreated control ($p<0.05$). The concentrations- 1000 µg/ml, 100 µg/ml, 10 µg/ml, 1 µg/ml or 0.1 µg/ml OA pretreatment prior to subsequent H_2O_2 exposure showed a slight, but not significantly ($p>0.05$) improved mean cell viability to $65.52 \pm 4.44\%$, $63.02 \pm 6.62\%$, $69.95 \pm 6.42\%$, $68.74 \pm 8.35\%$, and $63.63 \pm 5.05\%$ respectively. Pretreatment with 10 µg/ml, 1 µg/ml, 0.1 µg/ml and 0.01 µg/ml OL improved the mean cell viability to $61.03 \pm 4.49\%$, $64.11 \pm 3.96\%$, $62.35 \pm 4.39\%$ and $69.89 \pm 2.51\%$ respectively. Again the improvement was not significant ($p>0.05$).
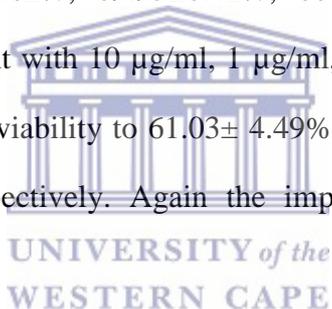
The OA and OL applied as a free drug, was thus not able to protect the H9c2 cells against H_2O_2 - induced stress. To test whether OA or OL, when applied intracellular, as opposed to in the incubation medium, could afford better protection selected concentrations of OA or OL was encapsulated inside liposomes and used as a pretreatment.

A

B
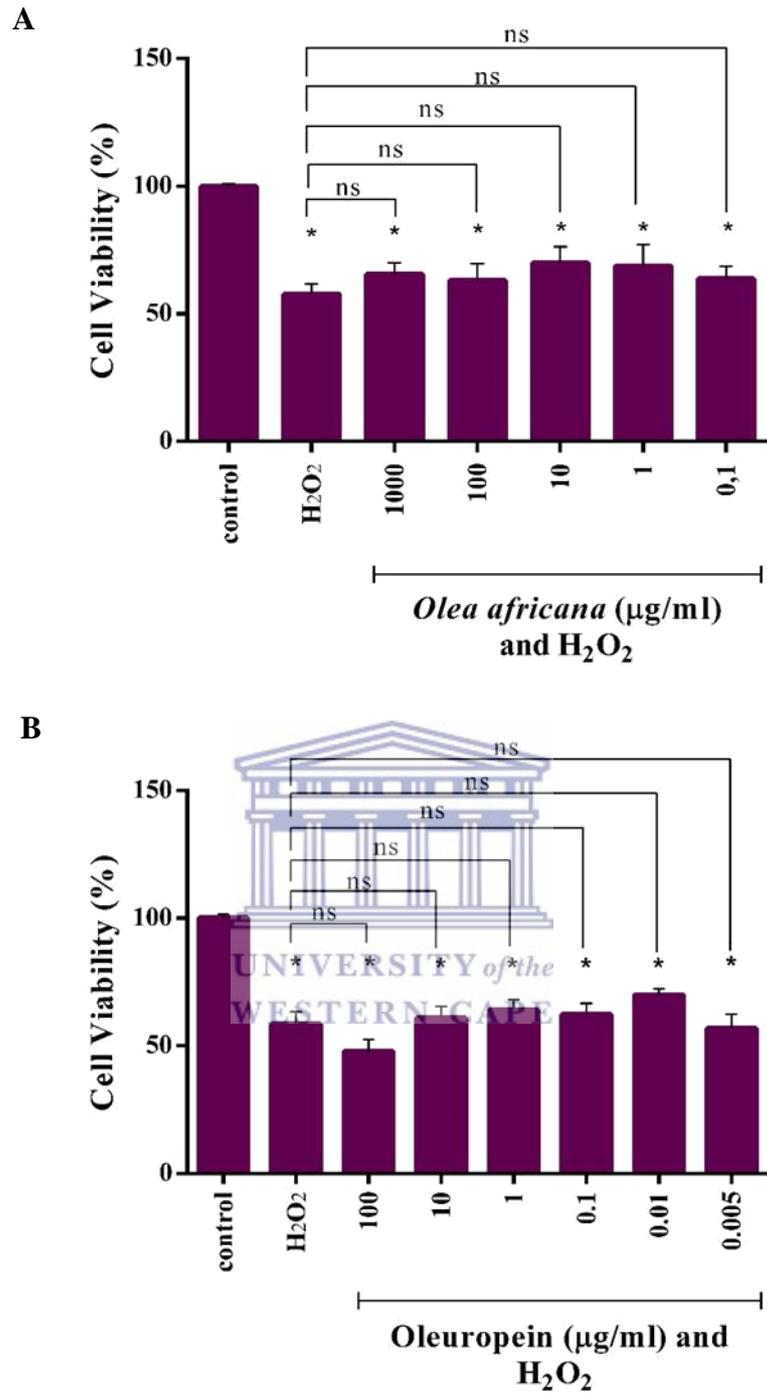
Figure 4.17: The effect of 24 hours OA or OL pretreatment on H_2O_2 induced stress in H9c2 cells.
*$p<0.05$ as compared to the control.

To ensure that the liposome itself was not toxic to the cells, cells were treated with

different concentrations of liposomes (1000 µg/ml, 100 µg/ml 10 µg/ml and 1

μg/ml) containing a selected concentration of OA (1000 µg/ml or OL (0.1 µg/ml) encapsulated inside the liposome. Cell viability was assessed using the MTT assay to determine a concentration that will not significantly increase or decrease cell viability. The results are shown in Figure 4.18A and Figure 4.18B.

After encapsulation of the OA or OL, H9c2 cells were treated with different concentrations of liposomes. OA –or OL containing liposomes did not cause any significant increase or decrease in cell viability at any of the concentrations tested as shown in Figure 4.18A and Figure 4.18B (p>0.05) and were all suited to be used in subsequent experiments in which the potential cardioprotective effects of the encapsulated drugs were evaluated. The results showing the effects of a 24 hour AO or OL pretreatment prior to H_2O_2 –induced oxidative stress is shown in Figure 4.19A and Figure 4.19B.

A

a – 1000 µg/ml
b – 100 µg/ml
c – 10 µg/ml
d – 1 µg/ml

B
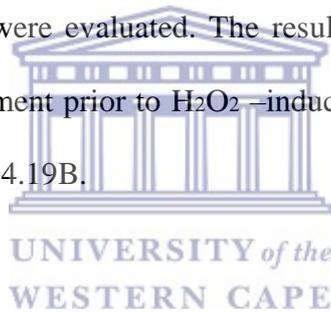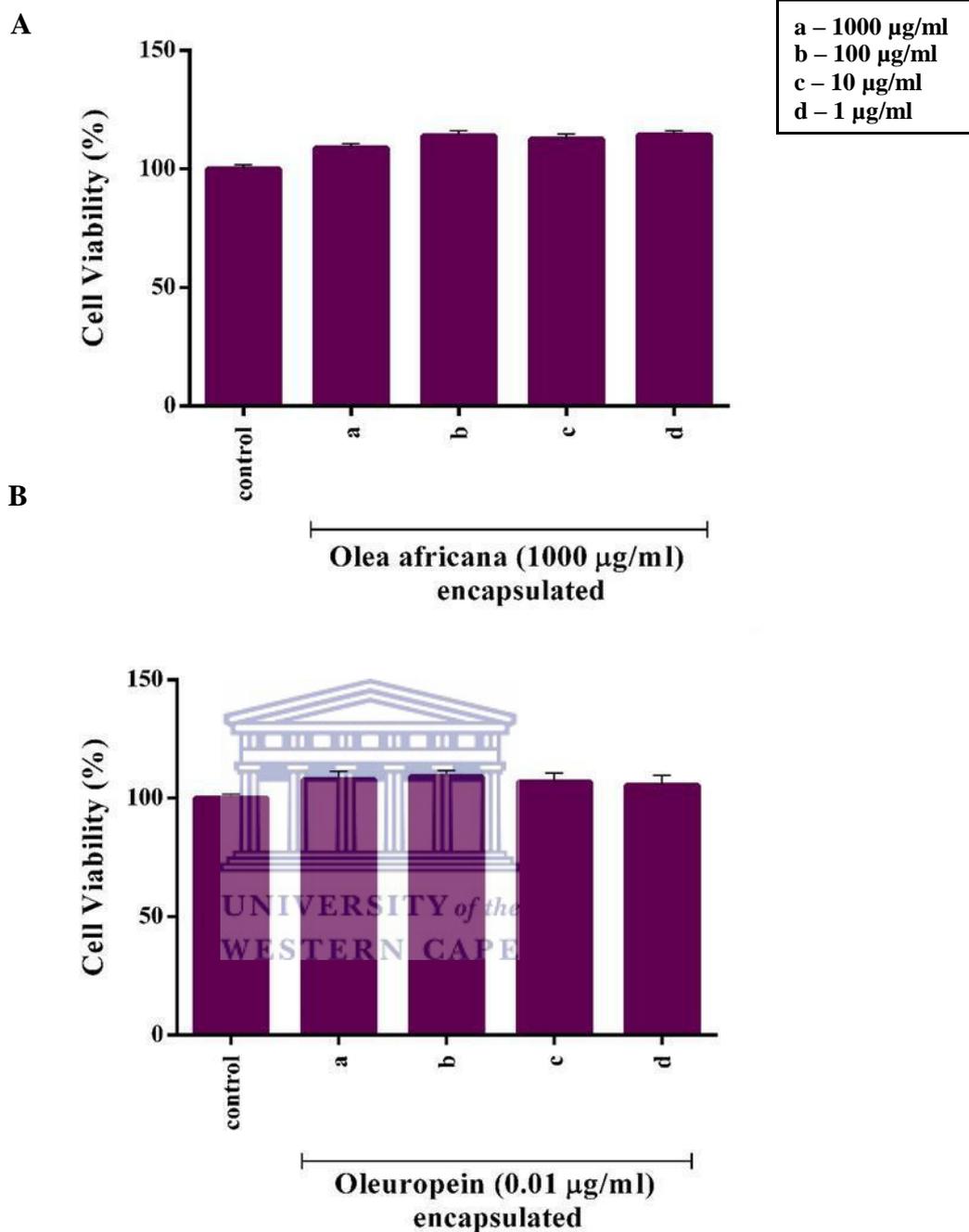
Figure 4.18: Effect of a 24-hour exposure to different liposome concentrations
(a-d) on cell viability.
Liposomes encapsulated with either 1000 µg/ml OA (A) or 0.01 µg/ml OL (B).
*$p < 0.05$ was considered statistically significant as compared to the control.

.

A

Olea africana (1000 µg/ml)
encapsulated and H₂O₂

a – 1000 µg/ml
b – 100 µg/ml
c – 10 µg/ml
d – 1 µg/ml

B

Oleuropein (0.01 µg/ml)
encapsulated and H₂O₂
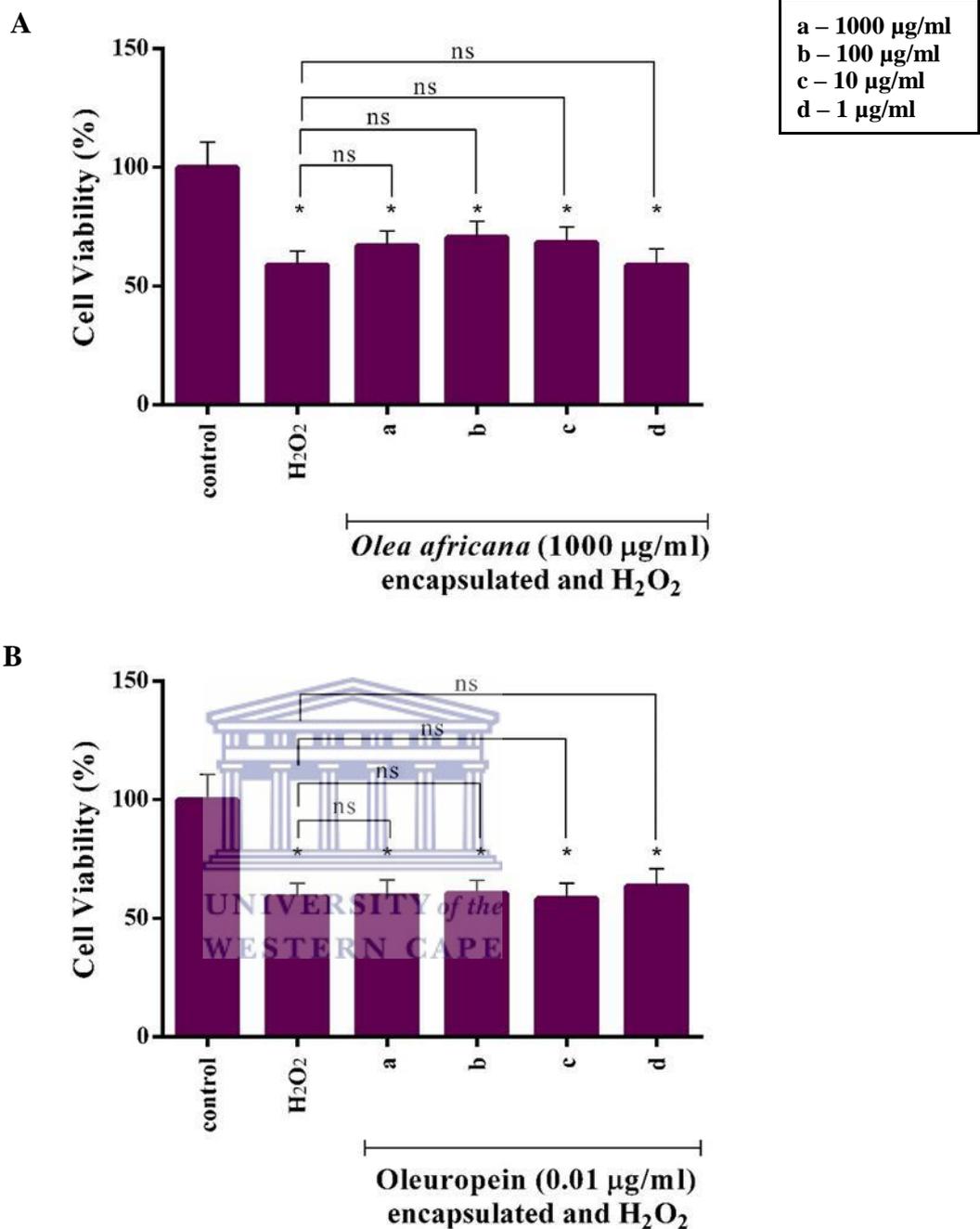
Figure 4.19: The effect of 1000 µg/ml encapsulated OA (A) or 0.01 µg/ml encapsulated OL (B) pretreatment on H₂O₂ induced cell death- as evaluated by the MTT assay.
*p<0.05 are considered statistically significant as compared to the control.

H₂O₂ decreased cell viability significantly as compared to the control (p<0.05). OA

containing liposomes (Figure 4.19A) could not significantly increase cell viability

as compared to the H₂O₂ control at any of the concentrations tested (p>0.05). OL

containing liposomes, shown in Figure 4.19B, were thus also not able to protect the H9c2 cells against H_2O_2 damage (p>0.05).

The MTT results/ measures mitochondrial cell viability and is a commonly used for an initial cell viability screening. Before cell death, H_2O_2 destabilizes the mitochondrial membrane potential (Li *et al*., 2003). The above set of experiments were thus repeated (H9c2 cells were pretreated with different concentrations of OA and OL as free drugs and encapsulated drugs for 24 hours) and MMP depolarization was assessed using the JC-1 assay. The results are shown in figure 4.20 and figure 4.21.
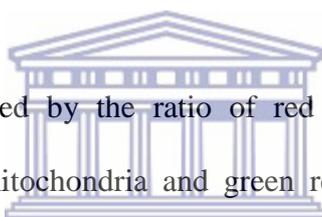
The MMP was calculated by the ratio of red over green fluorescence. Red represents the normal mitochondria and green represents the MMP instability. H_2O_2 caused significant mitochondrial hyperpolarization in H9c2 cells (p<0.05). A 24-hour pretreatment with OA or OL as a free-drug (Figure 4.20A and Figure 4.20B) or encapsulated (Figure 4.21A and Figure 4.21B) was not able to stabilize the MMP of H9c2 cells (p>0.05).
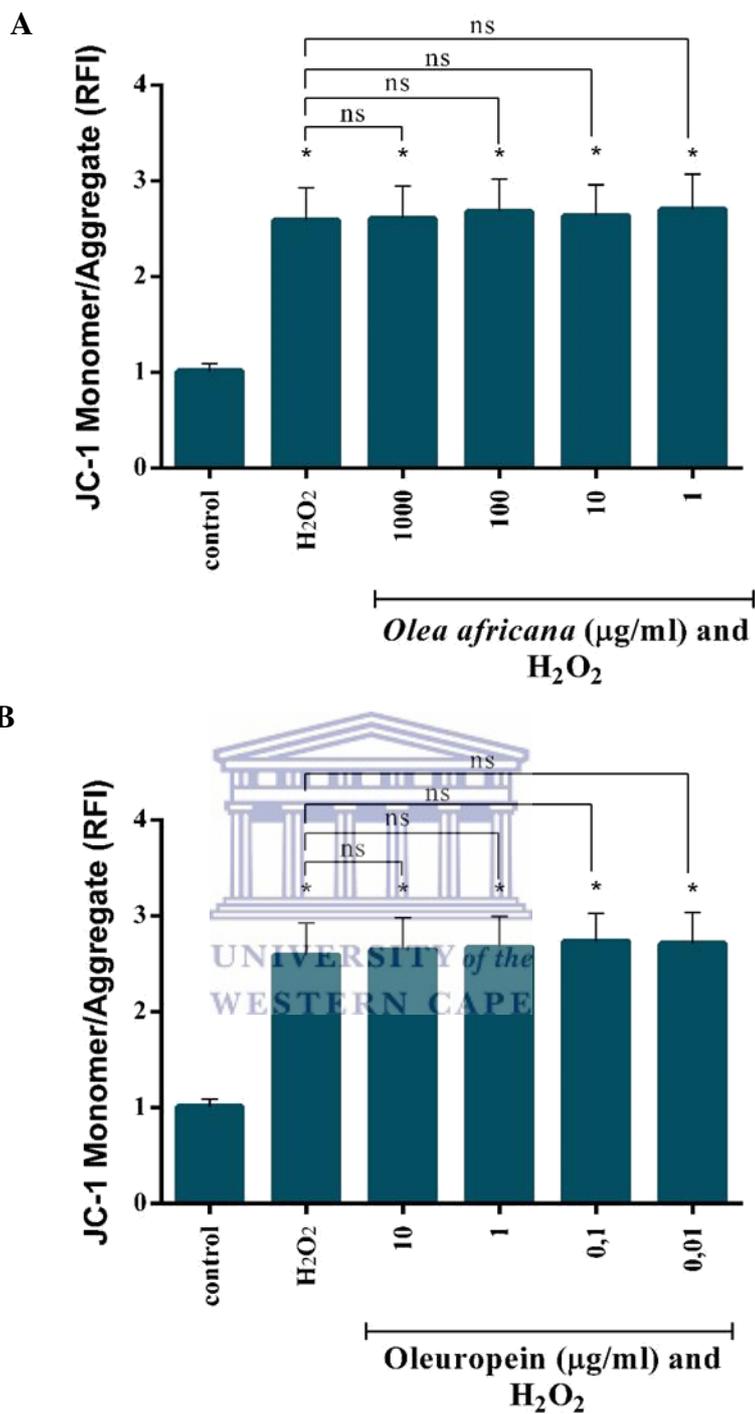
Figure 4.20: The effect of 1000 µg/ml encapsulated OA (A) or 0.01µg/ml encapsulated OL (B) pretreatment on H_2O_2 induced cell death- as evaluated by the JC-1 assay.

 *p<0.05 are considered statistically significant as compared to the control.
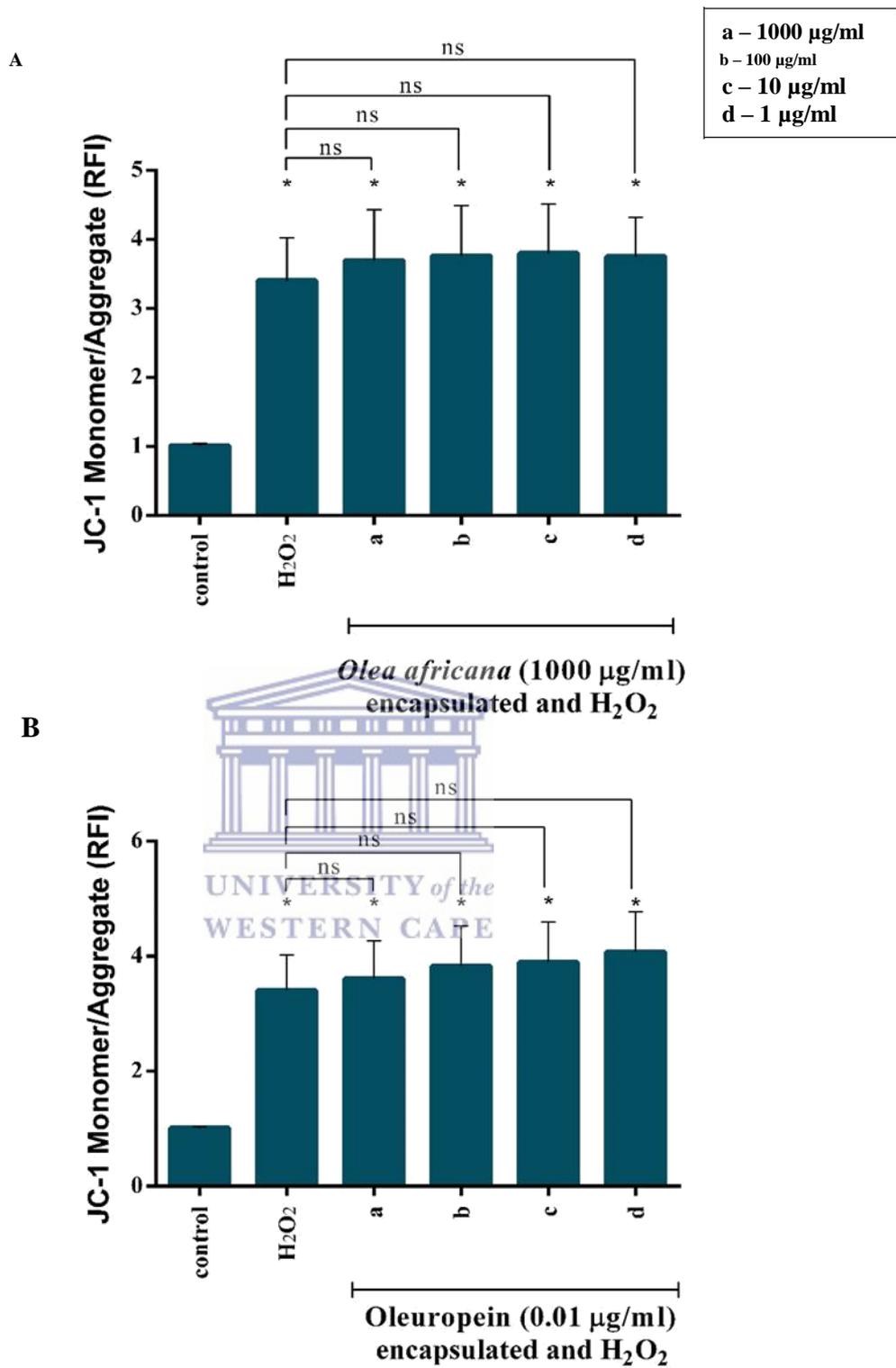
Figure 4.21: The effect of 1000 μg/ml encapsulated OA (A) or 0.01μg/ml encapsulated OL (B) pretreatment on H_2O_2 induced cell death- as evaluated by the JC-1 assay.

To further evaluate the ability of OA and OL to protect H9c2 cells from oxidative stress, a different stressor and endpoint was chosen. The results are shown in Figure 4.22A, Figure 4.22B, Figure 4.23A and Figure 4.23B.

Doxorubicin significantly decreased the mean cell viability to 60.46± 2.32% ($p < 0.05$) and a 24-hour pretreatment with OA (Figure 22A) or OL (Figure 22B) had no significant increase in the cell viability as compared to the dox-only control ($p > 0.05$).

OA and OL containing liposomes were also not able to significantly protect the H9c2 cells against dox toxicity as shown in Figure 4.23A and Figure 4.23B ($p > 0.05$).
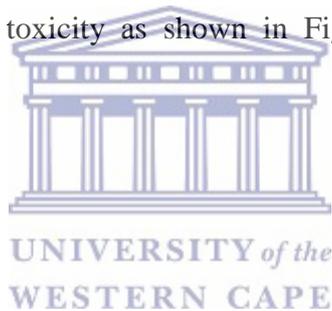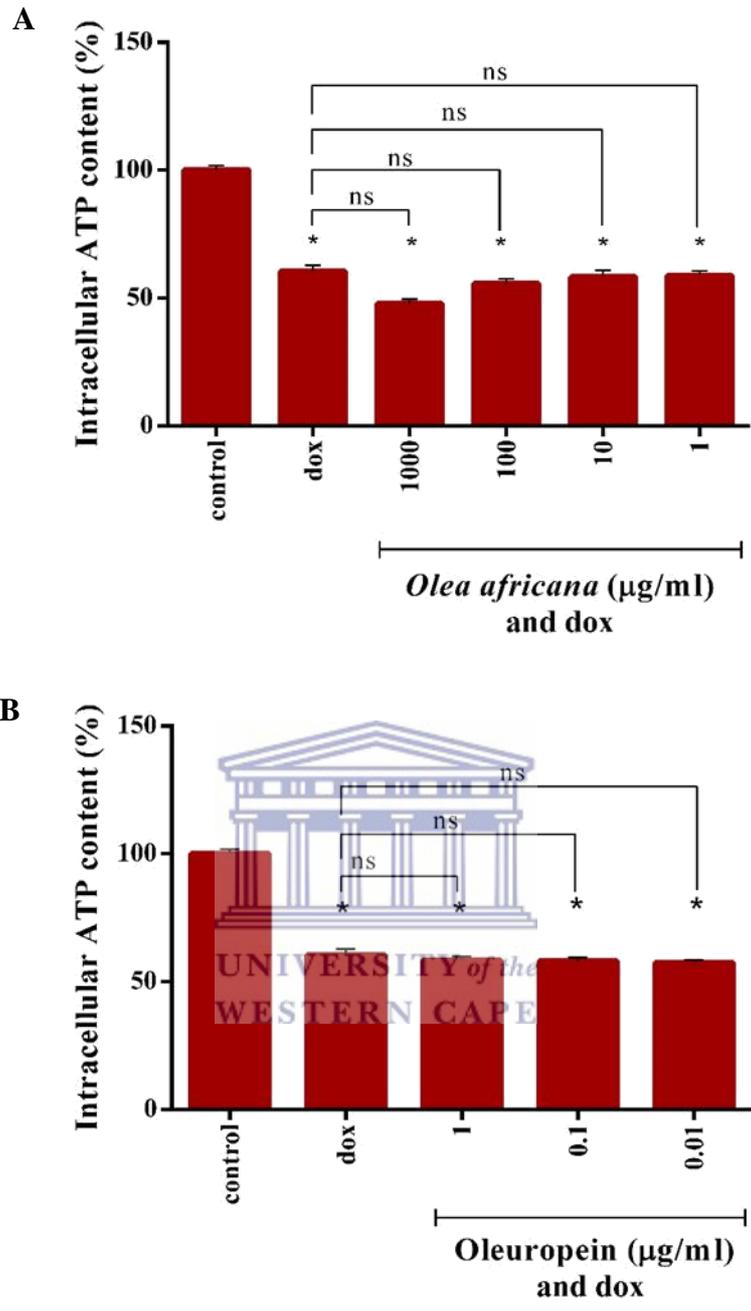
Figure 4.22: The effect of a 24 hour OA or OL pretreatment on doxorubicin-induced cell damage in H9c2 cells.
*p<0.05 was considered statistically significant as compared to the control.
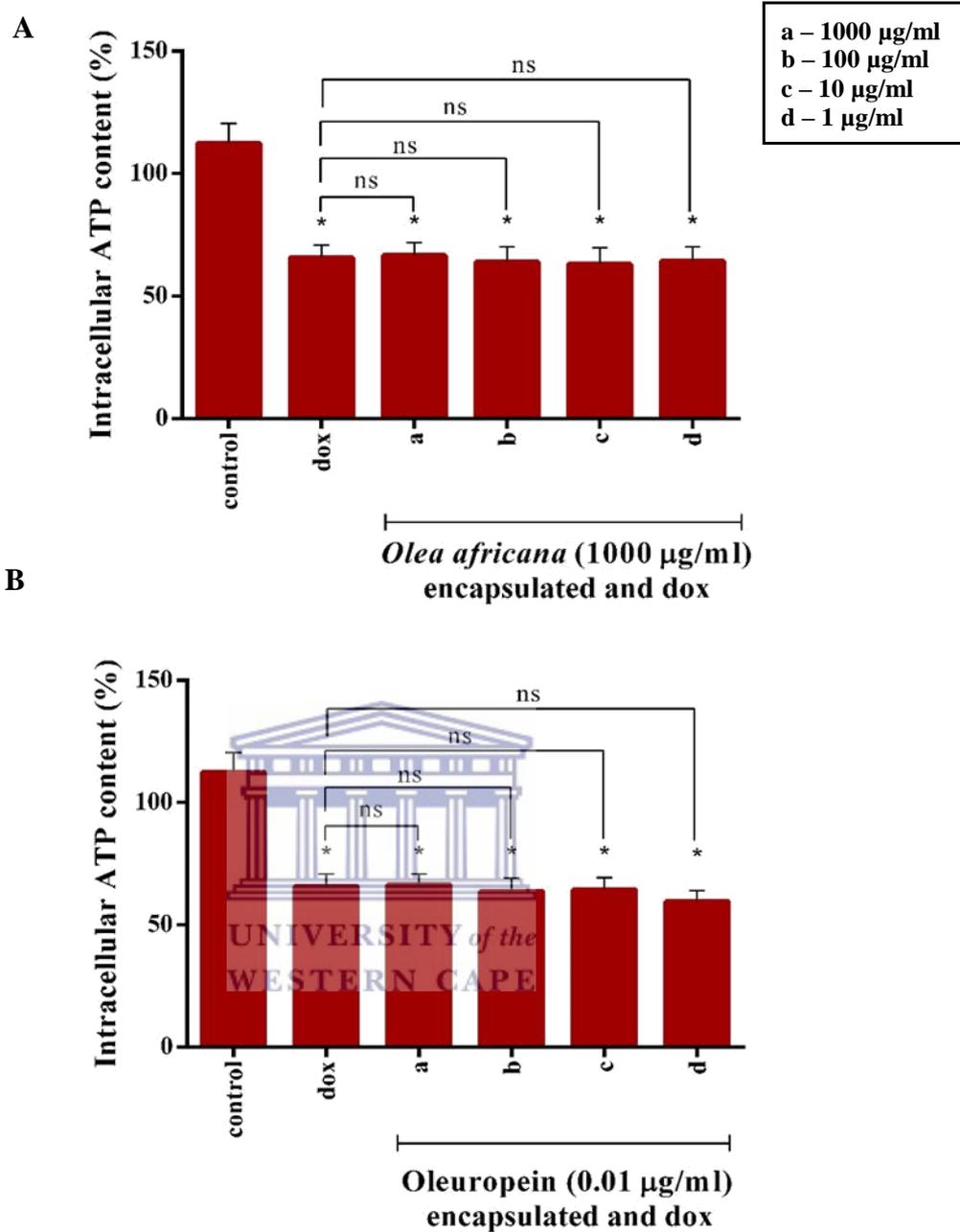
Figure 4.23: The effect of 1000 µg/ml encapsulated OA (A) or 0.01 µg/ml OL encapsulated (B) pretreatment on doxorubicin-induced cell death- as evaluated by the ATP assay.

*p<0.05 was considered statistically significant as compared to the control.

CHAPTER 5: DISCUSSION

5.1 Prepare an aqueous extract and characterize the extract using HPLC-MS

According to tribal tradition, plants are extracted with water (Ahmed-Qasem *et al*., 2013). We have therefore decided to use an aqueous extract in our experiments. Additional motivation is provided by the observation that an aqueous extract of OA was more effective than an ethanolic extract at decreasing the mean arterial blood pressure and heart rate of hypertensive rats (Osim *et al*., 1999). Using an aqueous extract, we obtained a yield of 33% and 12% for *Olea europaea* subsp. *africana* (OA) and *Olea exasperata* (OE) respectively. A yield of 25% was obtained from OA leaves in the study by Masoko and Makgapeetja (2015) when extracting with water. Our results however confirmed previous reports (Obied *et al.,* 2005) that the lyophilized sample is hygroscopic but remains stable for several months if stored in the dark at -20 °C.

To assist polyphenol leaching, the leaves of OA and OE were dried and then finely ground into a powder to aid in the breakdown of the cellular matrix which is known to facilitate the release of polyphenols (Mediani *et al*., 2014, Ahmad-Qasem *et al*., 2013). Masoko and Makgapeetja (2015) reported that OA leaf extracts contained more than twice the radical – scavenging activity of a *Camelia sinensis* (green tea) extract. The antioxidant activity was mostly conferred by the polar compounds, which can be extracted by water (Masoko and Makgapeetja, 2015).

A study by Afaneh *et al* (2015) showed higher Oleuropein (OL) recovery (1%) from dried leaves as compared to fresh leaves (Afaneh *et al*., 2015). Malik (2008) reported that OL was present in *Olea europaea* at 7.3% on a dry weight basis (Malik and Bradford, 2008). In our study, OL in the OA extract was present at a concentration of 0.1%, which was lower than reported above. This could be due to the method used in processing the extract.

In our experiments, the isocratic method was found a simple and reliable method to determine the OL content. Preliminary experiments showed that OL eluted at a retention time (R_T) of 2.996 minutes. OL has a molecular mass of 540 gram/ mole. The peak at m/z 538.07 on the mass spectra, represents that of OL in this study. A higher resolution mass spectra would probably have given values closer to 540 m/z. Furthermore, the UV-vis spectra of OL show a λ_{max} at 244 nm and 280 nm according to Klen *et al* (2010). In this study, we found that OL peaked at about 240 nm and 280 nm on the UV-vis spectra.

After the OL was detected with HPLC, the method used for its detection was validated based on the linearity, range, accuracy, precision, the limit of detection and limit of quantitation. Our results show that the linearity of the method was $r^2=$ 0.9991 over the range of 1 ppm to 300 ppm and the RSD values for concentrations of 2 ppm, 50 ppm, and 300 ppm were 102.6±1.30%, 98.31±1.01% and 98.33±0.78% respectively (Table 4.1). Despite a relatively poor separation from other compounds, OL had a peak purity of 1.4 and there was no co-elution with other compounds. This was confirmed by the UV spectra that shows that OL is the only compound in the peak. Our method thus met the criteria for accuracy,

repeatability and precision as described (Al-Rimawi, 2014) over a wide range. The LOD of the method was 1 ppm and the LOQ was determined to be 4 ppm which would allow OL in the *Olea* to be detected at a very low concentration. This is important since OL is sometimes present in trace amounts (Al-Rimawi, 2014).

In OA the OL recovery was 0.1% per dry weight basis and there was no OL present in the OE extract. It is, however, important to note that the plant material used in this study comes from one tree. The enzymatic oxidation of polyphenols, such as OL, results in brown products, as seen with maturing olive fruit. This could be because as soon as polyphenols are extracted, it also allows for the extraction of enzymes that break down OL (Garciá *et al.*, 2008, Lee, 1992). The aqueous extracts of OA and OE had a brown colour. This would probably not affect the antioxidant properties of the extract, as OL, if hydrolyzed, becomes hydrolyzed to hydroxytyrosol which has been described as having, like OL, biological activities such as antioxidant and anti-inflammatory properties (Khalatbary and Zarrinjoei, 2012).

In the OE extract, there was a peak eluting with an RT at 2.921 minutes on the HPLC chromatogram. This was seemingly OL. The UV-vis spectra of the peak were evaluated and it did not have the same λmax trends of OL. The presence of OL was then evaluated on the MS. The MS did not show any mass - to - charge ratio (m/z) that appears to be that of OL. The OE extract was then left out of subsequent experiments, as OL was used the compound for encapsulation determination and is the main bioactive compound in the olive leaf extract responsible for the pharmacological properties (Briante *et al.*, 2001).

Most bioactive compounds in plants are water-soluble, including OL (Saraf, 2010b, Jerman Klen et al., 2015). It is their poor lipid solubility that severely limits their ability to cross over the lipid-rich cell membranes and enter into cells (Saraf, 2010b). A suitable method to alter the biodistribution of poorly lipophilic agents is to encapsulate it into liposomes (Saraf, 2010b).

5.2 Preparation of a nanocarrier

Liposomes were formed using the lipid film hydration technique. For use in drug delivery applications, mono-dispersed liposomes in the 20 - 200 nm size range are preferred, with 100 nm particles being described as an ideal carrier size (Chen *et al*., 2016). In this study, extrusion was used to reduce the size of the MLVs. The extrusion of the liposomes was fast and easy. There was no congestion of the polycarbonate membrane. This could be because of the lipid - to – cholesterol ratio being 7:3 as well as a high temperature at which we worked. When the cholesterol content is higher the membrane would be less flexible. The membrane, with a 200 nm pore size, yielded liposomes with an average size of 134 nm in diameter. After extrusion through a 100 nm polycarbonate membrane, liposomes had a mean diameter of 109.6 nm and a PDI of 0.098. Ong *et al* (2016) found that when they extruded through a 200 nm polycarbonate membrane the liposome sizes were smaller than the membrane pore size and a pore size of 100 nm yielded liposomes sizes that were bigger than the polycarbonate membrane filter size. These results were confirmed by our own observations. Another method to reduce the size of nanoparticles is sonication, but results based on the size and PDI of liposomes by Ong (2016) show that extrusion was a superior method. The charge of the liposomes

in our study was -20.3 mV. Guzman-Villanueva *et al* (2015) also used phosphatidylcholine and cholesterol in a 7:3 ratio and found that liposomes formed had a charge of -31 mV. Furthermore, the study also used 100 nm polycarbonate filter to extrude their liposomes and found the average size to be 70 nm with a PDI of 0.2. The liposomes formed in their study then remained stable for 6 months (Guzman-Villanueva *et al*., 2015). Similarly, in our study, we observed that size and charge play a role in the stability of the liposomes.

Our liposome batch remained stable for 6 months. The particles seemed to be stable as confirmed by their size (111.2 nm) and charge (-24 mV). Furthermore, the results indicate that the liposomes were stable not only because of electrostatic repulsion offered by the charge, but size also played a role in the stability of the particles. Unextruded particles had the same charge, but there was flocculation of the particles (Figure 1A in the appendix). The pellet formed was easily dislodged by gentle agitation. This is because larger particle forms a sediment faster than smaller particles. In the 100 nm extruded batch, there were no visible sedimentation and particles did not aggregate or flocculate during the 6 month period tested. When the size and charge were taken, there was no change in size or charge and any small changes in the results were just because of the batch to batch variability that is associated with the dynamic light scattering technique.

The efficient entrapment of a drug in a liposome is important. Not only is it more economical, but if the drug entrapment is high, fewer liposomes can be used to treat cells. This would lead to cells being less saturated with lipids and reduce the incidence of lipid oxidation (Kirby and Gregoriadis, 1984). The encapsulation

efficiency of liposomes was 24%. The lipid-film hydration, used in this study has been described to result in poor encapsulation of drugs. It was, however, the most practical method to be employed in our laboratory. Using the lipid- film hydration technique, Yuan *et al*., (2017) found that encapsulating hydroxytyrosol at the aqueous phase, like we did with our compounds, produced an encapsulation efficiency of 45.08% (Yuan *et al*., 2017). Two ways to improve the encapsulation efficiency of our experiments is explained below. The freeze-thaw method allows for an increase in the entrapped volume into the liposome, and consequently a better encapsulation of water-soluble drugs. The repeated physical disruption of the lipid membrane allows the encapsulation efficiency to be increased (Popovska, 2014). Another way by which the encapsulation efficiency can be improved is by increasing the drug to lipid ratio when liposomes are formed. Using the latter method Plangsombat *et al* (2016) were able to improve the encapsulation of an aqueous extract, added to the aqueous – phase of liposome formation, from 14.02% to 55.71%, depending on the drug-lipid ratio (Plangsombat *et al*., 2016). The HPLC data, however, was not done in our department and due to delays in obtaining the results we had to proceed without knowing the encapsulation efficiency or having the opportunity to improve the encapsulation efficiency of our products.

Liposomes can be tagged with fluorescent dyes by post-formation, conjugation or incorporation of a fluorescent molecule during liposome formation. This allows for the tracking of the liposome inside the cell, the quantitation of liposome uptake or to do drug release studies (Costanzo *et al*., 2016, Claassen, 1992). By tagging the nanoparticles with rhodamine 123, we could evaluate the uptake of nanoparticles by the cell using confocal microscopy. We found that nanoparticles were

115 | P a g e

present in the H9c2 cells at the 24 hour time point. The nanoparticles did not localize to a specific site in the cell and instead were distributed evenly in the cytoplasm. There was also no nanoparticles adsorbed on the surface of the cell and it is assumed that the particles were taken up by endocytosis.

5.3 Evaluate the potential cardioprotective effects of OA and OL

In this study, cells were grown to 80% confluence and incubated with serum-free medium. This was done to minimize cell proliferation. Cardiomyocytes proliferate during foetal development. After birth, however, proliferation ceases as cells withdraw from the cell cycle. This suggests that any events happening in adult cardiomyocytes proceed under cell arrest (Oyama *et al*., 2011). H9c2 cells are foetal cardiomyoblast that has been transformed into a proliferating cell line. In humans, heart cells are post-mitotic and still remain in the G_0/G_1 cell cycle. When cells are grown to 80% confluence and exposed to the serum - free medium, cells enter the cell cycle in the phase G_0/G_1.

At first, cells were exposed to OA and OL only. This was to test whether any survival of cells observed was in fact associated with cell survival, rather than cell proliferation. Furthermore, we exposed cells to OA and OL only, to ensure that the treatments do not cause any decrease in cell viability. OA and OL at all the concentrations tested did not significantly affect cell viability as compared to the non-treated control. Similar to our results, Choi *et al* (2015) reported that OL (1-100 µM) had no effects on cell viability of human vascular progenitor cells.

After a 24 hour pretreatment with OA and OL, the H9c2 cells were exposed to H_2O_2. Hydrogen peroxide has been used extensively in the *in vitro* induction of oxidative stress. Subconfluent H9c2 cells were treated with H_2O_2 to identify the cytotoxic range of H_2O_2. The concentration of hydrogen peroxide used in subsequent experiments was 550 µM, which reduced cell viability to 58%. Photomicrographs reveal that H9c2 cells when exposed to 550 µM cells showed morphological changes and cells become detached (Figure 2A in the appendix), indicating cell death. Detachment is an indication of apoptosis in adherent cells (Oliveira-Ferrer *et al*., 2008).

OLE and OL could not protect against hydrogen peroxide - induced stress, when assayed by MTT and JC-1. We thus used a different stressor, doxorubicin, and a more sensitive assay, the ATP assay, to evaluate the cardioprotective effects of OA and OL. At all the time points tested preincubation with OA and OL, as both an encapsulated and free drug did not afford protection.

The ability of olive leaf extracts and OL to protect different cell lines from oxidative stress have been reported recently. OL has been proven to have high antioxidant activity *in vitro* (Al-Azzawie and Alhamdani, 2006, Saija *et al*., 1998, Speroni *et al*., 1998). OL was able to significantly decrease intracellular ROS levels after angiotensin II treatment in human vascular progenitor cells (Choi *et al*., 2015). An ethanolic olive leave extract and OL protected INS-1 pancreatic cells against H_2O_2 – induced toxicity. It could however not completely ameliorate cell viability (Cumaoglu *et al*., 2011). The possible neuroprotective effect of an ethanolic olive leaf extract and its main phenolic constituent, OL, were also investigated in 6-

Hydroxydopamine (6-OHDA) – induced stress in the rat pheochromocytoma (PC12) cell line. The 6-OHDA stressor exerts its effects through oxidative damage of mitochondria via free radical-induced lipid peroxidation. Concentrations of 20 µg/ml and 25 µg/ml OL were able to protect against 6-OHDA–induced cell death and this concentration completely ameliorated cell viability as compared to the control. Furthermore, 200 µg/ml, 400 µg/ml and 600 µg/ml of the olive leaf extract also protected the cells from oxidative stress. Both the olive leaf extract and OL worked by scavenging intracellular ROS (Pasban-Aliabadi *et al*., 2013). The ethanolic olive leaf extract and OL were able to protect H9c2 cardiomyocytes from 4-Hydroxynonenal-induce toxicity *in vitro* (Bali *et al*., 2014).
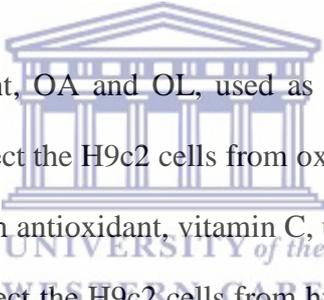
In our current experiment, OA and OL, used as a free drug or encapsulated in liposomes could not protect the H9c2 cells from oxidative stress. This was a rather unexpected result since an antioxidant, vitamin C, used in previous experiments in our laboratory could protect the H9c2 cells from hydrogen peroxide stress (results not shown). Furthermore, water extracts from the OA leaves have been proven to have angiotensin converting enzyme (ACE) inhibitor properties, which should also improve cell viability via a PKB signaling pathway. Experiments (not published) from our laboratory showed that an olive leave extract, added to the drinking water of rats for four weeks, increase PKB levels in the heart significantly. The ACE blocking activities of the OA extract had been attributed to the activity of OL (Hashmi *et al*., 2015, Parzonko *et al*., 2013). The deviant result in our study possibly could be because of the pre-incubation time and other improvements that could be made in this study as listed below.

In conclusion, we found that OL was present in our OA extract but was not present in our OE extract. We determined the OL content of our OA extract by HPLC and mass spectrometry and validated the method for linearity, range, accuracy, precision, limit of detection and limit of quantification. Furthermore, we designed a suitable nanocarrier that had a good size and charge and that was stable for 6 months. The liposomes designed were able to enter H9c2 cells and was able to encapsulate the compounds tested. Finally, we assessed the ability of OL and the aqueous extract to protect H9c2 cells from oxidative stress. We found that OA or OL as a free drug, or encapsulated in nanoliposomes, did not protect the H9c2 cells against hydrogen peroxide or doxorubicin-induced stress.

Shortcomings and Future directions

To improve this study we could:

1. Improve the encapsulation efficiency of our compound

2. Include a drug release study to ensure that the liposome releases/ their contents into the cells. Just because liposomes entered the cell, does not mean that the drugs were released.

3. The liposomes could be targeted to the mitochondria since the mitochondria are the main source of ROS formation.

4. Determine the phenol content of the extract.

Include a positive control such as vitamin C which, in our hands, was shown to protect H9c2 cells from hydrogen peroxide - induced toxicity.

BIBLIOGRAPHY

ADAMS, L. S., SEERAM, N. P., HARDY, M. L., CARPENTER, C. & HEBER, D. 2006. Analysis of the interactions of botanical extract combinations against the viability of prostate cancer cell lines. *Evidence-Based Complementary and Alternative Medicine,* 3**,** 117-124.

AFANEH, I., YATEEM, H. & AL-RIMAWI, F. 2015. Effect of olive leaves drying on the content of oleuropein. *American Journal of Analytical Chemistry,* 6**,** 246.

AHMAD-QASEM, M. H., BARRAJÓN-CATALÁN, E., MICOL, V., MULET, A. & GARCÍA-PÉREZ, J. V. 2013. Influence of freezing and dehydration of olive leaves (var. Serrana) on extract composition and antioxidant potential. *Food Research International,* 50**,** 189-196.

AKBARZADEH, A., REZAEI-SADABADY, R., DAVARAN, S., JOO, S. W., ZARGHAMI, N., HANIFEHPOUR, Y., SAMIEI, M., KOUHI, M. & NEJATI-KOSHKI, K. 2013. Liposome: classification, preparation, and applications. *Nanoscale research letters,* 8**,** 1.

AL-AZZAWIE, H. F. & ALHAMDANI, M.-S. S. 2006. Hypoglycemic and antioxidant effect of oleuropein in alloxan-diabetic rabbits. *Life sciences,* 78**,** 1371-1377.

AL-RIMAWI, F. 2014. Development and validation of a simple reversed-phase HPLC-UV method for determination of oleuropein in olive leaves. *journal of food and drug analysis,* 22**,** 285-289.

AMES, B. N., SHIGENAGA, M. K. & HAGEN, T. M. 1993. Oxidants, antioxidants, and the degenerative diseases of aging. *Proceedings of the National Academy of Sciences,* 90**,** 7915-7922.

ARMSTRONG, R. N. 1997. Structure, catalytic mechanism, and evolution of the glutathione transferases. *Chemical research in toxicology,* 10**,** 2-18.

ARVIZO, R. R., MIRANDA, O. R., THOMPSON, M. A., PABELICK, C. M., BHATTACHARYA, R., ROBERTSON, J. D., ROTELLO, V. M., PRAKASH, Y. & MUKHERJEE, P. 2010. Effect of nanoparticle surface charge at the plasma membrane and beyond. *Nano letters,* 10**,** 2543-2548.

ATALE, N., CHAKRABORTY, M., MOHANTY, S., BHATTACHARYA, S., NIGAM, D., SHARMA, M. & RANI, V. 2013. Cardioprotective role of Syzygium cumini against glucose-induced oxidative stress in H9C2 cardiac myocytes. *Cardiovascular toxicology,* 13**,** 278-289.

BALI, E. B., ERGIN, V., RACKOVA, L., BAYRAKTAR, O., KÜÇÜKBOYACi, N. & KARASU, Ç. 2014. Olive leaf extracts protect cardiomyocytes against 4-hydroxynonenal-induced toxicity in vitro: Comparison with oleuropein, hydroxytyrosol, and quercetin. *Planta medica,* 80**,** 984-992.

BANERJEE, R., TYAGI, P., LI, S. & HUANG, L. 2004. Anisamide-targeted
stealth liposomes: A potent carrier for targeting doxorubicin to human
prostate cancer cells. *International journal of cancer,* 112**,** 693-700.

BARBARO, B., TOIETTA, G., MAGGIO, R., ARCIELLO, M., TAROCCHI, M.,
GALLI, A. & BALSANO, C. 2014. Effects of the olive-derived
polyphenol oleuropein on human health. *International journal of
molecular sciences,* 15**,** 18508-18524.

BARENHOLZ, Y. 2003. Relevancy of drug loading to liposomal formulation
therapeutic efficacy. *Journal of liposome research,* 13**,** 1-8.

BLANCO, E., SHEN, H. & FERRARI, M. 2015. Principles of nanoparticle
design for overcoming biological barriers to drug delivery. *Nature
biotechnology,* 33**,** 941-951.

BOCK, M., THORSTENSEN, E. B., DERRAIK, J. G., HENDERSON, H. V.,
HOFMAN, P. L. & CUTFIELD, W. S. 2013. Human absorption and
metabolism of oleuropein and hydroxytyrosol ingested as olive (Olea
europaea L.) leaf extract. *Molecular nutrition & food research,* 57**,** 2079-
2085.

BONIFÁCIO, B. V., DA SILVA, P. B., DOS SANTOS RAMOS, M. A., NEGRI, K. M. S., BAUAB, T. M. & CHORILLI, M. 2014. Nanotechnology-based drug delivery systems and herbal medicines: a review. *International journal of nanomedicine,* 9**,** 1.

BOZZUTO, G. & MOLINARI, A. 2015. Liposomes as nanomedical devices. *International journal of nanomedicine,* 10**,** 975.

BRIANTE, R., LA CARA, F., TONZIELLO, M. P., FEBBRAIO, F. & NUCCI, R. 2001. Antioxidant activity of the main bioactive derivatives from oleuropein hydrolysis by hyperthermophilic β-glycosidase. *Journal of agricultural and food chemistry,* 49**,** 3198-3203.

BULOTTA, S., CELANO, M., LEPORE, S. M., MONTALCINI, T., PUJIA, A. & RUSSO, D. 2014. Beneficial effects of the olive oil phenolic components oleuropein and hydroxytyrosol: focus on protection against cardiovascular and metabolic diseases. *Journal of translational medicine,* 12**,** 1-22.

CARLUCCIO, M. A., SICULELLA, L., ANCORA, M. A., MASSARO, M., SCODITTI, E., STORELLI, C., VISIOLI, F., DISTANTE, A. & DE CATERINA, R. 2003. Olive oil and red wine antioxidant polyphenols inhibit endothelial activation antiatherogenic properties of mediterranean diet phytochemicals. *Arteriosclerosis, thrombosis, and vascular biology,* 23**,** 622-629.

CHEN, G., ROY, I., YANG, C. & PRASAD, P. N. 2016. Nanochemistry and nanomedicine for nanoparticle-based diagnostics and therapy. *Chemical reviews,* 116**,** 2826-2885.

CHEN, L., WRIGHT, L. R., CHEN, C.-H., OLIVER, S. F., WENDER, P. A. & MOCHLY-ROSEN, D. 2001. Molecular transporters for peptides: delivery of a cardioprotective ϵPKC agonist peptide into cells and intact ischemic heart using a transport system, R 7. *Chemistry & biology,* 8**,** 1123-1129.

CHEN, Q. M., TU, V. C., WU, Y. & BAHL, J. J. 2000. Hydrogen peroxide dose dependent induction of cell death or hypertrophy in cardiomyocytes. *Archives of biochemistry and biophysics,* 373**,** 242-248.
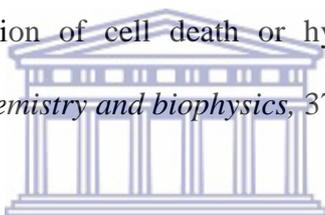
CHOI, S. H., JOO, H. B., LEE, S. J., CHOI, H. Y., PARK, J. H., BAEK, S. H. & KWON, S. M. 2015. Oleuropein prevents angiotensin II-mediated. *International journal of cardiology,* 181**,** 160-165.

CLAASSEN, E. 1992. Post-formation fluorescent labelling of liposomal membranes: in vivo detection, localisation and kinetics. *Journal of immunological methods,* 147**,** 231-240.

CONI, E., DI BENEDETTO, R., DI PASQUALE, M., MASELLA, R., MODESTI, D., MATTEI, R. & CARLINI, E. 2000. Protective effect of oleuropein, an olive oil biophenol, on low density lipoprotein oxidizability in rabbits. *Lipids,* 35**,** 45-54.

COOK, C., COLE, G., ASARIA, P., JABBOUR, R. & FRANCIS, D. P. 2014. The annual global economic burden of heart failure. *International journal of cardiology,* 171**,** 368-376.

COSTANZO, M., CARTON, F., MARENGO, A., BERLIER, G., STELLA, B., ARPICCO, S. & MALATESTA, M. 2016. Fluorescence and electron microscopy to visualize the intracellular fate of nanoparticles for drug delivery. *European journal of histochemistry: EJH,* 60.

CRISTIANA, F., NINA, Z. & ELENA, A. 2012. Homocysteine in Red Blood Cells Metabolism-Pharmacological Approaches. *Blood Cell-An Overview of Studies in Hematology.* InTech.

CZAPLICKI, S. 2013. Chromatography in Bioactivity Analysis of Compounds. *Column Chromatography.* InTech.

DAI, D.-F., CHIAO, Y. A., MARCINEK, D. J., SZETO, H. H. & RABINOVITCH, P. S. 2014. Mitochondrial oxidative stress in aging and healthspan. *Longev Healthspan,* 3**,** 1-22.

DAI, D.-F. & RABINOVITCH, P. S. 2009. Cardiac aging in mice and humans: the role of mitochondrial oxidative stress. *Trends in cardiovascular medicine,* 19**,** 213-220.

DE CASTRO, M. L. & CAPOTE, F. P. Extraction of Oleuropein and Related Phenols from Olive Leaves and Branches-Chapter 28.

DEMMING, A. 2011. Nanotechnology under the skin. *Nanotechnology,* 22**,** 260201.

DUARTE, T. L. & JONES, G. D. 2007. Vitamin C modulation of H 2 O 2-induced damage and iron homeostasis in human cells. *Free Radical Biology and Medicine,* 43**,** 1165-1175.

EKHTERAE, D., LIN, Z., LUNDBERG, M. S., CROW, M. T., BROSIUS, F. C. & NÚÑEZ, G. 1999. ARC inhibits cytochrome c release from mitochondria and protects against hypoxia-induced apoptosis in heart-derived H9c2 cells. *Circulation research,* 85**,** e70-e77.
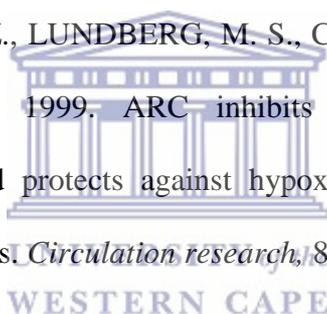
ESMAEILI, M. A. & SONBOLI, A. 2010. Antioxidant, free radical scavenging activities of Salvia brachyantha and its protective effect against oxidative cardiac cell injury. *Food and Chemical Toxicology,* 48**,** 846-853.

EZE, M. O. 1991. Phase transitions in phospholipid bilayers: lateral phase separations play vital roles in biomembranes. *Biochemical education,* 19**,** 204-208.

FINKEL, T. & HOLBROOK, N. J. 2000. Oxidants, oxidative stress and the biology of ageing. *Nature,* 408**,** 239-247.

FREITAS, R. A. 2005. What is nanomedicine? *Nanomedicine: Nanotechnology, Biology and Medicine,* 1**,** 2-9.

GARCÍA, A., ROMERO, C., MEDINA, E., GARCÍA, P., DE CASTRO, A. & BRENES, M. 2008. Debittering of olives by polyphenol oxidation. *Journal of agricultural and food chemistry,* 56**,** 11862-11867.

GATOO, M. A., NASEEM, S., ARFAT, M. Y., MAHMOOD DAR, A., QASIM, K. & ZUBAIR, S. 2014. Physicochemical properties of nanomaterials: implication in associated toxic manifestations. *BioMed research international,* 2014.
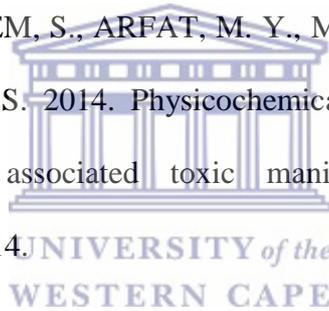
GIORDANO, F. J. 2005. Oxygen, oxidative stress, hypoxia, and heart failure. *The Journal of clinical investigation,* 115**,** 500-508.

GOFFART, S., VON KLEIST-RETZOW, J.-C. & WIESNER, R. J. 2004. Regulation of mitochondrial proliferation in the heart: power-plant failure contributes to cardiac failure in hypertrophy. *Cardiovascular Research,* 64**,** 198-207.

GUIMARÃES-FERREIRA, L. 2014. Role of the phosphocreatine system on energetic homeostasis in skeletal and cardiac muscles. *Einstein (São Paulo),* 12**,** 126-131.

GUZMAN-VILLANUEVA, D., MENDIOLA, M. R., NGUYEN, H. X. & WEISSIG, V. 2015. Influence of triphenylphosphonium (TPP) cation hydrophobization with phospholipids on cellular toxicity and mitochondrial selectivity. *SOJ Pharm Pharm Sci,* 2**,** 1-9.

HALLIWELL, B. 1994. Free radicals and antioxidants: a personal view. *Nutrition reviews,* 52**,** 253-265.

HAN, H., LONG, H., WANG, H., WANG, J., ZHANG, Y. & WANG, Z. 2004. Progressive apoptotic cell death triggered by transient oxidative insult in H9c2 rat ventricular cells: a novel pattern of apoptosis and the mechanisms. *American Journal of Physiology-Heart and Circulatory Physiology,* 286**,** H2169-H2182.

HASHMI, M. A., KHAN, A., HANIF, M., FAROOQ, U. & PERVEEN, S. 2015. Traditional uses, phytochemistry, and pharmacology of Olea europaea (olive). *Evidence-Based Complementary and Alternative Medicine,* 2015.

HEO, J. M., KIM, H. J., HA, Y. M., PARK, M. K., KANG, Y. J., LEE, Y. S., SEO, H. G., LEE, J. H., YUN-CHOI, H. S. & CHANG, K. C. 2007. YS 51, 1-(β-naphtylmethyl)-6, 7-dihydroxy-1, 2, 3, 4,-tetrahydroisoquinoline, protects endothelial cells against hydrogen peroxide-induced injury via carbon monoxide derived from heme oxygenase-1. *Biochemical pharmacology,* 74**,** 1361-1370.

HESCHELER, J., MEYER, R., PLANT, S., KRAUTWURST, D., ROSENTHAL, W. & SCHULTZ, G. 1991. Morphological, biochemical, and electrophysiological characterization of a clonal cell (H9c2) line from rat heart. *Circulation research,* 69**,** 1476-1486.
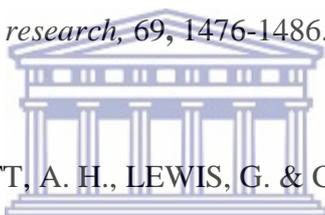
HUTCHINGS, A., SCOTT, A. H., LEWIS, G. & CUNNINGHAM, A. B. 1996. *Zulu medicinal plants: an inventory,* University of Kwazulu Natal Press.

JEONG, J. J., HA, Y. M., JIN, Y. C., LEE, E. J., KIM, J. S., KIM, H. J., SEO, H. G., LEE, J. H., KANG, S. S. & KIM, Y. S. 2009. Rutin from Lonicera japonica inhibits myocardial ischemia/reperfusion-induced apoptosis in vivo and protects H9c2 cells against hydrogen peroxide-mediated injury via ERK1/2 and PI3K/Akt signals in vitro. *Food and Chemical Toxicology,* 47**,** 1569-1576.

JERMAN KLEN, T., GOLC WONDRA, A., VRHOVSEK, U. K. & MOZETIC
VODOPIVEC, B. 2015. Phenolic profiling of olives and olive oil process-
derived matrices using UPLC-DAD-ESI-QTOF-HRMS analysis. *Journal
of agricultural and food chemistry,* 63**,** 3859-3872.

JIA, G., AROOR, A. R. & SOWERS, J. R. 2014. Estrogen and mitochondria
function in cardiorenal metabolic syndrome. *Progress in molecular
biology and translational science,* 127**,** 229.

KHALATBARY, A. & ZARRINJOEI, G. R. 2012. Anti-inflammatory effect of
oleuropein in experimental rat spinal cord trauma. *Iranian red crescent
medical journal,* 14**,** 229.

KIRBY, C. & GREGORIADIS, G. 1984. Dehydration-rehydration vesicles: a
simple method for high yield drug entrapment in liposomes. *Nature
Biotechnology,* 2**,** 979-984.

KUMARI, A., KUMAR, V. & YADAV, S. 2012. Nanotechnology: a tool to
enhance therapeutic values of natural plant products. *Trends in Medical
Research,* 7**,** 34-42.

LALL, N. & KISHORE, N. 2014. Are plants used for skin care in South Africa
fully explored? *Journal of ethnopharmacology,* 153**,** 61-84.

LAMMERS, T. 2013. Smart drug delivery systems: back to the future vs. clinical reality. *International journal of pharmaceutics,* 454**,** 527-529.

LAZAROVITS, J., CHEN, Y. Y., SYKES, E. A. & CHAN, W. C. 2015. Nanoparticle–blood interactions: the implications on solid tumour targeting. *Chemical Communications,* 51**,** 2756-2767.

LEE, C. Y. 1992. Enzymatic oxidation of phenolic compounds in fruits. ACS Publications.

LI, J.-M., ZHOU, H., CAI, Q. & XIAO, G.-X. 2003. Role of mitochondrial dysfunction in hydrogen peroxide-induced apoptosis of intestinal epithelial cells. *World journal of gastroenterology,* 9**,** 562.

LINDGREN, M., HÄLLBRINK, M., PROCHIANTZ, A. & LANGEL, Ü. 2000. Cell-penetrating peptides. *Trends in pharmacological sciences,* 21**,** 99-103.

LONG, H., TILNEY, P. & VAN WYK, B.-E. 2010. The ethnobotany and pharmacognosy of Olea europaea subsp. africana (Oleaceae). *South African Journal of Botany,* 76**,** 324-331.

MAIOLI, E., TORRICELLI, C., FORTINO, V., CARLUCCI, F., TOMMASSINI, V. & PACINI, A. 2009. Critical appraisal of the MTT assay in the presence of rottlerin and uncouplers. *Biological procedures online,* 11**,** 227.

MALIK, N. S. & BRADFORD, J. M. 2008. Recovery and stability of oleuropein and other phenolic compounds during extraction and processing of olive (Olea europaea L.) leaves. *Journal of Food Agriculture and Environment,* 6**,** 8.

MANNA, C., MIGLIARDI, V., GOLINO, P., SCOGNAMIGLIO, A., GALLETTI, P., CHIARIELLO, M. & ZAPPIA, V. 2004. Oleuropein prevents oxidative myocardial injury induced by ischemia and reperfusion. *The journal of nutritional biochemistry,* 15**,** 461-466.

MASOKO, P. & MAKGAPEETJA, D. M. 2015. Antibacterial, antifungal and antioxidant activity of Olea africana against pathogenic yeast and nosocomial pathogens. *BMC complementary and alternative medicine,* 15**,** 409.

MCCORD, J. M. & FRIDOVICH, I. 1969. Superoxide dismutase an enzymic function for erythrocuprein (hemocuprein). *Journal of Biological chemistry,* 244**,** 6049-6055.

MEDIANI, A., ABAS, F., TAN, C. P. & KHATIB, A. 2014. Effects of different drying methods and storage time on free radical scavenging activity and total phenolic content of Cosmos caudatus. *Antioxidants,* 3**,** 358-370.

MITRAGOTRI, S., LAMMERS, T., BAE, Y. H., SCHWENDEMAN, S., DE SMEDT, S., LEROUX, J.-C., PEER, D., KWON, I. C., HARASHIMA, H. & KIKUCHI, A. 2017. Drug Delivery Research for the Future: Expanding the Nano Horizons and Beyond. *Journal of controlled release: official journal of the Controlled Release Society,* 246**,** 183.

MOURTZINOS, I., SALTA, F., YANNAKOPOULOU, K., CHIOU, A. & KARATHANOS, V. T. 2007. Encapsulation of olive leaf extract in β-cyclodextrin. *J. of Agricultural and Food Chemistry,* 55**,** 8088-8094.

MYLONAKI, S., KIASSOS, E., MAKRIS, D. P. & KEFALAS, P. 2008. Optimisation of the extraction of olive (Olea europaea) leaf phenolics using water/ethanol-based solvent systems and response surface methodology. *Analytical and Bioanalytical Chemistry,* 392**,** 977-985.

NII, T. & ISHII, F. 2005. Encapsulation efficiency of water-soluble and insoluble drugs in liposomes prepared by the microencapsulation vesicle method. *International journal of pharmaceutics,* 298**,** 198-205.

OHNISHI, N., YAMAMOTO, E., TOMIDA, H., HYODO, K., ISHIHARA, H., KIKUCHI, H., TAHARA, K. & TAKEUCHI, H. 2013. Rapid determination of the encapsulation efficiency of a liposome formulation

using column-switching HPLC. *International journal of pharmaceutics,* 441**,** 67-74.

OLIVEIRA-FERRER, L., HAUSCHILD, J., FIEDLER, W., BOKEMEYER, C., NIPPGEN, J., CELIK, I. & SCHUCH, G. 2008. Cilengitide induces cellular detachment and apoptosis in endothelial and glioma cells mediated by inhibition of FAK/src/AKT pathway. *Journal of Experimental & Clinical Cancer Research,* 27**,** 86.

OSIM, E., MBAJIORGU, E., MUKARATI, G., VAZ, R., MAKUFA, B., MUNJERI, O. & MUSABAYANE, C. 1999. Hypotensive effect of crude extract Olea. africana (Oleaceae) in normo and hypertensive rats. *The Central African journal of medicine,* 45**,** 269-274.
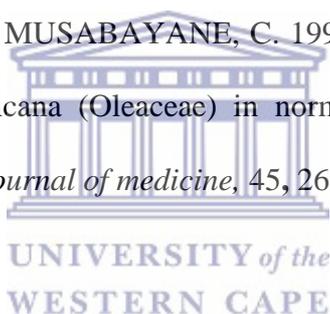
OYAMA, K., TAKAHASHI, K. & SAKURAI, K. 2011. Hydrogen peroxide induces cell cycle arrest in cardiomyoblast H9c2 cells, which is related to hypertrophy. *Biological and Pharmaceutical Bulletin,* 34**,** 501-506.

PAGANO, R. E. & WEINSTEIN, J. N. 1978. Interactions of liposomes with mammalian cells. *Annual review of biophysics and bioengineering,* 7**,** 435-468.

PARZONKO, A., CZERWIŃSKA, M. E., KISS, A. K. & NARUSZEWICZ, M. 2013. Oleuropein and oleacein may restore biological functions of endothelial progenitor cells impaired by angiotensin II via activation of Nrf2/heme oxygenase-1 pathway. *Phytomedicine,* 20**,** 1088-1094.

PASBAN-ALIABADI, H., ESMAEILI-MAHANI, S., SHEIBANI, V., ABBASNEJAD, M., MEHDIZADEH, A. & YAGHOOBI, M. M. 2013. Inhibition of 6-hydroxydopamine-induced PC12 cell apoptosis by olive (Olea europaea L.) leaf extract is performed by its main component oleuropein. *Rejuvenation research,* 16**,** 134-142.

PERAGÓN, J., RUFINO-PALOMARES, E. E., MUÑOZ-ESPADA, I., REYES-ZURITA, F. J. & LUPIÁÑEZ, J. A. 2015. A new HPLC-MS method for measuring maslinic acid and oleanolic acid in HT29 and HepG2 human cancer cells. *International journal of molecular sciences,* 16**,** 21681-21694.

PERRY, S. W., NORMAN, J. P., BARBIERI, J., BROWN, E. B. & GELBARD, H. A. 2011. Mitochondrial membrane potential probes and the proton gradient: a practical usage guide. *Biotechniques,* 50**,** 98.
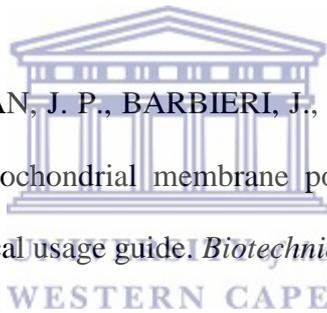
PETRONI, A., BLASEVICH, M., SALAMI, M., PAPINI, N., MONTEDORO, G. F. & GALLI, C. 1995. Inhibition of platelet aggregation and eicosanoid production by phenolic components of olive oil. *Thrombosis research,* 78**,** 151-160.

PINSUWAN, S., AMNUAIKIT, T., UNGPHAIBOON, S. & ITHARAT, A. 2010. Liposome-containing Hibiscus sabdariffa calyx extract formulations with increased antioxidant activity, improved dermal penetration and reduced dermal toxicity. *Journal of the Medical Association of Thailand= Chotmaihet thangphaet,* 93**,** S216-26.

PLANGSOMBAT, N., RUNGSARDTHONG, K., KONGKANERAMIT, L., WARANUCH, N. & SARISUTA, N. 2016. Anti-inflammatory activity of liposomes of Asparagus racemosus root extracts prepared by various methods. *Experimental and therapeutic medicine,* 12**,** 2790-2796.

POPOVSKA, O. 2014. An overview: methods for preparation and characterization of liposomes as drug delivery systems. *International Journal of Pharmaceutical and Phytopharmacological Research,* 3.

RANI, D. 2013. Liposome as a potential drug delivery system: a review. *International Research Journal of Pharmacy,* 4**,** 1-12.

RANKI, H. J., BUDAS, G. R., CRAWFORD, R. M., DAVIES, A. M. & JOVANOVIĆ, A. 2002. 17β-estradiol regulates expression of KATP channels in heart-derived H9c2 cells. *Journal of the American College of Cardiology,* 40**,** 367-374.

RASKIN, I., RIBNICKY, D. M., KOMARNYTSKY, S., ILIC, N., POULEV, A., BORISJUK, N., BRINKER, A., MORENO, D. A., RIPOLL, C. & YAKOBY, N. 2002. Plants and human health in the twenty-first century. *TRENDS in Biotechnology,* 20**,** 522-531.

RICE-EVANS, C., MILLER, N. & PAGANGA, G. 1997. Antioxidant properties of phenolic compounds. *Trends in plant science,* 2**,** 152-159.

RICHTER, M. 2003. Traditional medicines and traditional healers in South Africa. *Treatment action campaign and AIDS law project,* 17**,** 4-29.

SACHSE, A., LEIKE, J. U., RÖLING, G. L., WAGNER, S. E. & KRAUSE, W. 1993. Preparation and evaluation of lyophilized iopromide-carrying liposomes for liver tumor detection. *Investigative radiology,* 28**,** 838-844.

SAHOO, S., PARVEEN, S. & PANDA, J. 2007. The present and future of nanotechnology in human health care. *Nanomedicine: Nanotechnology, Biology and Medicine,* 3**,** 20-31.

SAIJA, A., TROMBETTA, D., TOMAINO, A., CASCIO, R. L., PRINCI, P., UCCELLA, N., BONINA, F. & CASTELLI, F. 1998. In vitro'evaluation of the antioxidant activity and biomembrane interaction of the plant phenols oleuropein and hydroxytyrosol. *International Journal of Pharmaceutics,* 166**,** 123-133.

SARAF, A. 2010a. Phytochemical and antimicrobial studies of medicinal plant Costus speciosus (Koen.). *Journal of Chemistry,* 7**,** S405-S413.

SARAF, S. 2010b. Applications of novel drug delivery system for herbal formulations. *Fitoterapia,* 81**,** 680-689.

SCHNEIDER, T., SACHSE, A., RÖBLING, G. & BRANDL, M. 1995. Generation of contrast-carrying liposomes of defined size with a new continuous high pressure extrusion method. *International journal of pharmaceutics,* 117**,** 1-12.

SCHRÖDER, E. & EATON, P. 2008. Hydrogen peroxide as an endogenous mediator and exogenous tool in cardiovascular research: issues and considerations. *Current opinion in pharmacology,* 8**,** 153-159.

SHEU, S.-S., NAUDURI, D. & ANDERS, M. 2006. Targeting antioxidants to mitochondria: a new therapeutic direction. *Biochimica et Biophysica Acta (BBA)-Molecular Basis of Disease,* 1762**,** 256-265.

SHI, J., VOTRUBA, A. R., FAROKHZAD, O. C. & LANGER, R. 2010. Nanotechnology in drug delivery and tissue engineering: from discovery to applications. *Nano letters,* 10**,** 3223-3230.

ŠKÁRKA, L. & OŠTÁDAL, B. 2002. Mitochondrial membrane potential in cardiac myocytes. *Physiol Res,* 51**,** 425-434.

SOMOVA, L., SHODE, F., RAMNANAN, P. & NADAR, A. 2003. Antihypertensive, antiatherosclerotic and antioxidant activity of triterpenoids isolated from Olea europaea, subspecies africana leaves. *Journal of ethnopharmacology,* 84**,** 299-305.

SPERONI, E., GUERRA, M., MINGHETTI, A., CRESPI-PERELLINO, N., PASINI, P., PIAZZA, F. & RODA, A. 1998. Oleuropein evaluated in vitro and in vivo as an antioxidant. *Phytotherapy Research,* 12.

STRAMBEANU, N., DEMETROVICI, L., DRAGOS, D. & LUNGU, M. 2015. Nanoparticles: Definition, Classification and General Physical Properties. *Nanoparticles' Promises and Risks.* Springer.

SWARTZ, M. 2010. HPLC detectors: a brief review. *Journal of Liquid Chromatography & Related Technologies,* 33**,** 1130-1150.

TAKAHASHI, M., KITAMOTO, D., ASIKIN, Y., TAKARA, K. & WADA, K. 2009. Liposomes encapsulating Aloe vera leaf gel extract significantly enhance proliferation and collagen synthesis in human skin cell lines. *Journal of oleo science,* 58, 643-650.

TAKAHASHI, R., KAWAWA, A. & KUBOTA, S. 2006. Short time exposure to hypoxia promotes H9c2 cell growth. *Biochimica et Biophysica Acta (BBA)-General Subjects,* 1760**,** 1293-1297.

TAYLOR, J., RABE, T., MCGAW, L., JÄGER, A. & VAN STADEN, J. 2001. Towards the scientific validation of traditional medicinal plants. *Plant growth regulation,* 34**,** 23-37.

TSAI, W.-C., LI, W.-C., YIN, H.-Y., YU, M.-C. & WEN, H.-W. 2012. Constructing liposomal nanovesicles of ginseng extract against hydrogen peroxide-induced oxidative damage to L929 cells. *Food Chemistry,* 132**,** 744-751.

TSUKAMOTO, H., HISADA, S., NISHIBE, S. & ROUX, D. G. 1984. Phenolic glucosides from Olea europaea subs. africana. *Phytochemistry,* 23**,** 2839-2841.

TUCK, K. L. & HAYBALL, P. J. 2002. Major phenolic compounds in olive oil: metabolism and health effects. *The Journal of nutritional biochemistry,* 13**,** 636-644.

VAN BLADEREN, P. J. 2000. Glutathione conjugation as a bioactivation reaction. *Chemico-biological interactions,* 129**,** 61-76.

VAN TONDER, A., JOUBERT, A. M. & CROMARTY, A. D. 2015. Limitations of the 3-(4, 5-dimethylthiazol-2-yl)-2, 5-diphenyl-2H-tetrazolium bromide (MTT) assay when compared to three commonly used cell enumeration assays. *BMC research notes,* 8**,** 47.

VISIOLI, F. & GALLI, C. 1994. Oleuropein protects low density lipoprotein from oxidation. *Life sciences,* 55**,** 1965-1971.

WAGNER, S., GONDIKAS, A., NEUBAUER, E., HOFMANN, T. & VON DER KAMMER, F. 2014. Spot the difference: engineered and natural nanoparticles in the environment—release, behavior, and fate. *Angewandte Chemie International Edition,* 53**,** 12398-12419.

WALLACE, D. C. 2006. A mitochondrial paradigm of metabolic and degenerative diseases, aging, and cancer: a dawn for evolutionary medicine. *The FASEB Journal,* 20**,** A1474.

WISEMAN, S. A., MATHOT, J. N., DE FOUW, N. J. & TIJBURG, L. B. 1996. Dietary non-tocopherol antioxidants present in extra virgin olive oil increase the resistance of low density lipoproteins to oxidation in rabbits. *Atherosclerosis,* 120**,** 15-23.

WITTING, P. K., LIAO, W.-Q., HARRIS, M. J. & NEUZIL, J. 2006. Expression of human myoglobin in H9c2 cells enhances toxicity to added hydrogen peroxide. *Biochemical and biophysical research communications,* 348**,** 485-493.

WU, L., ZHANG, J. & WATANABE, W. 2011. Physical and chemical stability of drug nanoparticles. *Advanced drug delivery reviews,* 63**,** 456-469.

YUAN, J.-J., QIN, F. G., TU, J.-L. & LI, B. 2017. Preparation, Characterization, and Antioxidant Activity Evaluation of Liposomes Containing Water-Soluble Hydroxytyrosol from Olive. *Molecules,* 22**,** 870.

ZHANG, J., WANG, X., VIKASH, V., YE, Q., WU, D., LIU, Y. & DONG, W. 2016. ROS and ROS-mediated cellular signaling. *Oxidative medicine and cellular longevity,* 2016.

ZHANG, Y., CHAN, H. F. & LEONG, K. W. 2013. Advanced materials and processing for drug delivery: the past and the future. *Advanced drug delivery reviews,* 65**,** 104-120.

ZHOU, X., SETO, S. W., CHANG, D., KIAT, H., RAZMOVSKI-NAUMOVSKI, V., CHAN, K. & BENSOUSSAN, A. 2016. Synergistic effects of Chinese herbal medicine: a comprehensive review of methodology and current research. *Frontiers in pharmacology,* 7.

ZOROV, D. B., JUHASZOVA, M. & SOLLOTT, S. J. 2014. Mitochondrial reactive oxygen species (ROS) and ROS-induced ROS release. *Physiological reviews,* 94**,** 909-950.

APPENDIX

Figure A1: Liposomes flocculating
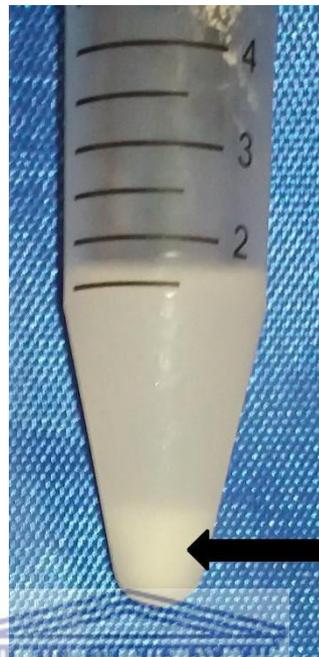
Liposomes settling to the bottom of the conical tube
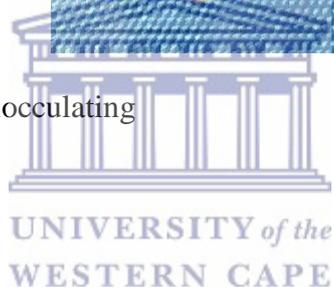
A
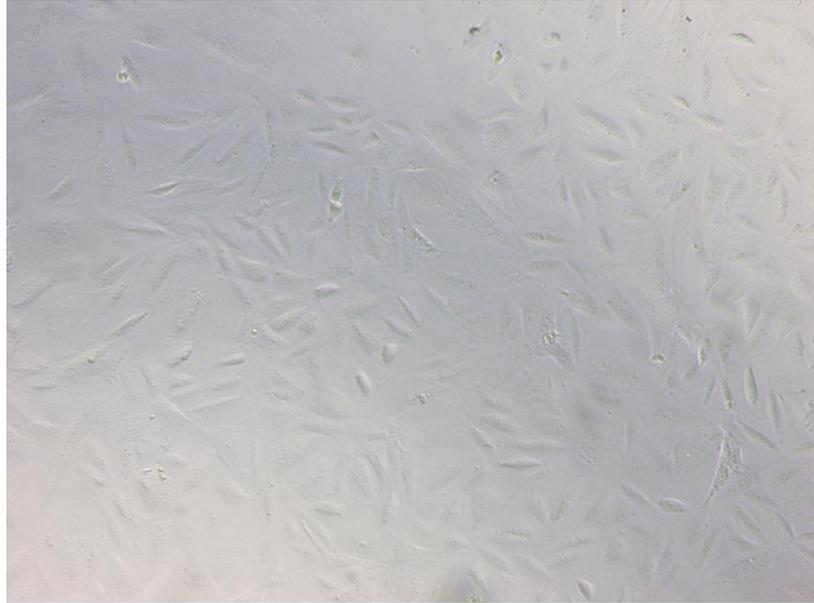
B

Figure A2: Untreated cells having no damage (A) and cells exposed to hydrogen peroxide being damaged (B) at10x magnification.

Table A1: The OL concentration calculated based on the linear regression with coefficients (4915.065856; -55962.26988)

|	Peak area	OL concentration (μg/mL)	OL concentration (%)
	1130210.175	241.33	24.133
	1150100.426	245.38	24.538
	1137521.429	242.82	24.282
Average	**1139277,343**	**243,1767**	**24,31767**
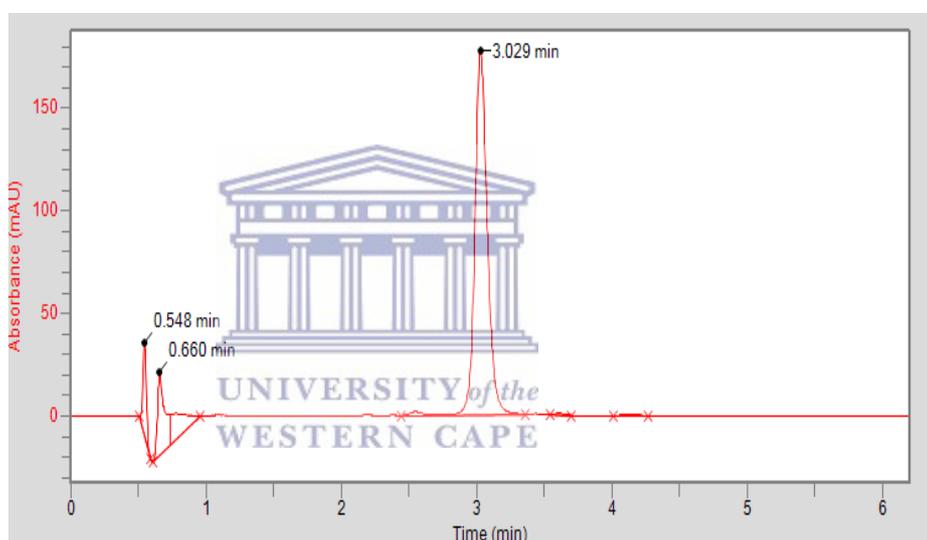


Figure A3: OL peak at 3.029 minutes on the HPLC chromatogram.
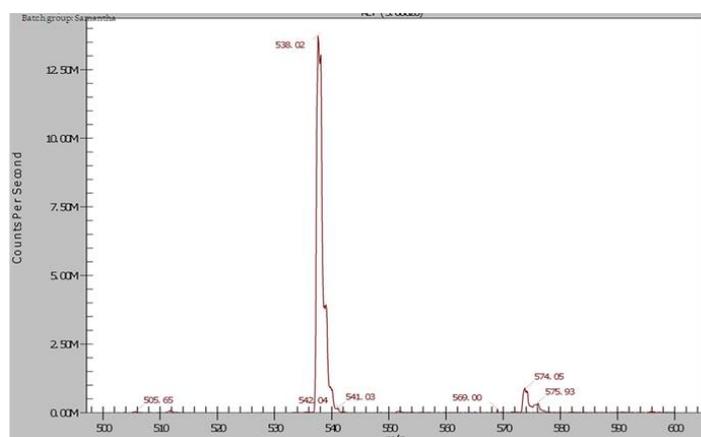
Figure A4: OL had a peak of 538.02 on the MS.